



**CIVIL ENGINEERING STUDIES**

Illinois Center for Transportation Series No. 16-016

UIIU-ENG-2016-2016

ISSN: 0197-9191

# **EFFECTIVENESS OF EXTERIOR BEAM ROTATION PREVENTION SYSTEMS FOR BRIDGE DECK CONSTRUCTION**

Prepared By

**Md Ashiquzzaman**

**Li Hui**

**Justin Schmeltz**

**Carlos Merino**

**Bora Bozkurt**

**Ahmed Ibrahim**

**Will Lindquist**

**Riyadh Hindi**

Saint Louis University

Research Report No. FHWA-ICT-16-015

A report of the findings of

**ICT PROJECT R27-140**

**Effectiveness of Exterior Beam Rotation Prevention Systems  
for Bridge Deck Construction**

---

**Illinois Center for Transportation**

**June 2016**



**TECHNICAL REPORT DOCUMENTATION PAGE**

<b>1. Report No.</b> FHWA-ICT-16-015		<b>2. Government Accession No.</b>		<b>3. Recipient's Catalog No.</b>	
<b>4. Title and Subtitle</b> Effectiveness of Exterior Beam Rotation Prevention Systems for Bridge Deck Construction				<b>5. Report Date</b> June 2016	
				<b>6. Performing Organization Code</b>	
<b>7. Author(s)</b> Md Ashiquzzaman, Li Hui, Justin Schmeltz, Carlos Merino, Bora Bozkurt, Ahmed Ibrahim, Will Lindquist, Riyadh Hindi				<b>8. Performing Organization Report No.</b> ICT-16-016 UILU-ENG-2016-2016	
<b>9. Performing Organization Name and Address</b> Saint Louis University 3450 Lindell Blvd St Louis, MO 63103				<b>10. Work Unit No.</b>	
				<b>11. Contract or Grant No.</b> R27-140	
<b>12. Sponsoring Agency Name and Address</b> Illinois Department of Transportation (SPR) Bureau of Material and Physical Research 126 East Ash Street Springfield, IL 62704				<b>13. Type of Report and Period Covered</b> Jan. 1, 2014, through June 30, 2016	
				<b>14. Sponsoring Agency Code</b> FHWA	
<b>15. Supplementary Notes</b> Conducted in cooperation with the U.S. Department of Transportation, Federal Highway Administration.					
<b>16. Abstract</b> Bridge decks often overhang past the exterior girders in order to increase the width of the deck while limiting the required number of longitudinal girders. The overhanging portion of the deck results in unbalanced eccentric loads to the exterior girders, which are generally greatest during construction. These eccentric loads mainly come from the bridge placing and finishing equipment as well as fresh concrete and other construction live loads that can create rotation of the exterior girders in the transverse direction. The rotations can also affect both the global and local stability of the girders as well as the bridge. In this study, the current bracing systems used by the Illinois Department of Transportation (IDOT) were evaluated through field instrumentation, finite element analysis (FEA), and the use of the Torsional Analysis Exterior Girders (TAEG) program. Alternative bracing systems were evaluated through an experimental study and FEA. Based on this work, it is recommended that intermediate cross frames with top and bottom angles in addition to cross-angle sections in the exterior panels be specified to limit exterior girder rotation during construction. An alternative approach is to place transverse ties and diagonal pipes in the exterior panels at a spacing to maintain the spacing-to-girder-depth ratio below 3.94.					
<b>17. Key Words</b> Overhang width, exterior girder rotation, rotation prevention system, TAEG program, experimental study			<b>18. Distribution Statement</b> No restrictions. This document is available through the National Technical Information Service, Springfield, VA 22161.		
<b>19. Security Classif. (of this report)</b> Unclassified		<b>20. Security Classif. (of this page)</b> Unclassified		<b>21. No. of Pages</b> 82 + appendices	<b>22. Price</b>



# ACKNOWLEDGMENT, DISCLAIMER, MANUFACTURERS' NAMES

This publication is based on the results of ICT-R27-140, **Effectiveness of Exterior Beam Rotation Prevention Systems for Bridge Deck Construction**. ICT-R27-140 was conducted in cooperation with the Illinois Center for Transportation; the Illinois Department of Transportation; and the U.S. Department of Transportation, Federal Highway Administration.

Members of the Technical Review panel were the following:

- Mark Thomson, TRP Chair, Illinois Department of Transportation
- Dan Brydl, Federal Highway Administration
- Douglas Dirks, Illinois Department of Transportation
- Ted Nemsky, Illinois Department of Transportation
- Kevin Riechers, Illinois Department of Transportation
- Jayme Schiff, Illinois Department of Transportation
- Mark Shaffer, Illinois Department of Transportation

The contents of this report reflect the view of the authors, who are responsible for the facts and the accuracy of the data presented herein. The contents do not necessarily reflect the official views or policies of the Illinois Center for Transportation, the Illinois Department of Transportation, or the Federal Highway Administration. This report does not constitute a standard, specification, or regulation.

Trademark or manufacturers' names appear in this report only because they are considered essential to the object of this document and do not constitute an endorsement of product by the Federal Highway Administration, the Illinois Department of Transportation, or the Illinois Center for Transportation.

## EXECUTIVE SUMMARY

Bridge decks often overhang past the exterior girders in order to increase the width of the deck while limiting the required number of longitudinal girders. The overhanging portion of the deck results in unbalanced eccentric loads to the exterior girders, which are generally largest during construction. These eccentric loads come primarily from the bridge placing and finishing equipment as well as fresh concrete and other construction live loads that can create rotation of the exterior girders in the transverse direction. The rotations can also affect both the global and local stability of the girders as well as the bridge. In this study, the current bracing systems used by the Illinois Department of Transportation (IDOT) were evaluated through field instrumentation, finite element analysis (FEA), and the use of the Torsional Analysis Exterior Girders (TAEG) program. Alternative bridge bracing systems were proposed and evaluated through both experimental testing and FEA.

The objectives of the proposed research were to evaluate current IDOT bracing policies and procedures and to develop improved and practical alternatives to minimize or prevent exterior girder rotation during new bridge deck construction. The specific objectives of the study included the following:

- Evaluate current bracing systems commonly used in the state of Illinois to determine effectiveness.
- Investigate and develop improved systems and construction bracing techniques to limit exterior girder rotation.
- Evaluate the TAEG program and identify how to properly model and analyze bracing systems appropriate for IDOT use.
- Develop bracing requirements that are dependent on specific bridge geometries, including beam depth-to-cantilever ratio, cross frame/diaphragm spacing, and finishing-machine rail locations.

Six steel girder bridges and one concrete girder bridge were instrumented with multiple sensors to measure girder rotation during deck construction. Basic geometric and construction information for all bridges was provided by IDOT engineers. The bridges monitored for the study were divided into four groups based on girder section size and type, number of spans, diaphragm spacing, bridge skew, and deck construction techniques. All girders and bracing systems were monitored using tilt sensors and strain gages installed at various locations on the top and bottom flanges of the exterior and first interior girders, girder webs, and tie bars and brackets used in the current bracing system. The results in this report are presented in two forms: the maximum measured rotation during deck placement and the residual (stable) rotation after completion of the bridge deck.

Construction loads were observed to have a significant effect on exterior girder rotations. Skewed bridges had more rotation compared with non-skewed bridges due to increased torsional moments produced as a result of the bridge geometry. For bridges with smaller W-sections, the first interior and exterior girder experienced differential rotations, whereas the deeper plate girders experienced

much smaller rigid body rotation. The single concrete girder bridge experienced minimal rotation due to the torsional stiffness and rigidity of the girders. The arrangement and spacing of diaphragms along the longitudinal and transverse directions also played a significant role in the measured rotation. In general, rotations of the first interior girders were negligible compared with the exterior girders. The ratio of the permanent diaphragm spacing to girder depth also had a noteworthy effect on exterior girder rotation. The three bridges that exceeded IDOT's overhang deflection limit also had the highest diaphragm spacing-to-girder-depth ratio.

In addition to the experimental field study, an analytical study was performed using the comprehensive FEA software Abaqus/CAE. The goals of the FE study were to verify and validate data collected from the bridges monitored in the field. The FE models were created based on plans provided by IDOT for all bridges and included the girders, diaphragms, bridge deck, and permanent and temporary bracing systems. After validation, these models were used to predict stresses and rotations at sections difficult to monitor in the field.

The TAEG program developed at the University of Kansas is frequently used by bridge designers to design bracing systems to prevent exterior girder rotation. The program is widely used and works well for bridges with straightforward geometry and applied loads. The program requires many variables including the geometry of overhang brackets, screed load, concrete weight, and the number and spacing of temporary lateral supports (tie bars and timber blocks). Five of the bridges in this study were analyzed using the TAEG program, and the results were compared with those measured in the field. The TAEG program did not always yield results consistent with those from the data collected from the field due to the limited ability of the program to account for the wide range of situations encountered during deck placement. Limitations of the program included its inability to account for multiple spacings between permanent lateral supports, inability to properly determine and model diaphragm connections, loading conditions, and alternative bracing systems..

The last part of this study included an experimental program utilizing a scaled bridge prototype with the goal of evaluating traditional girder rotation prevention systems used by IDOT in a controlled environment. The study also included an investigation of new methods and alternatives to prevent exterior girder rotation during deck placement. Multiple combinations of bracing elements (transverse ties, diagonal ties, intermediate cross frames, timber blocks, and horizontal and diagonal steel pipes) were evaluated in the study. The most effective bracing system in limiting exterior girder rotation was intermediate cross frames with top and bottom angles in addition to the transverse ties (straight and diagonal) currently used by IDOT. An alternative is to place transverse ties and diagonal pipes in the exterior panels while maintaining a spacing-to-girder-depth ratio below 3.94. Employing adjustable diagonal tie rods and horizontal pipes in the exterior panels could be another solution to minimize rotation.

# CONTENTS

<b>CHAPTER 1: INTRODUCTION .....</b>	<b>1</b>
<b>1.1 OVERVIEW.....</b>	<b>1</b>
<b>1.2 PROJECT OBJECTIVES .....</b>	<b>2</b>
<b>1.3 SCOPE .....</b>	<b>3</b>
<b>1.4 CHAPTER ORGANIZATION .....</b>	<b>3</b>
<b>CHAPTER 2: BACKGROUND INFORMATION AND LITERATURE REVIEW .....</b>	<b>4</b>
<b>2.1 INTRODUCTION .....</b>	<b>4</b>
2.1.1 Definition.....	4
2.1.2 Specifications for Deck Overhang .....	4
<b>2.2 CONSTRUCTION OF DECK OVERHANG .....</b>	<b>5</b>
2.2.1 Overhang Formwork System.....	5
2.2.2 Load Application.....	6
<b>2.3 SYSTEMS TO PREVENT EXTERIOR GIRDER ROTATION.....</b>	<b>7</b>
<b>CHAPTER 3: FIELD MONITORING AND FINITE ELEMENT ANALYSIS OF BRIDGES.....</b>	<b>9</b>
<b>3.1 GENERAL INFORMATION ABOUT THE BRIDGES.....</b>	<b>9</b>
<b>3.2 SENSORS USED FOR FIELD INSTRUMENTATION.....</b>	<b>9</b>
3.2.1 Tilt Sensor.....	9
3.2.2 Strain Gage .....	10
<b>3.3 FIELD DATA COLLECTION AND ANALYSIS .....</b>	<b>12</b>
3.3.1 Group 1 Bridges.....	12
3.3.2 Group 2 Bridges.....	15
3.3.3 Group 3 Bridges.....	18
3.3.4 Group 4 Bridges.....	20
<b>3.4 FINITE ELEMENT ANALYSIS .....</b>	<b>22</b>
3.4.1 Finite Element Modeling.....	22
3.4.2 Material Modeling.....	24
3.4.3 Finite Element Analysis for Group 1 Bridges .....	24
3.4.4 Finite Element Analysis for Group 2 Bridges.....	26



3.4.5 Finite Element Analysis for Group 3 Bridges .....	29
3.4.6 Finite Element Analysis for Group 4 Bridges .....	30
<b>3.5 EFFECT OF B/D RATIO IN EXTERIOR GIRDER ROTATION.....</b>	<b>32</b>
<b>CHAPTER 4: EVALUATION AND ASSESSMENT OF TORSIONAL ANALYSIS OF EXTERIOR GIRDERS (TAEG) PROGRAM .....</b>	<b>34</b>
<b>4.1 TAEG RESULTS AND DISCUSSION .....</b>	<b>34</b>
<b>4.2 THE MODIFIED ANALYSIS METHOD (AVERAGE LATERAL SUPPORT SPACING) .....</b>	<b>37</b>
<b>4.3 TREND ANALYSIS .....</b>	<b>38</b>
<b>4.4 PARAMETRIC ANALYSIS .....</b>	<b>40</b>
<b>4.5 PROGRAM CONCLUSIONS .....</b>	<b>44</b>
<b>CHAPTER 5: EXPERIMENTAL PROGRAM .....</b>	<b>46</b>
<b>5.1 OVERVIEW.....</b>	<b>46</b>
<b>5.2 DESIGN OF THE LABORATORY BRIDGE SCALED MODEL.....</b>	<b>46</b>
<b>5.3 ELEMENTS OF THE EXPERIMENTAL SETUP .....</b>	<b>47</b>
<b>5.4 INSTRUMENTATION.....</b>	<b>48</b>
5.4.1 Data Acquisition System .....	48
5.4.2 Tilt Sensors .....	48
<b>5.5 TESTING PROGRAM .....</b>	<b>49</b>
5.5.1 Bracing Elements.....	49
5.5.2 Testing Matrix .....	49
5.5.3 Data Analysis Procedure .....	50
5.5.4 Experimental Results .....	51
5.5.5 Best Experimental Cases .....	57
5.5.6 Comparison of Conventional and New Dayton Superior Hangers.....	57
<b>5.6 FINITE ELEMENT ANALYSIS.....</b>	<b>58</b>
5.6.1 Abaqus Model .....	58
5.6.2 Test Results and Comparison with Finite Element Analysis Results.....	61
5.6.3 Additional Cases Evaluated Using FEA.....	64
<b>5.7 COST-EFFECTIVE ASSESSMENT.....</b>	<b>65</b>
<b>5.8 SUMMARY.....</b>	<b>66</b>

<b>CHAPTER 6: EVALUATION AND ASSESSMENT OF IMPROVED ROTATION PREVENTION SYSTEMS.....</b>	<b>68</b>
<b>6.1 FINITE ELEMENT ANALYSIS .....</b>	<b>68</b>
6.1.1 Evaluation of Intermediate Cross Frames.....	68
6.1.2 Evaluation of Diagonal Pipes (DP) Combined with Transverse Ties (TT).....	71
6.1.3 Assessment of Adjusted Diagonal Ties (ADT) Combined with Horizontal Pipes (HP) .....	72
<b>6.2 MAXIMUM ALLOWABLE B/D RATIO .....</b>	<b>74</b>
<b>6.3 SUMMARY .....</b>	<b>75</b>
<b>CHAPTER 7: CONCLUSIONS AND RECOMMENDATIONS.....</b>	<b>76</b>
<b>7.1 CONCLUSIONS.....</b>	<b>76</b>
<b>7.2 FIELD-MONITORED DATA.....</b>	<b>76</b>
<b>7.3 TAEG RESULTS .....</b>	<b>77</b>
<b>7.4 EXPERIMENTAL RESULTS.....</b>	<b>77</b>
<b>7.5 RECOMMENDATIONS .....</b>	<b>77</b>
7.5.1 Girders with W-Sections .....	77
7.5.2 Medium and Deep Steel Plate Girders .....	79
7.5.3 Concrete Girders .....	79
<b>7.6 FUTURE STUDIES.....</b>	<b>80</b>
<b>REFERENCES.....</b>	<b>81</b>
<b>APPENDIX A: DEPARTMENT OF TRANSPORTATION OVERHANG DESIGN GUIDELINES (FASL 2008) .....</b>	<b>83</b>
<b>APPENDIX B: DETAILS OF THE BRIDGES .....</b>	<b>84</b>
<b>B.1 FUNDAMENTAL INFORMATION OF THE MONITORED BRIDGES.....</b>	<b>84</b>
<b>B.2 PLAN VIEW OF GROUP 1 BRIDGES .....</b>	<b>84</b>
<b>B.3 PLAN VIEW OF GROUP 2 BRIDGES .....</b>	<b>86</b>
<b>B.4 PLAN VIEW OF GROUP 3 BRIDGES .....</b>	<b>88</b>
<b>B.5 PLAN VIEW OF GROUP 4 BRIDGES .....</b>	<b>90</b>

<b>APPENDIX C: TORSIONAL ANALYSIS OF EXTERIOR GIRDERS (TAEG)</b> .....	<b>91</b>
<b>C.1 DESCRIPTION OF ANALYSIS ASSUMPTIONS</b> .....	<b>91</b>
C.1.1 Description of Loading Conditions.....	91
C.1.2 Location of Maximum Rotation .....	91
C.1.3 Diaphragm Spacing .....	91
C.1.4 Overhang Width.....	92
C.1.5 Temporary Lateral Supports .....	92
<b>C.2 UNIFORM BRIDGE ANALYSIS</b> .....	<b>93</b>
<b>C.3 PROGRAM LIMITATIONS</b> .....	<b>94</b>
<b>APPENDIX D: ADDITIONAL INFORMATION FROM THE EXPERIMENTAL PROGRAM</b> .....	<b>96</b>
<b>D.1 DESCRIPTION OF THE SETUP ELEMENTS</b> .....	<b>96</b>
D.1.1 Girders .....	96
D.1.2 Tie Bars .....	96
D.1.3 Bracket.....	97
D.1.4 Hangers.....	98
D.1.5 Load Application System .....	101
D.1.6 Girder Supports .....	101
D.1.7 Cross Frames.....	102
D.1.8 Compression Struts .....	103
<b>D.2 LABORATORY LAYOUTS AND MOST RELEVANT CROSS-SECTIONS FROM THE TESTED     CASES IN THE EXPERIMENTAL PROGRAM</b> .....	<b>105</b>
<b>D.3 LABORATORY LAYOUTS AND MOST RELEVANT CROSS-SECTIONS FROM THE TESTED     CASES IN THE EXPERIMENTAL PROGRAM</b> .....	<b>111</b>



# CHAPTER 1: INTRODUCTION

## 1.1 OVERVIEW

To reduce costs, bridge engineers generally design superstructures using the least number of girders possible across the roadway width with the same section size. In most cases, the deck extends past the exterior girders to increase the effective width of the deck without the use of additional girders. The overhanging portion of the deck is typically proportioned so that the same girder section can be used for both the interior and exterior girders. The extended width of the deck, or overhang, is shown in Figure 1.1. During construction of steel or concrete girder bridges, construction loads on the overhang portion of the deck are supported by steel cantilever-forming brackets placed every 3 to 6 ft. along the length of the exterior girders. While this leads to economical designs, the construction of these overhangs results in torsional moments acting on the exterior girders causing rotation and stresses that are generally not considered during design. These moments can cause excessive rotations of the exterior girders—leading to thin decks, reduced concrete cover, poor rideability, and potential instabilities during construction, to name a few problems.



**Figure 1.1 Deck overhang in bridge.**

To prevent exterior girder rotation during construction, it is essential to select an appropriate bracing system that can carry the construction loads, and that can be installed and adjusted properly. Ineffective or improperly installed bracing systems may lead to excessive rotation due to overhang loading, as shown in Figure 1.2. Rotations can also affect both the global and local stability of the bridge girders. The objective of this study was to enhance the knowledge and understanding of exterior girder behavior due to unbalanced eccentric construction loads and to identify the critical factors affecting rotation by recommending appropriate bracing systems to minimize or prevent rotation.

Prior to construction of the deck, engineers often predict exterior girder rotation expected during deck placement using practical experience, software, or both. A common software package used in Illinois is TAEG. This program calculates the rotation of exterior girders using conservative assumptions, which in many cases can lead to inaccurate results. Therefore, it is important to

evaluate the performance of the TAEG program based on field measurements and detailed finite element analyses (FEA).

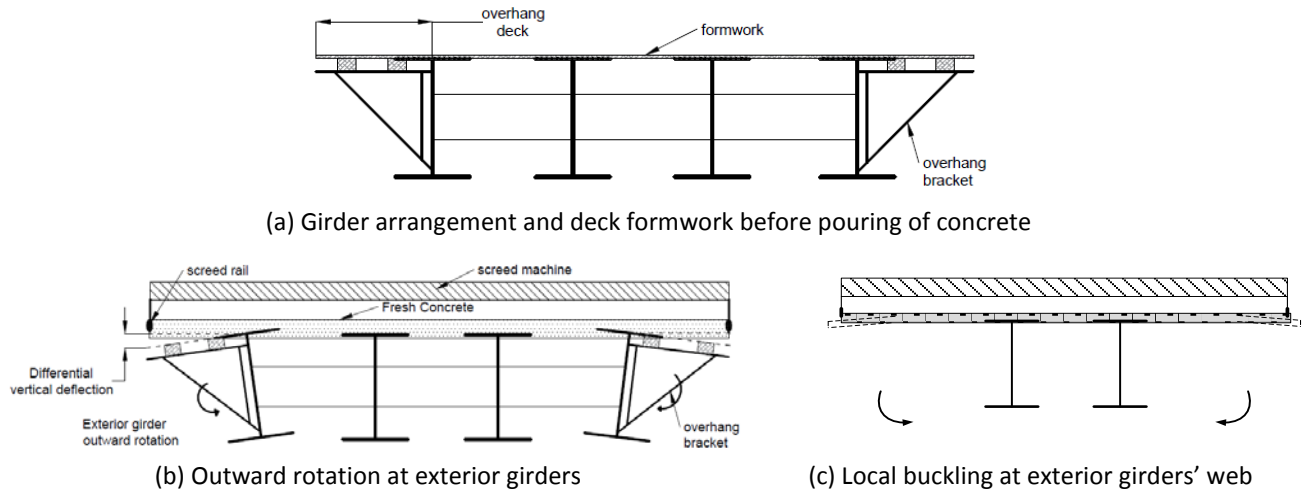


**Figure 1.2. Exterior girder rotation due to unbalanced eccentric load on deck overhang.**

The Illinois Department of Transportation (IDOT) funded this research investigation, entitled “Effectiveness of Exterior Beam Rotation Prevention Systems for Bridge Deck Construction,” to improve bracing systems and to prevent or minimize exterior girder rotations in both steel and concrete girder bridges. In this study, the overhang geometry and its deformed shape were measured and identified. In this report, recommendations are made to improve rotation prevention systems, and suggestions are offered to improve bridge deck overhang construction.

The remainder of this chapter provides a discussion on the scope of the research as well as a brief outline of the remainder of this report.

## 1.2 PROJECT OBJECTIVES

The specific objectives of the study are as follows:

- Evaluate current bracing systems commonly used in the state of Illinois to determine their effectiveness.
- Investigate and develop improved systems and construction bracing techniques to limit exterior girder rotation.
- Evaluate the TAEG program and identify how to properly model and analyze bracing systems appropriate for IDOT.
- Develop comprehensive bracing requirements that are dependent on specific bridge geometries, including beam depth-to-cantilever ratio, cross frame/diaphragm spacing, and finishing machine rail locations.

### 1.3 SCOPE

This research project included field monitoring, laboratory testing, and a parametric FEA. Seven bridges were monitored during construction as part of the field testing. The bridges included three W30 girder bridges (both skewed and non-skewed); a straight, medium-depth plate girder bridge; two deep plate girder bridges (both skewed and non-skewed); and a skewed concrete bulb T-beam bridge. The field data was used to validate the FEA models. In addition to field monitoring, experimental laboratory tests on key elements of steel twin-girder systems were evaluated for further refinement of the FEA models. The validated FEA models were used to conduct a parametric study to improve understanding of the behavior of concrete and steel girder systems during deck construction. Three improved bracing systems are recommended in this report to minimize girder rotation resulting from the overhang loads. Finally, the TAEG program was evaluated to determine its ability to predict actual exterior girder rotation observed in the field. The results of this report are helpful to bridge engineers for predicting girder rotation using TAEG and for selecting bracing systems.

### 1.4 CHAPTER ORGANIZATION

This report consists of the following seven chapters:

**Chapter 1: Introduction**—Provides an introduction to the project scope and objectives.

**Chapter 2: Background Information and Literature Review**—Provides background information on the influence of overhang construction on girder design. Background information and a description of the TAEG program are presented. Chapter 2 also summarizes the available literature on overhang tests, FEA modeling, and overhang design in addition to presenting case studies of bridges that experienced problems during construction.

**Chapter 3: Field Monitoring and Finite Element Analysis of Bridges**—Presents field-monitored data for seven bridges. The chapter also presents the results of field data validation using FEA performed with the commercial FE software Abaqus.

**Chapter 4: Evaluation and Assessment of the Torsional Analysis of Exterior Girders (TAEG) Program**—Contains an introduction to the TAEG program and presentation of the assumptions for analyses. The chapter also discusses the evaluation of the TAEG program that was conducted using the field data collected from all bridges considered in this study.

**Chapter 5: Experimental Program**—Presents and discusses the results of the laboratory testing of a steel twin-girder system. Results from the FEA of the experimental section are also presented. Improved rotation prevention systems are proposed based on the experimental and FEA data.

**Chapter 6: Evaluation and Assessment of Improved Rotation Prevention Systems**—Presents and discusses the results of full-scale bridge models (using FEA).

**Chapter 7: Conclusions and Recommendations**—Presents a summary of the important findings, along with recommendations from the study and design guidelines for future studies.

## CHAPTER 2: BACKGROUND INFORMATION AND LITERATURE REVIEW

### 2.1 INTRODUCTION

#### 2.1.1 Definition

There is no consistent definition for deck overhang used by bridge engineers, but for the purposes of this study, the deck overhang (for both concrete and steel girder bridges) is defined as the width of the deck extended from the centerline of the exterior girder to the edge of the deck, as shown in Figure 2.1.



Figure 2.1 Deck overhang in a steel girder bridge.

#### 2.1.2 Specifications for Deck Overhang

Overhang widths and bracing systems vary significantly from state to state. Most states specify a maximum allowable overhang width based on factors such as girder spacing, girder depth, and deck thickness. The 2012 IDOT Bridge Manual limits the overhang width to 3'-8" for steel beams and PPC I-Beams and 4'-6" for Bulb T Beams. A summary of overhang requirements for several other states is provided in Appendix A. The current bracing system requirements for Illinois are described in Article 503.06 of the Illinois Standard Specifications for Road and Bridge Construction (April 2016). Article 503.06 requires transverse ties (No. 4 bars with a maximum spacing of 8 ft.) attached from one exterior girder to the opposite exterior girder with hardwood 4 × 4 in. blocks wedged between the webs of the exterior and first interior beams within 6 in. of the bottom flanges. Guide Bridge Special Provision (GBSP) #78 was developed as an alternative to the standard specification and requires diagonal No. 4 ties that attach the top flange of the exterior girder to the bottom flange of the first interior girder. GBSP #78 also requires hardwood timber blocks.



## 2.2 CONSTRUCTION OF DECK OVERHANG

### 2.2.1 Overhang Formwork System

The deck overhang is usually formed by wood sheathing supported with steel brackets spaced across the length of the bridge. Several studies have evaluated commercially available overhang brackets and hangers (Ariyasajakorn 2006; Clifton 2008; and Grubb 1990).

Formwork (both for steel and concrete girders, as shown in Figure 2.2) is used to support the plastic concrete on the deck overhang. A large variety of overhang steel brackets is currently available for use on both steel and concrete girders. Manufacturers include Dayton Superior and Meadow Burke, and they offer different types of overhang brackets that allow vertical leg adjustment, horizontal leg adjustment, and adjustment of the horizontal leg angle.

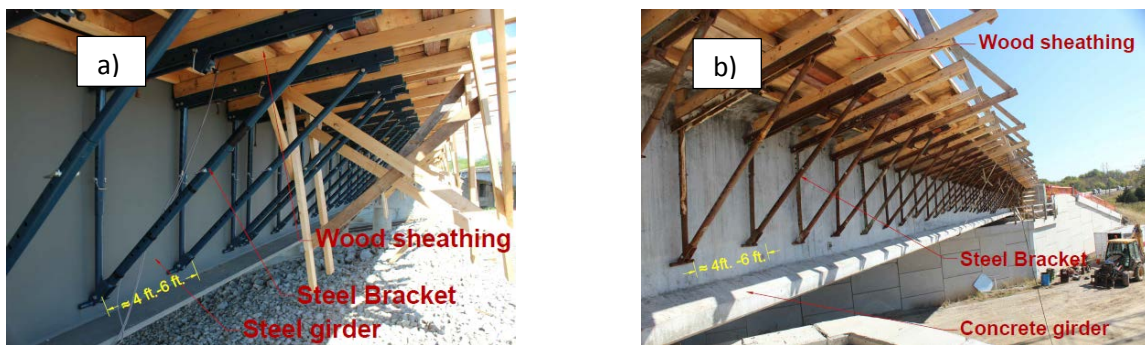
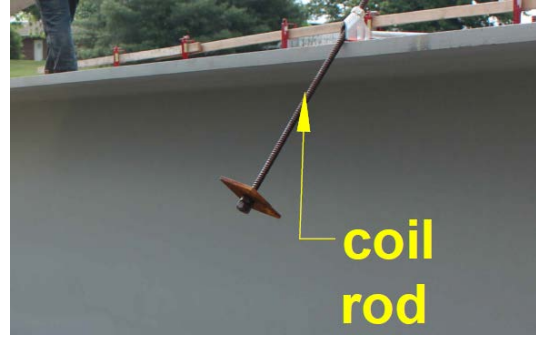


Figure 2.2 Formwork for overhang deck: (a) steel girder bridge, (b) concrete girder bridge.

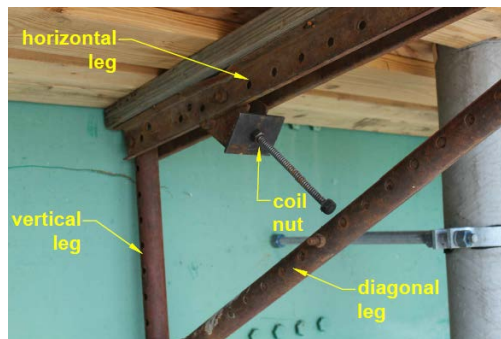
Figure 2.3 shows the bracket assembly. In step 1, steel hangers (Dayton Superior 2015) were attached to the top flange of the girder, which was embedded in the concrete during construction. In step 2, the hanger and steel bracket were connected by the coil rod. In step 3, overhanging brackets that support the plywood overhang formwork were installed.



Step 1: Attaching hanger to the girder



Step 2: Coil rod dropping from hanger



Step 3: Installing hanger with coil rod and then placing wood sheathing on top of bracket

**Figure 2.3 Installation of steel brackets.**

## 2.2.2 Load Application

Several types of construction loads are applied to the exterior girder through overhang brackets. Figure 2.4 shows a bridge during concrete deck placement. Typical construction loads include fresh concrete, finishing screed, and overhang formwork, as well as the weight of construction personnel. Each of these loads results in torsional moments acting on the exterior girder.

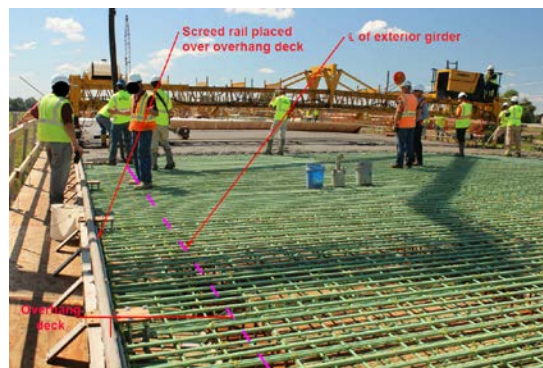


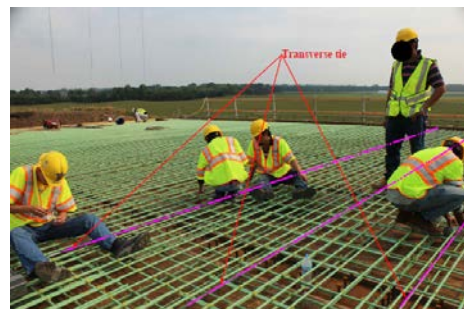
**Figure 2.4 Screed rail placed on the overhang formwork.**

## 2.3 SYSTEMS TO PREVENT EXTERIOR GIRDER ROTATION

The source of rotation is based on the overhang width and loading as well as the bracing system used to restrict girder rotation during construction. It is possible to reduce the net torsional moment caused by these loads by placing the machine rails directly on the exterior girder (zero eccentricity) rather than on the overhang formwork. The reduction in torsional moment must be weighed against potential construction difficulties because the overhang requires hand placing and finishing. Most contractors prefer to place the screed rail on the overhang form because, in that configuration, the finishing machine can reach 95% of the deck surface and because movement of the screed rails during placement is not necessary (Suprenant 1994). To prevent exterior girder rotation caused by local or global buckling, it is important to implement an appropriate bracing system. The bracing system used can vary significantly from state to state. Figures 2.5 through 2.7 show different types of bracing systems used to prevent exterior girder rotation.

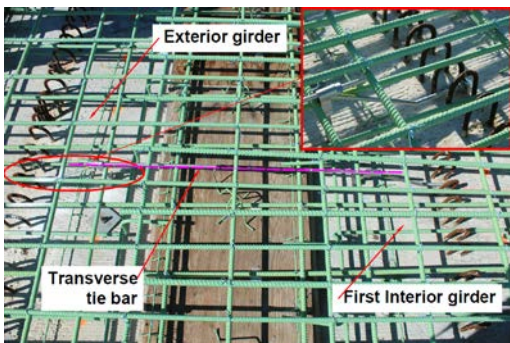


(a) Diagonal tie bar (connected from exterior girder to first interior girder)



(b) Transverse tie bars (connected from exterior girder to exterior girder)

**Figure 2.5 Rotation prevention systems for steel girder bridges.**



(a) Transverse tie bar (connected from exterior girder to first interior girder), with end tightened by nut



(b) Transverse tie bar (connected from exterior girder to first interior girder), welded end (Yang 2009)

**Figure 2.6 Rotation prevention systems for concrete girder bridges.**



**Figure 2.7 Timber blocking in addition to transverse tie bars.**

# CHAPTER 3: FIELD MONITORING AND FINITE ELEMENT ANALYSIS OF BRIDGES

## 3.1 GENERAL INFORMATION ABOUT THE BRIDGES

Six steel girder bridges and one concrete girder bridge were instrumented with multiple sensors to measure girder rotation during deck construction. The basic geometric and construction information for all bridges is shown in Table B.1 (Appendix B).

The bridges were divided into four different groups based on girder size, number of spans, and other unique attributes, as shown in Table 3.1.

**Table 3.1 Bridge Groups**

<b>Group 1</b>	<b>Group 2</b>	<b>Group 3</b>	<b>Group 4</b>
Lincoln Bridge	Highland Bridge	Carlyle Bridge	Belleville-I Bridge
Greenup Bridge		Belleville-II Bridge	
Bloomington Bridge			

Different measures were taken into consideration in assigning the bridges to groups:

**Group 1**—Girder steel sections of W30, three-span bridge with depths similar to overhang width ratios (Lincoln: 1.3, Greenup: 1.2, Bloomington: 1.2)

**Group 2**—Inconsistent diaphragm spacing across the width of the bridge.

**Group 3**—Deep plate girder bridges constructed in two stages.

**Group 4**—Precast concrete girder bridge.

## 3.2 SENSORS USED FOR FIELD INSTRUMENTATION

### 3.2.1 Tilt Sensor

Dual-axis tilt sensors (CXTLA02) with a  $\pm 20^\circ$  range in both directions were installed to monitor the transverse rotations in exterior girders and in the first interior girder of all bridges. The main reason for selecting these two girders was their susceptibility to rotation during deck construction. The sensitivity of the tilt sensors was checked prior to installation. In nearly every case, two locations (bottom flange and web) were monitored at each section (generally, three sections were selected for each bridge). An open aluminum box was fabricated to accommodate the tilt sensor (as shown in Figure 3.1), which was attached to the girder temporarily during construction. The directions (transverse direction measured along the width of the deck, and longitudinal direction measured along the length of the span) of the tilt sensors were carefully maintained during their installation. For this project, all tilt sensors were mounted to the girders in the same direction and same pattern to maintain consistency in the data collected.

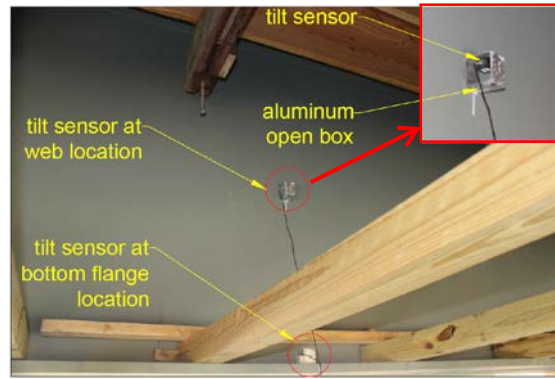


**Figure 3.1 Dual-axis tilt sensor installed on the bottom flange of the exterior girder.**

Strain gages (details provided in Section 3.2.2) were used to measure strain (and stress) in the brackets supporting the overhang deck as well as the ties intended to restrict girder rotation. Figure 3.2 shows the location of the tilt sensors and strain gages used at each section for the two different bracing systems evaluated in this study.

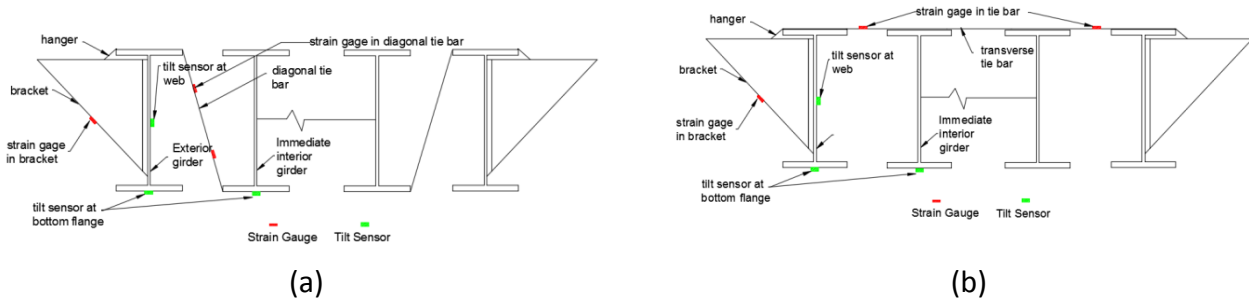


**Figure 3.2 Location of tilt sensors and strain gages: (a) bridge cross section with diagonal tie arrangement, (b) bridge cross section with transverse tie arrangement.**

### 3.2.2 Strain Gage

Foil strain gages (CEA-06-125UN-350/P2) were installed on bracing bars and ties to measure and investigate strains during and after construction, as shown in Figure 3.3. Self-fusing tape was used to protect the gages from moisture and other potential external distress.



(a) Strain gage in the transverse tie bar



(b) Strain gage in the diagonal leg

**Figure 3.3 Strain gage installation.**

Strain gages were installed on the bracing bars (diagonal ties and transverse ties) to evaluate the effectiveness of these elements and to validate the finite element (FE) models.

Exterior girders experience two types of rotation during bridge deck construction: transverse rotation about the longitudinal girder axes and longitudinal rotation about the transverse axis across the bridge width. Transverse rotations occur in both the inward and outward directions (as shown in Figure 1.2 in Chapter 1). In this report, outward transverse girder rotation is considered positive while inward transverse rotation is considered negative. All the recorded rotations are presented in a time–history format (rotation vs. time), as shown in Figures 3.4 and 3.5. Simple exponential smoothing (SES) was used to analyze the field data, where the SES equation takes the form of Equation 3.1.

$$\hat{y}_{i+1} = \alpha y_i + (1 - \alpha) \hat{y}_i \quad (3.1)$$

where  $\hat{y}_i$  is the known series values for time period  $i$ ,  $y_i$  is the forecast value of the variable  $Y$  for time period  $i$ ,  $\hat{y}_{i+1}$  is the forecast value for time period  $i + 1$ , and  $\alpha$  is the smoothing constant (Brown et al. 1961).

The SPSS (Statistical Package for the Social Sciences) software was used to calculate the maximum and stable girder rotation, as shown in Figure 3.4. The peak maximum rotation of any particular section occurs when the screed machine, fresh concrete (poured up to the particular section being considered), and other construction loads are positioned directly at that section. The stable or permanent rotation (forecasted rotation using the exponential smoothing system) is shown in Figures 3.4 and 3.5 and is determined after finishing construction of the bridge deck when all of the loads were removed except the weight of the concrete deck. This rotation became permanent as the concrete deck hardened, holding the girders in place.

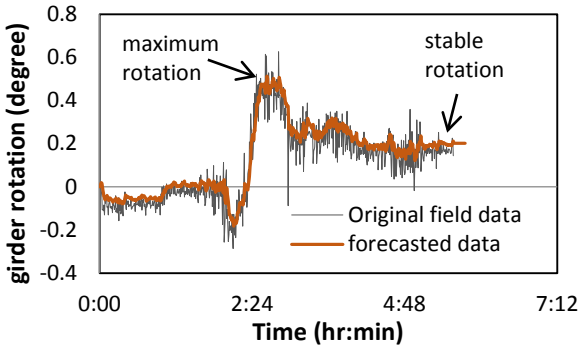


**Figure 3.4 Maximum and stable rotation by simple exponential smoothing.**

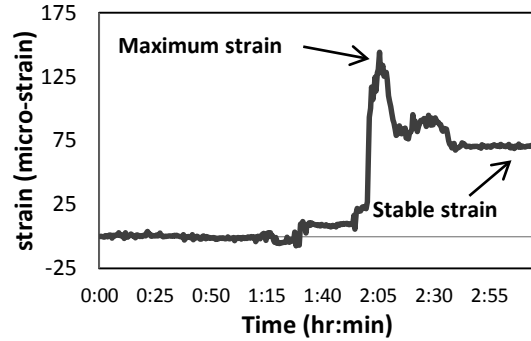


**Figure 3.5 Maximum and stable strains of tie bars.**

Bracing bars (transverse and diagonal ties) are subject to tensile strain during concrete placement. The peak “maximum strain of tie bars” at any particular section occurs when the screed machine, fresh concrete (poured up to the particular section being considered), and other construction loads are positioned at that section. The “stable/permanent/residual strain of tie bars” is shown in Figure 3.5 where the maximum and the residual strain is determined after finishing construction of the bridge deck when all loads are removed except the weight of the fresh concrete.

### 3.3 FIELD DATA COLLECTION AND ANALYSIS

#### 3.3.1 Group 1 Bridges

##### 3.3.1.1 Instrumentation Plan

Sensor locations are described in Table B.2 (Appendix B) for the three Group 1 bridges, with sections shown in plan view for each of the bridges in Appendix B (Figures B.1 through B.3). In general, rotations are measured at the bottom flange and mid-height of the web as shown in Figure 3.2.3.3.1.2 Field Data Collected on Girder Rotation

Figure 3.6 depicts the measured transverse rotation in the exterior girder at midspan (Section S1) for the Lincoln, Greenup, and Bloomington bridges. It can be seen that the maximum rotation of the exterior girder (outward direction) for this section was  $0.45^\circ$ ,  $0.53^\circ$ , and  $0.44^\circ$  for the Lincoln, Greenup, and Bloomington bridges, respectively. In each case, these maximum rotations occurred when the construction loads were applied directly at the section being considered. Stable rotations were  $0.34^\circ$ ,  $0.27^\circ$ , and  $0.30^\circ$  for the three bridges, respectively. Figure 3.6b shows the exterior girder web rotations measured at Section S1 for the Lincoln and Bloomington bridges. The maximum and stable rotations were  $0.50^\circ$  and  $0.39^\circ$  for the Lincoln bridge and  $0.46^\circ$  and  $0.31^\circ$  for the Bloomington bridge. It can be seen that the construction loads from the overhang deck acted with greater impact to the exterior girders.

The maximum and stable rotations of the first interior girders for the Lincoln bridge at midspan (Section S1) were small ( $0.025^\circ$  and  $-0.04^\circ$ ) and are shown in Figure 3.6c. This was likely caused by the lack of tightening of the diagonal ties and improperly shimmed timber blocks. The timber blocks were placed for lateral restraint and became effective only when the fresh concrete and other



construction live loads were applied and forced the first interior girder to rotate slightly in the outward direction, as shown in Figure 3.6c. On the other hand, by the end of construction—when the only load present was the weight of fresh concrete—the diagonal ties pulled the interior girder to rotate in the inward direction, as shown in Figure 3.6c. Girder rotations at diaphragm locations behaved differently where exterior girder rotations were nearly zero in the web because the diaphragm restricts rotation. The bottom flange experienced comparatively much higher rotation as a result of its unsupported length below the diaphragm. The exterior girder had the smallest rotation at Section S3, which was closest to the pier.

The field data collected for the skewed bridges (Greenup and Bloomington) was conceptually different than the data collected for the non-skewed bridge. The Greenup and Bloomington bridges were skewed  $24^\circ$  and  $3.8^\circ$ , respectively. Transverse rotations of the exterior girder in skewed bridges were always outward, and in most of the cases, they were larger than the corresponding values in the non-skewed bridge. Exterior girder rotations were measured at Section S2 for the three bridges, as shown in Figure 3.7. It can be seen that the maximum and stable rotations were  $0.34^\circ$  and  $0.25^\circ$  for the Lincoln bridge,  $0.38^\circ$  and  $0.20^\circ$  for the Greenup bridge, and  $0.45^\circ$  and  $0.29^\circ$  for the Bloomington bridge. Though the maximum exterior girder rotations occurred at midspan, the rotations at sections far from midspan (Sections S2 and S3) were significant enough to be taken into consideration. The maximum rotations at the web location for the three bridges at Section S3 were  $0.25^\circ$ ,  $0.51^\circ$ , and  $0.45^\circ$ , respectively, as shown in Figure 3.8, with corresponding stable rotations of  $0.17^\circ$ ,  $0.20^\circ$ , and  $0.26^\circ$ . These differences were attributed to the skewness of the bridge, the larger girder spacing, and the diaphragm locations.

During construction of the skewed bridges, the tie bars and the line of approach for concrete placement were perpendicular to the direction of roadway, which created unbalanced construction loads on the exterior girders (shown in Figure 3.9). Owing to these unbalanced loads (as a result of skewness of the bridges), the exterior girder rotations at Section S1 (shown in Figure 3.6) and Section S3 (shown in Figure 3.8) were similar for both the Greenup and Bloomington bridges.

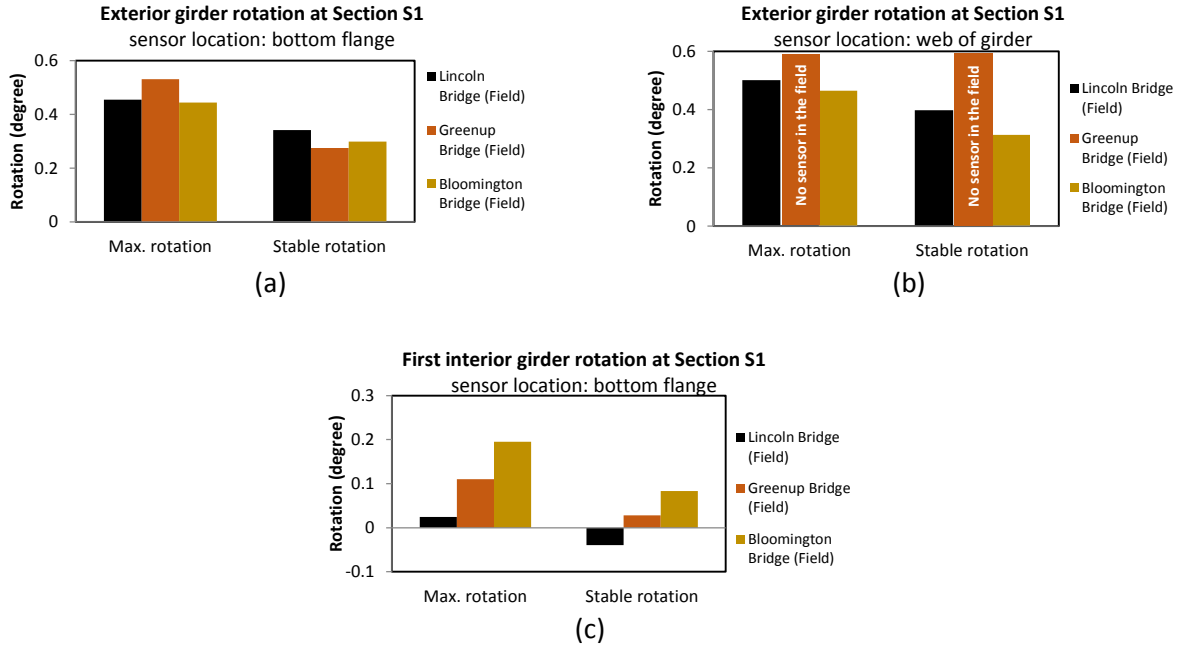


Figure 3.6 Girder rotation at Section S1 (Group 1).

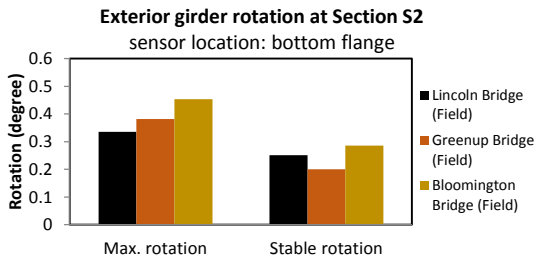


Figure 3.7 Girder rotation at Section S2 (Group 1).

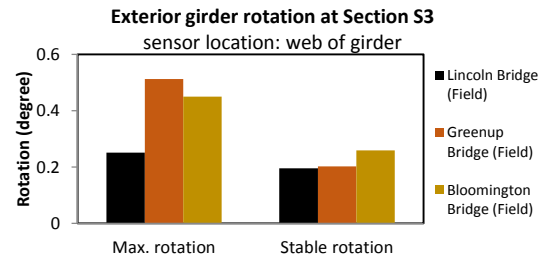


Figure 3.8 Girder rotation at Section S3 (Group 1).

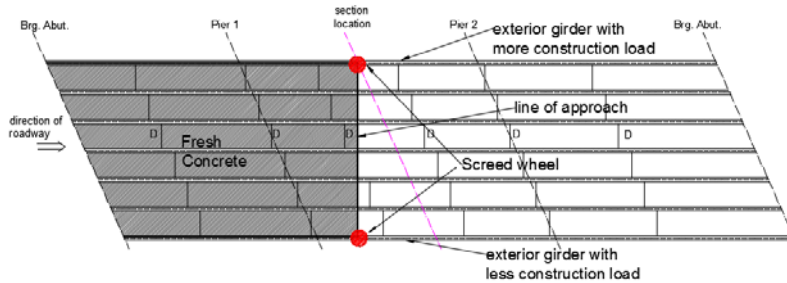
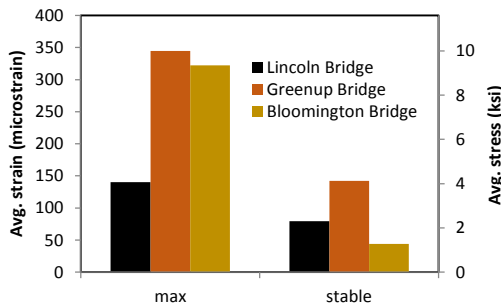


Figure 3.9 Unbalanced construction load on the two exterior girders, caused by bridge skewness.

### 3.3.1.3 Data Collected for Field Stresses/Strains on Tie Bars and Brackets

The strain data in the tie bars and brackets were recorded in micro-strain ( $\mu\epsilon$ ). The strain measured in the tie bars were used to calculate stresses using Hooke's law to determine stresses during and after construction. Figures 3.10 and 3.11 show the average maximum and stable strain and stress values in the bracing bars and the diagonal legs of the brackets for all bridges. The average maximum and stable strain values in the non-skewed bridge (Lincoln) were much smaller than the corresponding values in the case of skewed bridges (Greenup and Bloomington). The range of maximum strain values in the bracing bars for the skewed bridges was 325 to 350  $\mu\epsilon$ , which is 2.4 times the values obtained from the non-skewed bridge. After concrete placement, the strain values decreased significantly and represented the residual (stable) values in the considered members. The permanent strains were found to be 79, 142, and 44  $\mu\epsilon$  for the Lincoln, Greenup, and Bloomington bridges, respectively. The bracing bars in the non-skewed and small skewed bridges experienced minimal stresses, whereas the bracing bars in the bridge with the largest skew angle experienced comparatively higher values (see Figure 3.10). That could be attributed to the skew, which produced extra torsional stresses in addition to the unbalanced loads applied during deck placement.

The measured strains (and stresses) in the diagonal leg of the brackets are shown in Figure 3.11. All diagonal legs experienced compressive stresses related to deck construction loads. The average maximum compressive stress was 8.7 ksi in the Greenup bridge, which was much higher than the compressive stresses in the other bridges. This is most likely due to the 24° skew as well as the type of screed used to finish each bridge. A relatively light vibrating screed was used to finish the Lincoln bridge, a much larger and heavier finishing machine was used for the Greenup bridge due to the large deck width (50.3 ft.), and a smaller finishing machine was used to finish the Bloomington bridge with a relatively short width (16.2 ft.). The average permanent compressive strains and stresses for all bridges were very small compared with the corresponding maximum values, except for the Bloomington bridge, as shown in Figure 3.11.



**Figure 3.10** Field measurement of average tensile strains and stresses in tie bars.

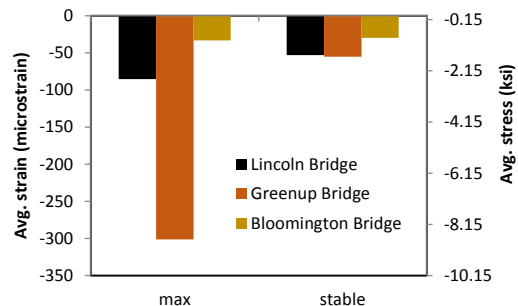


**Figure 3.11** Field measurement of average compressive strains and stresses in brackets.

## 3.3.2 Group 2 Bridges

### 3.3.2.1 Instrumentation Plan

This group consisted of one medium-depth (48 in.) steel plate girder bridge. This bridge was distinguished by its asymmetric diaphragms in the two exterior bays. The extra diaphragms were

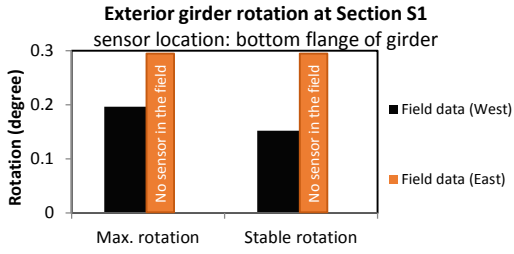
included in the design of this bridge to carry utility conduit. Sections for instrumentation are described in Table B.3 and the section locations on the bridge plans are shown in Figure B.4 (Appendix B). The locations of the sensors for each section (tilt sensor and strain gages) are shown in Figure 3.2.

### 3.3.2.2 *Field Data Collected on Girder Rotation*

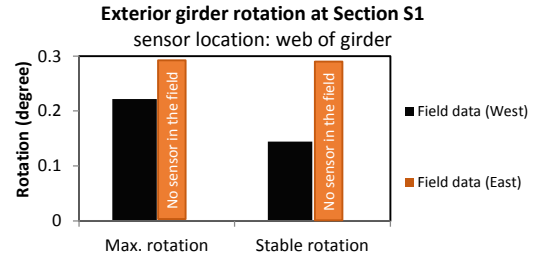
Girder rotations for Section S1 (shown in Figure 3.12) were  $0.20^\circ$  and  $0.22^\circ$  at the bottom flange and at the web, respectively. The stable rotations at the bottom flange and the web were  $0.15^\circ$  and  $0.14^\circ$ , respectively. The small difference between rotations measured at the flange and web indicated that the girder tilted as a rigid body. The maximum and stable rotations of the first interior girder in the west end were  $0.13^\circ$  and  $0.11^\circ$ , respectively. Tilt sensors were not installed in the east end of the bridge.

The exterior girder rotations in Section S2 (containing a continuous diaphragm) are shown in Figure 3.13. The tilt sensors were instrumented in the exterior girders at both the east and west ends of the bridge. At the west end, the maximum rotations at the bottom flange and the web were very close (approx.  $0.25^\circ$ ), and the stable rotations followed the same behavior for both the bottom flange and the web (approximately  $0.15^\circ$ ). On the other hand, at the east end, the maximum rotations at the bottom flange and the web were  $0.25^\circ$  and  $0.22^\circ$ , respectively, and stable rotations at the bottom flange and web were  $0.19^\circ$  and  $0.14^\circ$ , respectively. If a comparison of rotations at the east and the west ends is performed, it can be seen that the rotations at the west end were more likely occurring as rigid body rotation, whereas the east end experienced differential rotations between the bottom flange and the web. Another noticeable point is that the rotations at both ends were quite similar because of the presence of continuous diaphragms at those locations

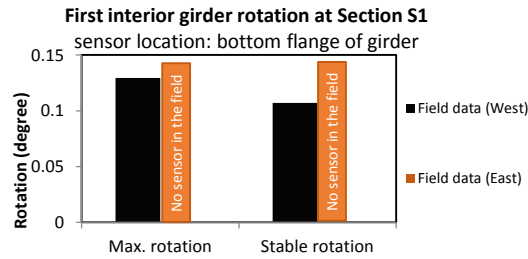
Girder rotations for Section S3 (with an intermediate diaphragm at the west end) are shown in Figure 3.14. The tilt sensors were installed on the exterior girders at both ends of the bridge at different locations. The exterior girder at the west end again showed rigid body rotation, with the maximum rotation at the bottom flange and the web at  $0.16^\circ$  and  $0.17^\circ$ , respectively. The exterior girder at the east end showed small maximum and stable rotations (nearly  $0.07^\circ$ ) at the bottom flange location.



(a)

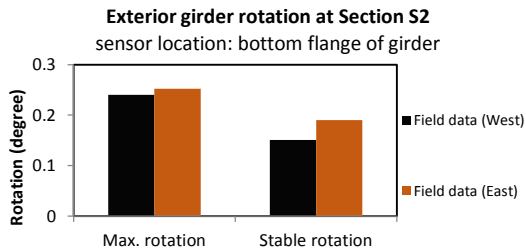


(b)

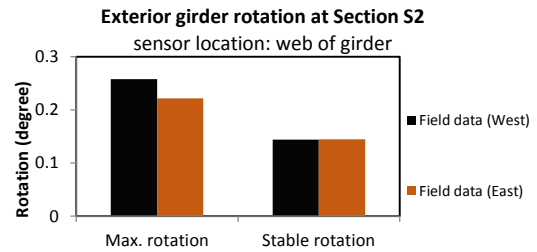


(c)

Figure 3.12 Field-monitored transverse rotations at Section S1 (Group 2).

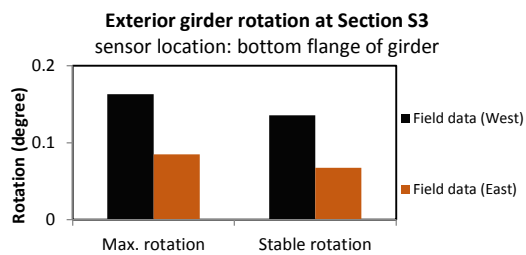


(a)

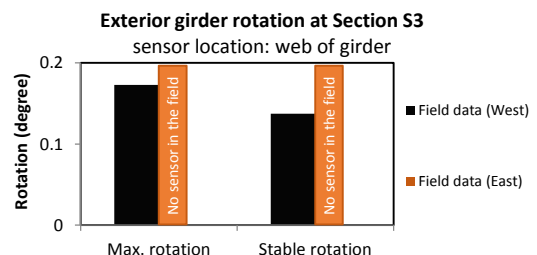


(b)

Figure 3.13 Field-monitored transverse rotations at Section S2 (Group 2).



(a)



(b)

Figure 3.14 Field-monitored transverse rotations at Section S3 (Group 2).

### 3.3.2.3 Collected Field Stresses/Strains on Tie Bars

The maximum strain (and stress) in the tie bar at Section S1 measured during construction was 142  $\mu\epsilon$  (4.1 ksi), and the stable strain (stress) was 72  $\mu\epsilon$  (2.1 ksi), as shown in Figure 3.15.

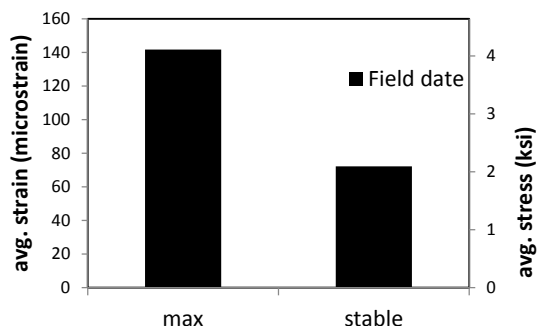


Figure 3.15 Field-monitored average stresses/strains in tie bars.

## 3.3.3 Group 3 Bridges

### 3.3.3.1 Instrumentation Plan

The Group 3 bridge sections for instrumentation are described in Table B.4 (Appendix B). Section locations are shown on the bridge plans in Appendix B (Figures B.5 and B.5). Sensor locations (tilt sensor and strain gages) are shown in Figure 3.2.

### 3.3.3.2 Field Data Collection on Girder Rotation

This group contained two deep plate girder bridges: the Carlyle (78-in. PLG) and Belleville-II (64-in. PLG) bridges. These bridges were constructed in two separate placements, with the second placement used for instrumentation, as shown in Appendix B (Figures B.5 and B.6).

It can be seen in Figures 3.16 through 3.18 that the rotations measured in both bridges were comparatively smaller than the steel girder bridges discussed previously. In the case of the Carlyle bridge, taking all sections into consideration (in both the web and flange locations), the maximum rotation was 0.092°, with negligible stable rotations (around 0.03°). The maximum rotation occurred at midspan.

The placement of concrete on the Belleville-II bridge deck was slightly different than for the other decks. The contractor was not able to use the screed at the beginning of the placement because of the skew of the bridge. Instead, a vibrating plate was used, as shown in Figure 3.19. In addition, the screed was not removed from the bridge after construction like it was for the other bridges included in the study. As a result, even after construction, the stable rotation values shown in Figures 3.16 through 3.18 are slightly higher at the screed location than the rotation measured for the Carlyle bridge. For all of the sections of the Belleville-II bridge, the largest maximum rotation was 0.17°, and it occurred at Section S2. The maximum rotation at Section S1 was slightly smaller than at Section S2 owing to the presence of a diaphragm. The stable rotations (approximately 0.05°) in all sections were very small compared with the IDOT limit, as shown in Figures 3.16 through 3.18.

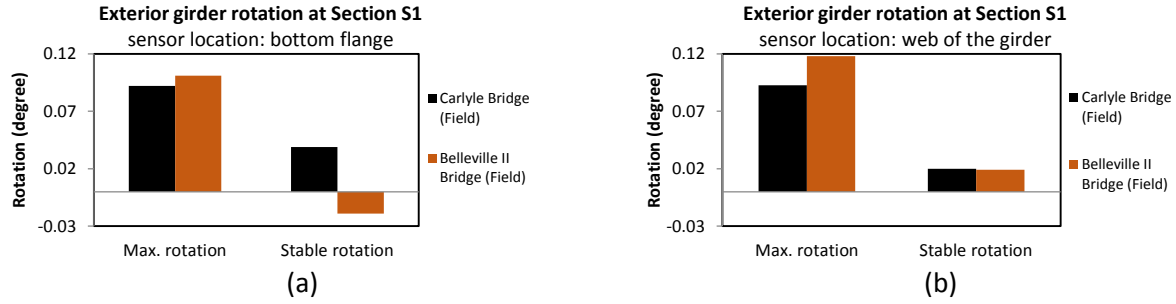


**Figure 3.16 Exterior girder rotation at Section S1 (Group 3).**

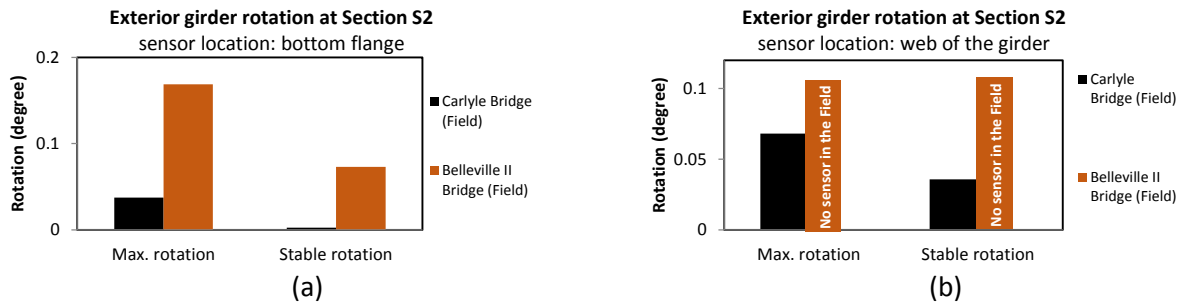


**Figure 3.17 Exterior girder rotation at Section S2 (Group 3).**

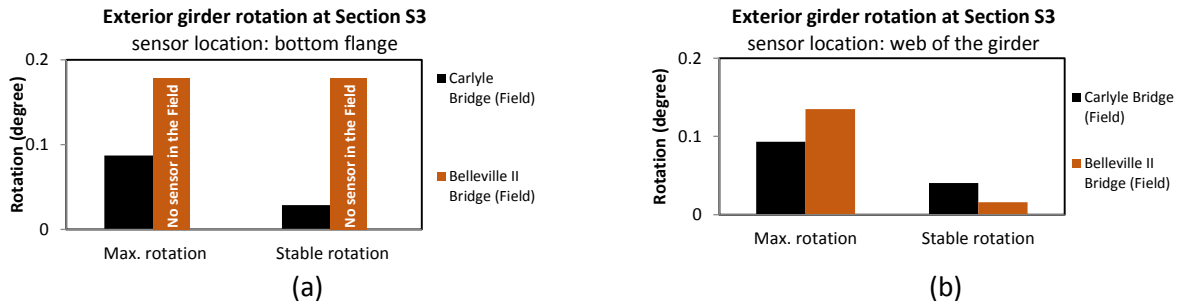


**Figure 3.18 Exterior girder rotation at Section S3 (Group 3).**



**Figure 3.19. Vibrating paving machine and the screed machine during construction.**

### **3.3.4 Group 4 Bridges**

#### *3.3.4.1 Instrumentation Plan*

There was only one bridge (concrete girder bridge) instrumented in this group. Sections for instrumentation are described in Table B.5 (Appendix B), with section locations overlaid on bridge plans, shown in Figure B.7 (Appendix B). Locations of the sensors are shown in Figure 3.2.

#### *3.3.4.2 Field Data Collected on Girder Rotation*

The tie bars (bracing bars) were different in this bridge from the other bridges. The tie bars were horizontal and connected from the exterior girder to the first interior girder, as shown in Figure 3.20. There was a smaller chance to observe sagging in this type of transverse tie bars because of their short length (approximately 3 ft.), as shown in Figure 3.20. Error in tightening tie bars can be reduced using this type of tie because there is much less interference with other bars. From a constructability standpoint, this bracing system appears to offer a viable alternative to the traditional system that spans across the entire bridge.

The field rotation data for the exterior girder indicated that rotation in the exterior girders was nearly rigid body rotation. In the case of Section S1 (shown in Figure 3.21), two important points can be noticed: (1) the maximum rotation was very small ( $0.059^\circ$ ) in both the bottom flange and the web, and (2) the exterior girder rotated as a rigid body. This phenomenon can result from the presence of properly tightened tie bars and the large rotational stiffness of the concrete girders.

Similar behavior can be seen in Sections S2 and S3, as shown Figures 3.22 and 3.23, respectively. In Section S2, the maximum and stable rotations were  $0.05^\circ$  and  $0.02^\circ$  at the bottom flange and web, respectively.



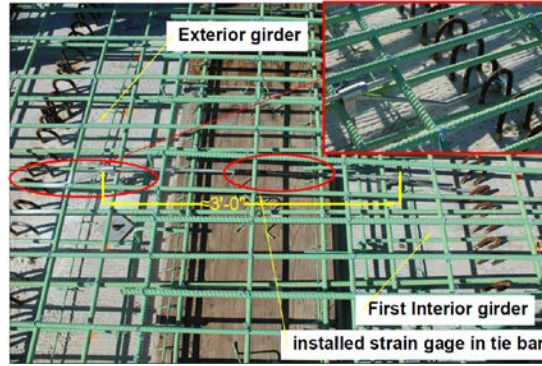
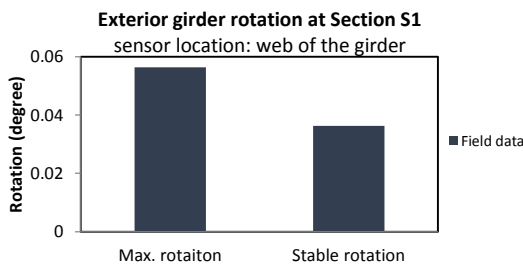
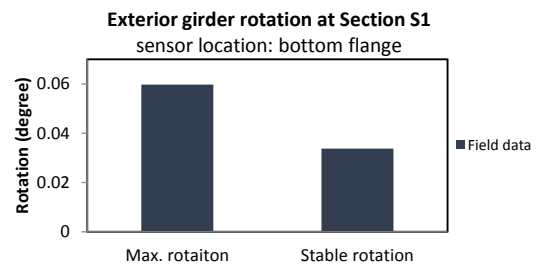


**Figure 3.20 Transverse tie bars in concrete girder bridge.**

At Section S3, the maximum rotation was  $0.07^\circ$  at both the bottom flange and the web of the exterior girder. The maximum rotation was small compared with the steel girder bridges and showed rigid body rotation in the field during construction.

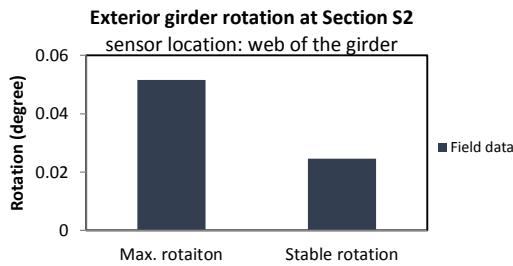


(a)

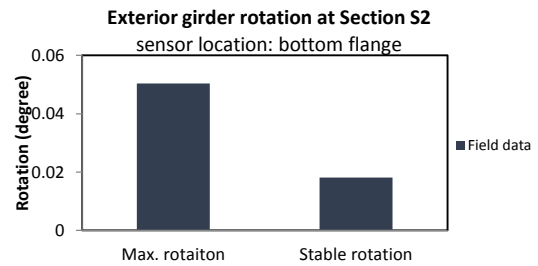


(b)

**Figure 3.21 Exterior girder rotation at Section S1 (Group 4).**



(a)



(b)

**Figure 3.22 Exterior girder rotation at Section S2 (Group 4).**

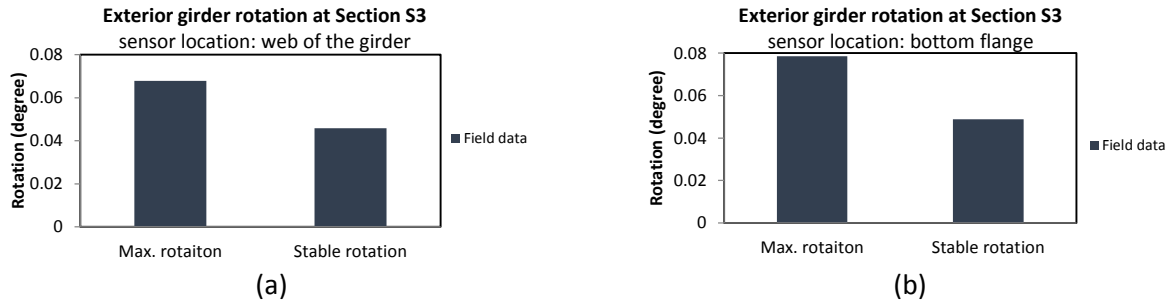


**Figure 3.23 Exterior girder rotation at Section S3 (Group 4).**

### 3.3.4.3 Field Data Collected on Tie Bar Stress/Strain

As shown Figure 3.24, the average maximum strain (stress) in the tie bars during construction was  $72 \mu\epsilon$  (2.1 ksi), and the stable strain (stress) was  $53 \mu\epsilon$  (1.5 ksi).

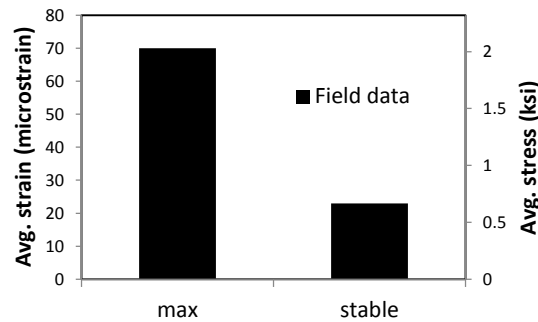


**Figure 3.24 Field-monitored average stress/strain in tie bars.**

## 3.4 FINITE ELEMENT ANALYSIS

### 3.4.1 Finite Element Modeling

Finite element models were built using the comprehensive FEA software Abaqus/CAE and validated using the data collected in the field. Figure 3.25 shows the full-scale FE model for the Highland bridge, which was built using the actual plan dimensions. In Abaqus, the bridge girders and diaphragms were modeled using shell elements. The bracing bars (diagonal tie bars and transverse tie bars) were modeled using a linear truss element, and a beam element was used to model the steel brackets used with the overhang deck. In the case of diagonal bracing bars, the angle of the hangers (usually  $45^\circ$  in the field) and the actual angle of the diagonal bracing bars were not same. To force adjust those angles, the diagonal bracing bars were bent in the field, as shown in Figure 3.26a. Bending of the diagonal bracing bars allowed the exterior girders to rotate freely some distance during construction prior to being fully mobilized. On the other hand, the transverse tie bars were affected by sagging (as shown in Figure 3.26) as a result of interference from other reinforcements, self-weight, and improper tightening, which can result in additional slack in the bars. In the FE study, a nonlinear link element (translator) was used with a gap to simulate the actual condition (as shown in Figure 3.26) of the diagonal and transverse bracing bars in the field. The  $4 \times 4$  in. timber blocks were assumed to be improperly shimmed because of the fillet at the corner of the web and bottom flange, as shown in

Figure 3.26, as well as other observations in the field. A truss element was used to represent the timber blocks with nonlinear translator links to simulate the gap between the timber block and the girder web. Surface-to-surface tie connections were assigned to connect the diaphragms/cross frames to girders.

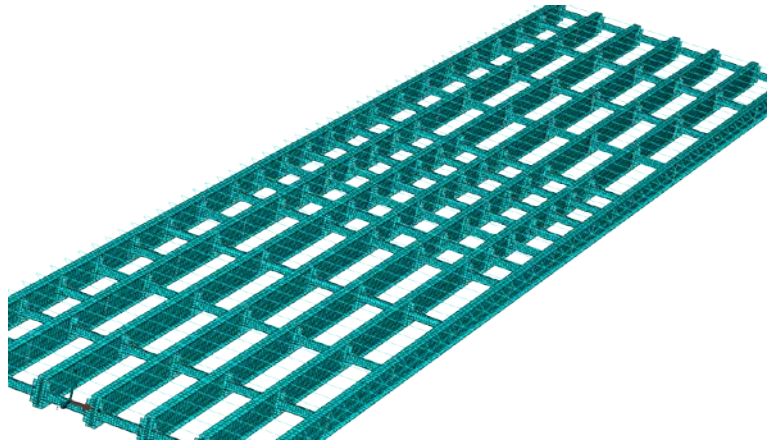


**Figure 3.25. Finite element model for Highland bridge.**

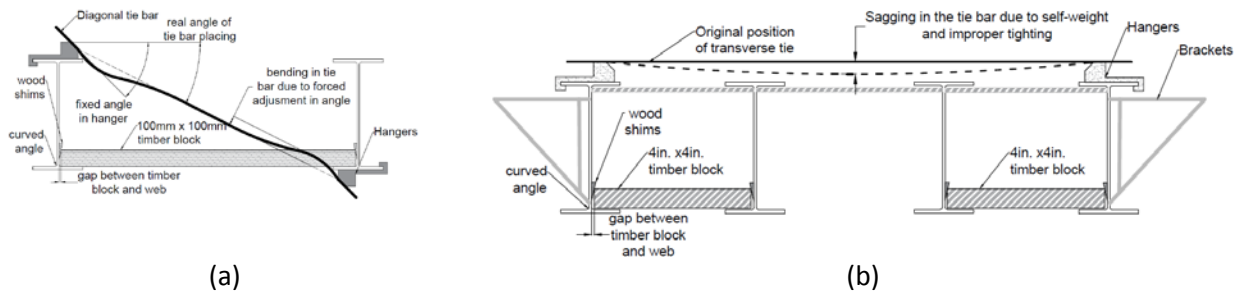


**Figure 3.26. Possible deviations that can introduce more girder rotation.**

The plastic concrete weight was divided based on the tributary area of the girder and then distributed over the surface area of the top flange of the girders. The deck overhang load was placed on the steel brackets. Different types of screed/paving machines (vibrating bridge paver, Bidwell M-3600, Gomaco C450, etc.) were used during construction with the weight, depending on the actual screed used as well as the width of the deck. The application of the loads depended on the section under consideration (sections defined in the field instrumentation plan as shown in Appendix B). For example, in the case of Section S1, to get the “maximum rotation,” the loads (concrete loads, screed, and overhang loads) were applied up to Section S1 from the start of concrete placement. On the other hand, only the weight of the fresh concrete was applied to the full span of the bridge to determine the “stable rotation.” Boundary conditions were assigned to simulate a continuous three-span bridge.

## 3.4.2 Material Modeling

### 3.4.2.1 Steel

Material properties for the steel used for modeling in Abaqus are shown in Table 3.2 (CEN 1995).

**Table 3.2 Material Properties of Steel**

Modulus of elasticity	E = 29000 ksi
Poisson's ratio in elastic stage	$\nu = 0.3$

### 3.4.2.2 Timber Blocks

The material properties of timber blocks were assigned in Abaqus and are shown in Table 3.3(CEN 1995).

**Table 3.3 Material Properties of Timber Blocks**

Modulus of elasticity	E = 1300 ksi
Poisson's ratio in elastic stage	$\nu = 0.37$

### 3.4.2.3 Concrete

The unit weight of reinforced concrete was considered to be 150 lb/ft<sup>3</sup>.

## 3.4.3 Finite Element Analysis for Group 1 Bridges

### 3.4.3.1 Comparison of Field Data and Finite Element Analysis Results

A detailed comparison of the field data and the results of the FEA for all three bridges in Group 1 are shown in Figures 3.27 through 3.29.

For the bottom flange of the exterior girder (shown in Figure 3.27a) at Section S1, the maximum rotations obtained from the FEA were 8.8%, 9.4%, and 4.5% smaller than the field data collected for the Lincoln, Greenup, and Bloomington bridges, respectively. The stable rotation obtained from the FE analysis were 10.9%, 8.3%, and 13.4% larger than the rotation monitored from the field in the Lincoln, Greenup, and Bloomington bridges, respectively. For the web of the exterior girder (shown in Figure 3.27b), there was not a tilt sensor attached at the web of the Greenup bridge, but the rotation of the exterior girder was calculated using FEA. The maximum and stable rotations were found to be 0.65° and 0.37°, respectively. The calculated rotation of the Greenup bridge was slightly higher and likely a result of local deformation in the girder web. The calculated maximum rotation values for the Lincoln and Bloomington bridges were 2.0% higher and 4.4% smaller than the field data, respectively. The field data and FEA results were in satisfactory agreement for all three bridges at the bottom flange of the first interior girder (shown in Figure 3.27c). Rotational values in the first interior girder were much smaller than the values in the other sections, and the FEA matched the field data very well.

Exterior girder rotation at Section S2 is shown in Figure 3.28. The calculated maximum rotation at the bottom flange for the Lincoln and Greenup bridges were 5.9% and 7.9% higher than the field maximum rotation, respectively, whereas the field maximum rotation was 25% larger than the rotation obtained from the FEA for the Bloomington bridge. For stable rotation, the results achieved from the FE analysis were 8%, 30%, and 0.035% higher than the rotation measured in the field for the Lincoln, Bloomington, and Greenup bridges, respectively.

At Section S3 for all three bridges (as shown in Figure 3.29), the FEA results for the maximum rotations of the exterior girder of the Lincoln and Greenup bridges at the web location were 19.0% and 1.6% higher than the corresponding rotation obtained from the field, respectively, but the FE values of maximum rotation was 2.4% smaller than the field data in the case of the Bloomington bridge.

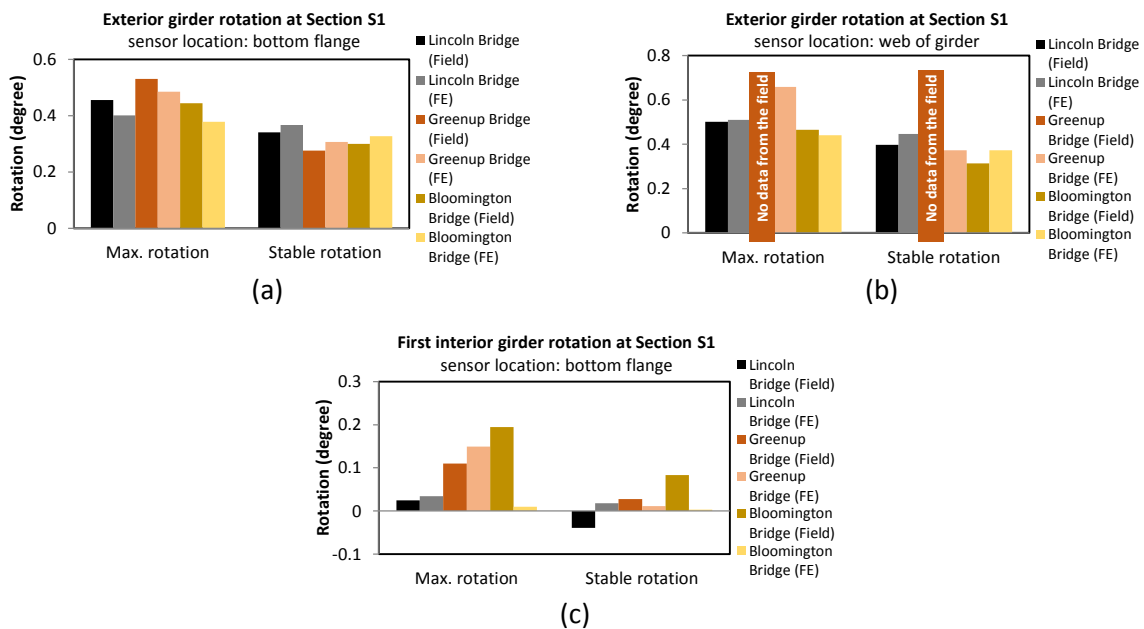


Figure 3.27 Comparison of field data and finite element analysis of Group 1 bridges at Section S1.

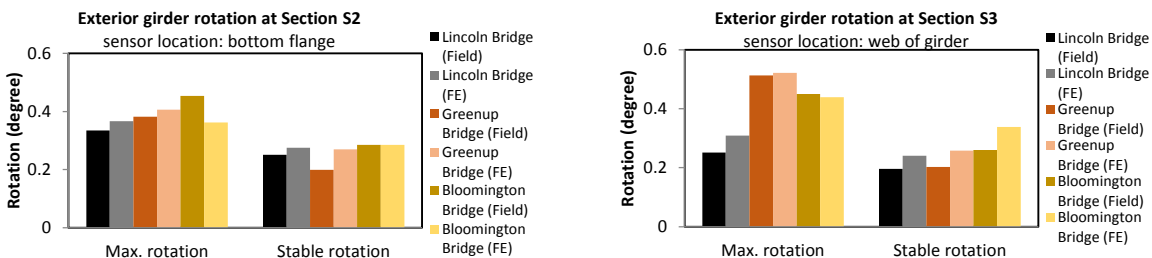
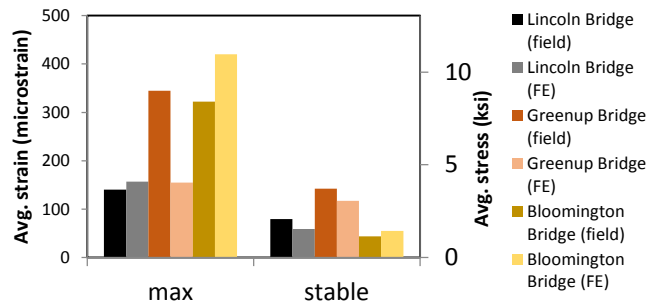


Figure 3.28 Comparison of field data and FEA of Group 1 bridges at Section S2.

Figure 3.29 Comparison of field data and FEA of Group 1 bridges at Section S3.

### 3.4.3.2 Comparison of Stress/Strain Values from Field Data and Finite Element Analysis Results

Comparison of the field data and the FEA results of stress/strain in the transverse tie bars is shown in Figure 3.30. A noticeable difference between the monitored average maximum strain/stress in the field and the results obtained from the FEA was observed for the Greenup Bridge. This observation could be a result of additional external loads applied to the deck system (screed load, workers stepping, weight of work bridge Terex work bridge, Gomaco work bridges, etc.) during deck placement. The stable strain/stress values from the field and the FEA results were in agreement following removal of the uncertain loads. Very small stresses were noticed in the diagonal tie bar in the Lincoln bridge, which demonstrated that initial bending in the tie bar decreased effectiveness.



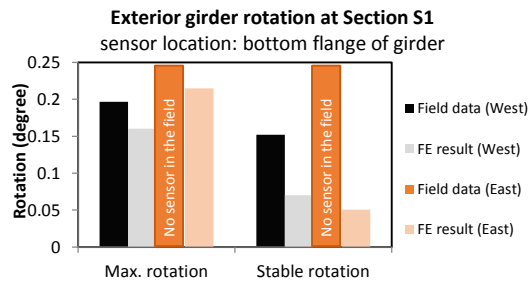
**Figure 3.30. Comparison of field data and FEA results for stress/strain in transverse tie bars.**

## 3.4.4 Finite Element Analysis for Group 2 Bridges

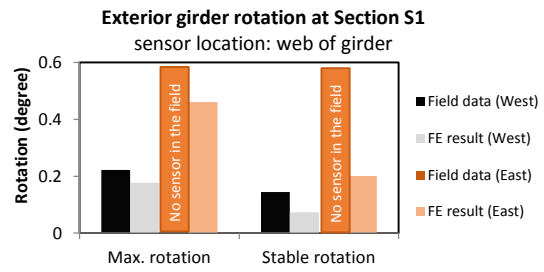
### 3.4.4.1 Comparison of Field Data and Finite Element Analysis Results for Girder Rotation

A detailed comparison of the field data and the results of the FEA for all three bridges of Group 2 is shown in Figures 3.31 through 3.33.

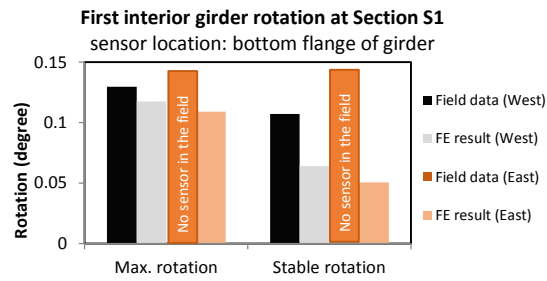
For the bottom flange of exterior girders at Section S1 (shown in Figure 3.31), the maximum rotation obtained from the FEA and the measured field data were similar ( $0.19^\circ$  to  $0.16^\circ$ , respectively), whereas the FEA results for stable rotation was approximately 50% lower than the field-monitored data. Because there was no tilt sensor installed on the east end of the bridge, the girder rotation was extrapolated from the FEA, and the maximum and stable girder rotations were found to be  $0.22^\circ$  and  $0.05^\circ$ , respectively. For the web of exterior girder at the west end, it can be seen that there is no big difference between field data and FEA results in terms of the maximum rotations ( $0.22^\circ$  and  $0.18^\circ$ , respectively) and the stable rotations ( $0.14^\circ$  and  $0.08^\circ$ , respectively). At the east end, the extrapolated maximum and stable rotations from the FEA were  $0.46^\circ$  and  $0.20^\circ$ , respectively, which were much higher than the rotations at the west end. The higher rotations in the web at the east end are due to the absence of the intermediate diaphragms. For the bottom flange of the first interior girder, the rotations were smaller than those of the exterior girder. At the west end, the maximum rotations in the field data and FEA results were similar, and in the case of stable rotations, the FEA and field monitored results were both small ( $0.06^\circ$  and  $0.10^\circ$ , respectively).



(a)

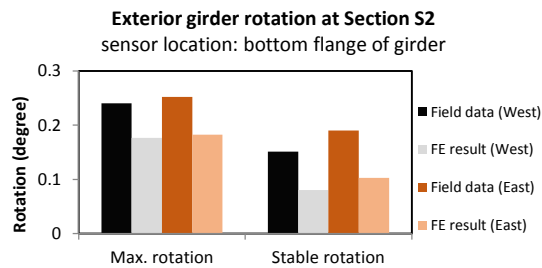


(b)

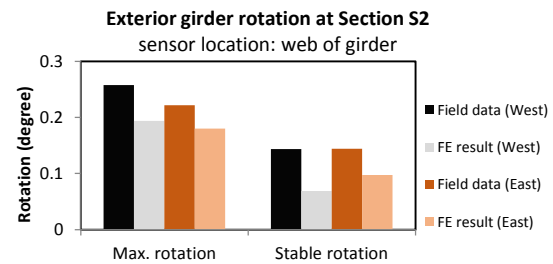


(c)

**Figure 3.31 Comparison of field data and FEA results for transverse rotations at Section S1.**



(a)



(b)

**Figure 3.32 Comparison of field data and FEA results for transverse rotations at Section S2.**

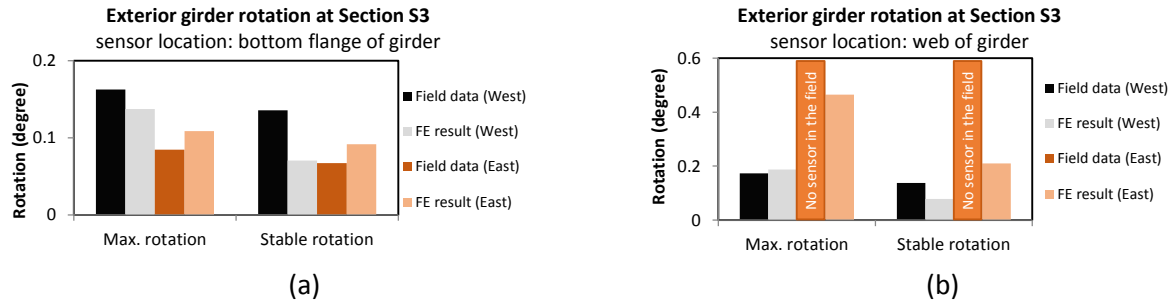


**Figure 3.33 Comparison of field data and FEA results for transverse rotations at Section S3.**

In Figure 3.32, a correlation is presented between the rotations from the field and the FEA at the bottom flange and at the web of the exterior girder at Section S2. Both the east and west ends of the bridge were instrumented with tilt sensors at two different locations, at the bottom flange and the web. For the bottom flange of the exterior girder, the maximum rotations from FEA for both the east and west ends were fairly similar ( $0.17^\circ$  and  $0.18^\circ$ , respectively) and reasonably close to the field data. The stable rotations at the west and east ends calculated from the FEA ( $0.07^\circ$  and  $0.10^\circ$ , respectively) were slightly smaller than the rotations monitored from the field ( $0.14^\circ$  and  $0.14^\circ$ , respectively). For the web of the exterior girder, the rotations from the FE analysis at the web nearly matched those at the bottom flange for both the east and west ends of the bridge, but the stable rotations were found to be 46.15% (west end) and 30.71% (east end) smaller than the rotations in the field. It can be seen that the exterior girders experienced nearly rigid body rotation, as shown in Figure 3.32.

Figure 3.33 presents the comparison of field data and FEA for transverse rotations at Section S3. For the bottom flange of the exterior girder, the maximum rotations from field data and the FEA results were in good agreement at both the east and west ends. In the west end, the field rotation was 14% higher than in the FEA, but the field rotation was 16% smaller than in the FEA for the east end. On the other hand, the calculated stable rotations from the FEA were around 46% smaller than the rotations from the field at the west end of the bridge. For the web of the exterior girder, both the field data and FEA results showed no significant difference in maximum rotations at the west end but with the stable rotations, the rotation achieved from FEA was 38% smaller than the monitored field rotation. At the east end of the bridge, there was no tilt sensor installed at the web location but the obtained FE maximum  $0.46^\circ$  and stable  $0.21^\circ$  rotations were even much bigger than the field rotations at the bottom flange. So, it can be deduced from Section S3 that the exterior girder at the west end experienced almost rigid body rotations, but in contrast, the exterior girder experienced differential rotations at the east end.

#### 3.4.4.2 Comparison of Stress/Strain Field Data and Finite Element Analysis Results

A comparison of the field data and FEA results for stress/strain in transverse tie bars is shown in Figure 3.34. It was observed that the monitored average maximum strain/stress in the field was 0.2% larger than the FEA results, and the average field stable rotation was 13% higher than found in the analysis.



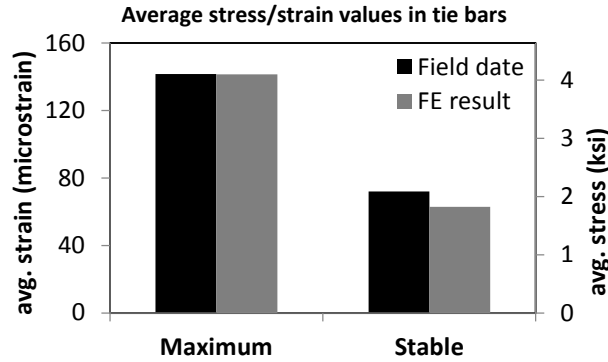


Figure 3.34 Comparison of field data and FE results for stress/strain in transverse tie bars.

### 3.4.5 Finite Element Analysis for Group 3 Bridges

#### 3.4.5.1 Comparison of Field Data and Finite Element Analysis Results

A detailed comparison of the field data and the results of the FE analysis for the two Group 3 bridges is shown in Figures 3.35 through 3.37. For the bottom flange (shown in Figure 3.35a) at Section S1, the FEA results of maximum rotations for the Carlyle and Belleville-II bridges were 33% smaller and 20% higher than the field results, respectively. The field data and FEA results of the stable rotations were in good agreement. For the web of the girder shown in Figure 3.35b, it was observed that the field maximum rotations (Carlyle bridge rotation = 0.09°, and Belleville II bridge rotation = 0.12°) were small and had a small difference with the results obtained from the FE analysis (Carlyle bridge rotation = 0.05° and Belleville II bridge rotation = 0.16°) for the Carlyle and Belleville-II bridges. The results obtained from the field data and the FE analyses for stable rotations were similar.

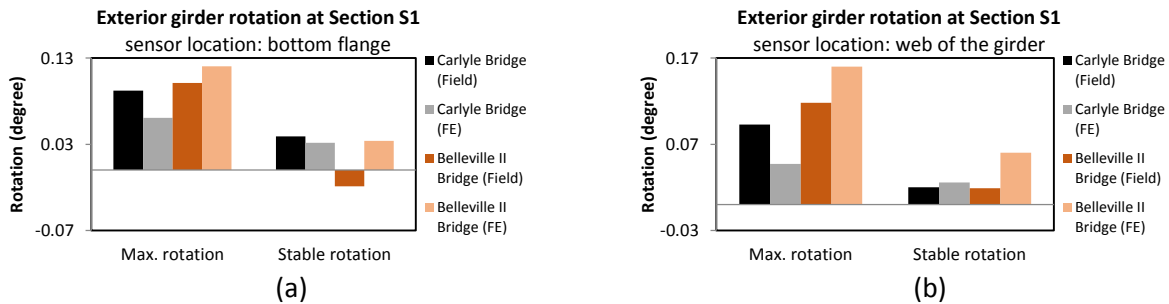
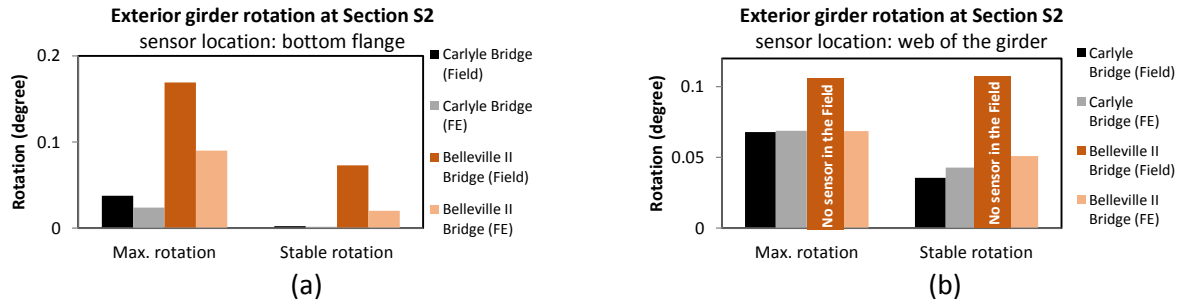
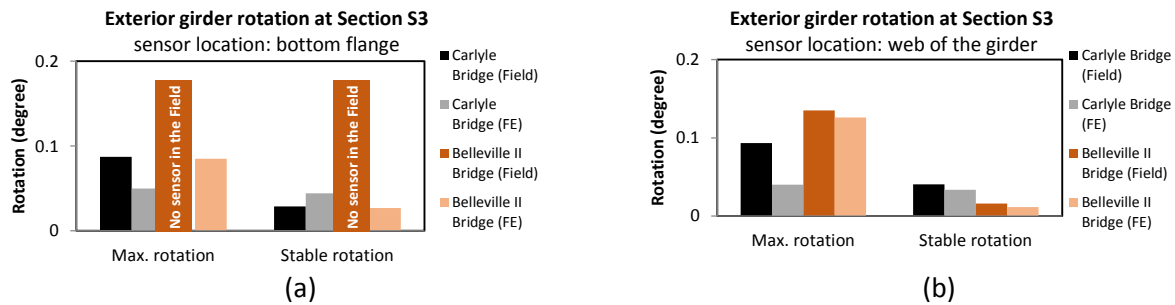


Figure 3.35 Comparison of field data and FEA results for transverse rotations at Section S1.



**Figure 3.36 Comparison of field data and FEA results for transverse rotations at Section S2.**



**Figure 3.37 Comparison of field data and FEA results for transverse rotations at Section S3.**

The bottom flange of the exterior girder at Section S2 is shown Figure 3.36. The maximum rotations obtained from the FEA of the Carlyle (0.03°) and Belleville-II (0.09°) bridges were similar and only slightly smaller than field monitored rotations (Carlyle: 0.04° and Belleville II: 0.16°). The stable rotation obtained from the field and FE analysis were nearly zero for the Carlyle bridge, but the field stable rotation was slightly higher than the FE analysis in the case of the Belleville-II bridge. For the web of the girder at the same Section S2, both the maximum and stable rotations of the Carlyle bridge were in good agreement when comparing the FE analysis and field data. A tilt sensor was not installed in the field at the web for Section S2, so the maximum and stable rotation of exterior girders were calculated using FE analysis, resulting in 0.07° and 0.05°, respectively.

Figure 3.37 presents a comparison of field data and FEA results for transverse exterior girder rotations at Section S3. A tilt sensor was not installed on the bottom flange for the Belleville-II bridge, but in examining Figure 3.37a, it can be seen that for the Carlyle bridge, rotations were comparatively small for both the maximum and stable rotations. For the girder web, the calculated maximum rotation for the Carlyle (0.04°) and Belleville-II (0.12°) bridges were found to be slightly smaller than the field rotation (Carlyle bridge rotation = 0.09° and Belleville-II bridge rotation = 0.13°). The stable rotations observed from field data and FE analysis in both of the bridges were negligibly small.

### 3.4.6 Finite Element Analysis for Group 4 Bridges

#### 3.4.6.1 Comparison of Field Data and Finite Element Analysis Results

This group consists of a single concrete girder bridge where tie bars connect the exterior girder to the first interior girder. In the FE analysis, because the bars were too short to have any measurable

sagging and the connection between the tie bars and the girders easily tightened (as shown in Figure 3.20), a gap element was not assigned while connecting the tie bars to the girders.

Figures 3.38 through 3.40 show the field exterior rotation and FEA results at the predefined sections. Figure 3.38 shows that the difference between the field and the FE rotations were negligibly small and in good agreement. For the bottom flange at Section S1, the girder web rotations measured in the field were about 25% higher than the rotation obtained from FE analysis.

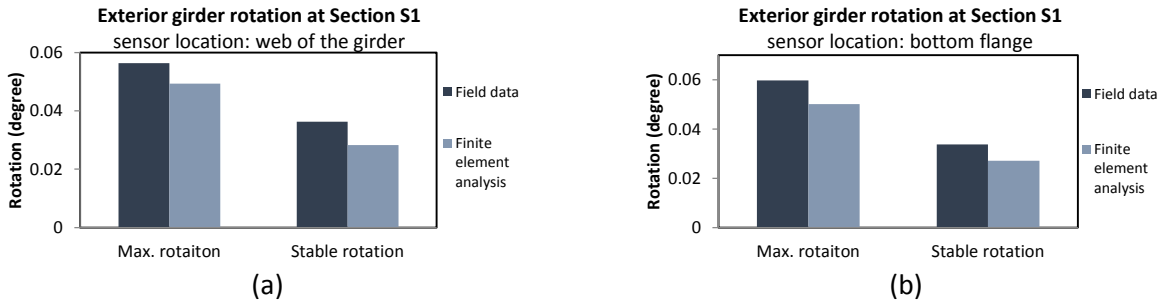


**Figure 3.38 Comparison of field data and FEA results for rotations at Section S1.**

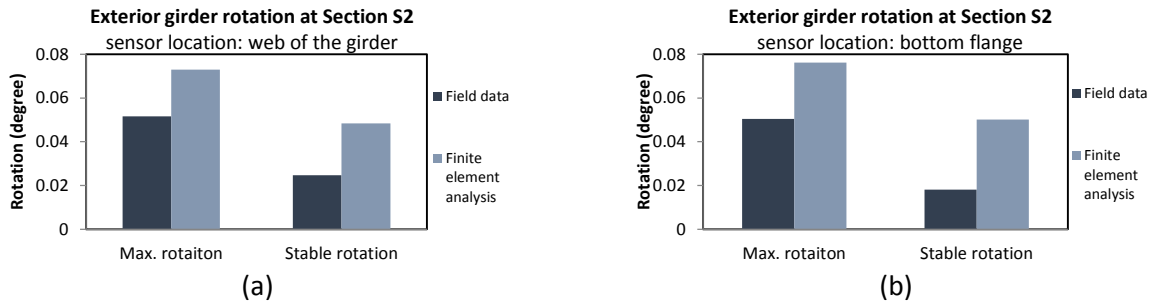


**Figure 3.39 Comparison of field data and FEA results for rotations at Section S2.**

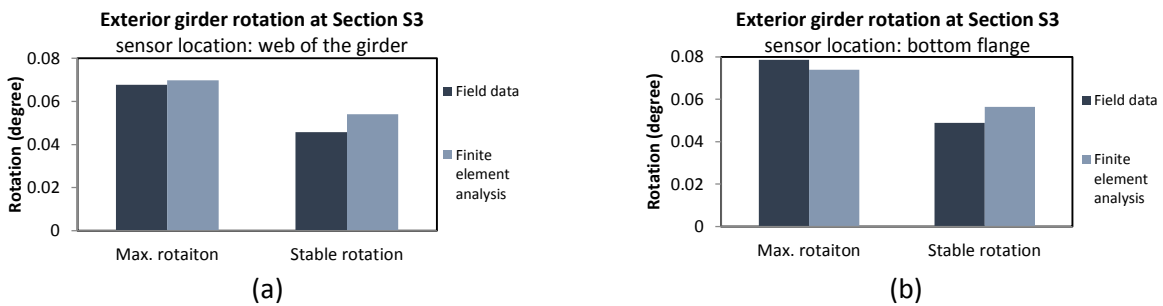


**Figure 3.40 Comparison of field data and FEA results for rotations at Section S3.**

In case of Section S2 shown in Figure 3.39, the FEA results were slightly higher than those of the measured field data but were still negligibly small. A similar observation was noticed at Section S3, as shown in Figure 3.40.

### 3.4.6.2 Comparison of Stress/Strain Values from Field Data and Finite Element Analysis Results

A comparison of field data and FEA results for stress/strain in transverse tie bars is shown in Figure 3.41. The monitored average maximum strain and stress in the field was 32% larger than the FEA results, but the average field stable rotation was 43% smaller than the FEA results. These inconsistencies are likely a result of difficulties in modeling the exact construction loading that occurred during deck placement at the location of these gages.

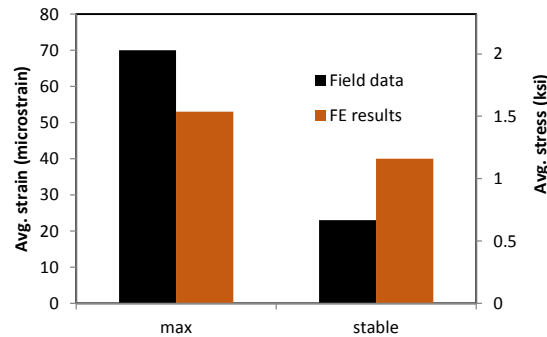


**Figure 3.41 Comparison of field data and FEA results for stress/strain in transverse tie bars.**

### 3.5 EFFECT OF B/D RATIO IN EXTERIOR GIRDER ROTATION

The ratio of the distance between diaphragms (B) in exterior panels to the girder depth (D) has a significant effect on exterior girder rotation (Figure 3.42).

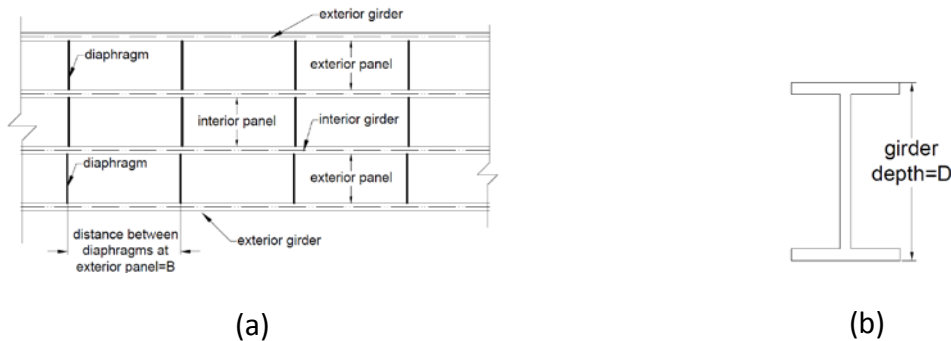


**Figure 3.42 (a) definition of B, and (b) definition of D.**

The Kansas Department of Transportation (KDOT) has a limit of  $1.0^\circ$  (Roddis et al. 2006) for exterior girder rotation. In contrast, instead of limiting exterior girder rotation directly, IDOT limits the vertical deflection of the tip of deck overhang. In the current study, the maximum vertical displacement ( $\Delta$ ) of the overhang was limited to  $3/16$  in., as recommended by IDOT (Figure 3.43), and the subsequent rotation ( $\theta$ ) of the exterior girder to create that displacement was treated as the limit. The overall comparison of the exterior girder rotation among all bridges is shown in Figure 3.44 (based on IDOT's

limit). Figure 3.44 also shows the effect of the diaphragm (permanent bracing) spacing (B) to girder depth (D) ratio (B/D). Only three bridges—Greenup, Bloomington, and Lincoln—exceeded the limit.

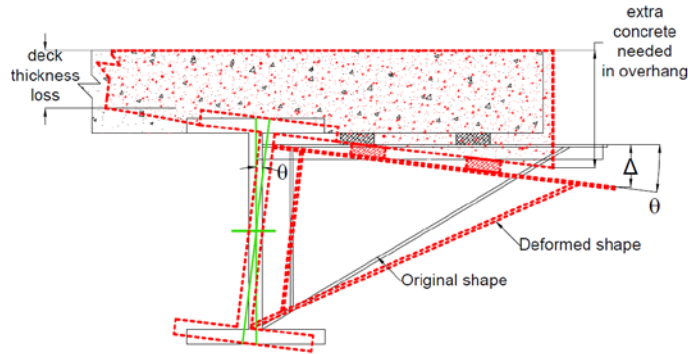


**Figure 3.43 Maximum overhang displacement (3/16 in.) during construction (suggested by IDOT).**

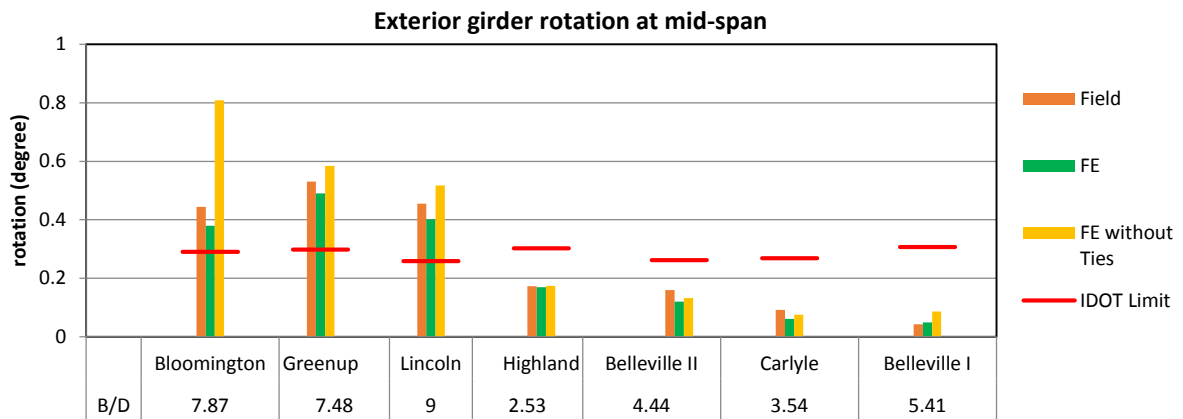


**Figure 3.44 Comparison of rotational values among all bridges.**

On the basis of that data in Figure 3.44, it appears clear that exterior girder rotations largely depend on B/D ratio.

## CHAPTER 4: EVALUATION AND ASSESSMENT OF TORSIONAL ANALYSIS OF EXTERIOR GIRDERS (TAEG) PROGRAM

One method commonly used by bridge designers and contractors to assess the potential for rotation of exterior bridge girders during construction is a program called Torsional Analysis of Exterior Girders (TAEG), developed by the University of Kansas and the Kansas Department of Transportation.

The program requires several inputs related to bridge geometry and supports to perform the analysis and calculate results:

- Geometric properties of the exterior girders, including the dimensions of the flanges and webs and the grade of the steel.
- Spacing and number of main girders, the spacing between permanent lateral supports, span lengths, and information related to the continuity of tie bars and timber blocks over the width of the bridge.
- Permanent lateral supports, including the dimensions and geometry of the diaphragms or cross frames and connection details.
- Temporary lateral supports, specifically tie bars and timber blocks. The program requires the number of temporary lateral supports spaced between permanent lateral supports, how they are spaced, and their cross-sectional areas.
- The geometry of the overhang brackets, the loads from the screed and finishing machine, and the unit weight of plastic concrete.

The main advantage of the TAEG program is the quick prediction of exterior girder rotation using a simplified approach. To calculate rotations, the TAEG program uses the simplified flexure analogy which also introduces a considerable amount of limitations. A comprehensive description of the program and its assumptions for analyzing bridges is presented in Appendix C. This chapter presents a comparison of the rotation obtained from the TAEG program to those measured in the field. A major factor affecting the field results was the effectiveness of the installed rotation prevention systems in the field. This undoubtedly resulted in differences as the program assumes an ideal installation.

### 4.1 TAEG RESULTS AND DISCUSSION

The rotation results from TAEG are presented with the percentage error compared with field rotation values for the bottom flange of the exterior girder when the screed was located at midspan. For each of the bridges, multiple temporary lateral support arrangements were input into the program and the results were obtained. The phrase “transverse tie bar” (or “tie bar”) is abbreviated as TT and “timber block” is abbreviated as TB in the data tables. For the Bloomington bridge, the results using the equivalent cross-sectional area had a noticeable difference, underestimating the rotation value by 38.7% compared with the rotation measured in the field. The results from using two standard-size tie bars and timber blocks in addition to one standard-size tie bar and timber block placed at the center

between diaphragms were reasonable, underestimating and overestimating rotation by only 3.5% and 5.9%, respectively. The results for all other conditions had a much higher error—consistently in excess of 30%, as shown in Table 4.1.

For the Greenup bridge, the results using the equivalent cross-sectional area had a noticeable discrepancy, underestimating the field value by 55.3%. The exterior girder rotation using two standard-size tie bars and timber blocks in addition to one standard-size tie bar and timber block placed between diaphragms was improved, but it still underestimated rotation by 29.9% and 11.2%, respectively. The results for the other conditions evaluated demonstrated much higher error, consistently registering well over 45%. The trend in the percentage error across the temporary lateral support arrangement was similar to that of the Bloomington bridge, which was most likely due to the similar size of the exterior girders, overhang width, and screed load. The full results of the TAEG program, the field-measured values that were used for comparison, and the corresponding percentage errors are shown in Table 4.2.

**Table 4.1 Bloomington Bridge**

	Rotation (°)	Percentage Error
Field Value	0.443	
Full or Equivalent Cross-Sectional Areas	0.272	-38.7
3 TT/TB	0.313	-29.5
2 TT/TB	0.428	-3.5
No TB and Full TT	1.848	316.5
No TT and Full TB	1.705	284.3
1 TB and 1 TT (Center)	0.47	5.9
No TB or TT	3.068	591.5

**Table 4.2 Greenup Bridge**

	Rotation (°)	Percentage Error
Field Value	0.530	
Full or Equivalent Cross-Sectional Areas	0.237	-55.3
3 TT/TB	0.271	-48.9
2 TT/TB	0.372	-29.9
No TB and Full TT	1.653	211.7
No TT and Full TB	1.535	189.4
1 TB and 1 TT (Center)	0.471	-11.2
No TB or TT	2.99	463.7

For the Carlyle bridge, the output of TAEG using the equivalent cross-sectional area demonstrated much smaller error—overestimating field-measured rotations by only 5.3%. The results using three standard-sized tie bars and timber blocks also differed slightly from the field value, resulting in a value 15.1% higher than the corresponding measured value in the field. The other conditions evaluated demonstrated noticeable uncertainty, as shown in Table 4.3, though the rotations were much closer to the field results than the results obtained for the Bloomington and Greenup bridges. This can be attributed to the greater depth of the girders used in the Carlyle bridge, which made the tie bars and timber blocks less effective in resisting the torsional moments caused by the construction equipment and therefore drawing less force compared with what was observed in the previous two bridges.

For the Lincoln bridge, the output of TAEG for the equivalent cross-sectional area demonstrated significant difference, underestimating the field value by 75.8%. None of the cases in the Lincoln bridge yielded reasonably close results, with the closest one underestimating the field value by 38.5%

when one standard-size tie bar and timber block was placed directly between permanent lateral supports. The summary of results is shown in Table 4.4.

**Table 4.3 Carlyle Bridge**

	Rotation (°)	Percentage Error
Field Value	0.092	
Full or Equivalent Cross-Sectional Areas	0.097	5.3
3 TT/TB	0.106	15.1
2 TT/TB	0.117	27.1
No TB and Full TT	0.121	31.4
1 TB and 1 TT (Center)	0.182	97.7
No TB or TT	0.127	37.9

**Table 4.4 Lincoln Bridge**

	Rotation (°)	Percentage Error
Field Value	0.455	-75.8
Full or Equivalent Cross-Sectional Areas	0.110	-63.3
3 TT/TB	0.167	-49.9
2 TT/TB	0.228	155.7
No TB and Full TT	1.163	142.5
1 TB and 1 TT (Center)	1.103	-38.5
No TB or TT	0.280	375.5

For the Highland bridge, the TAEG outputs consistently underestimated the rotation experienced in the field for both the short spacing and the longer spacing of permanent lateral supports. When the diaphragms were placed at the shorter spacing, an equivalent cross-sectional area was not necessary because two tie bars and timber blocks satisfied the 48-in. spacing requirement. This case yielded a significant underestimation of the rotation of 50.8% compared with the field value. The best estimation of the rotation of the shorter spacing scenario was achieved when the timber blocks were excluded from the model, giving a percentage difference of 29.4% below the measured field rotation.

The results were improved when the model was run with the longer spacing with the closest value underestimating the rotation measured in the field by 11.4% and when the timber blocks were excluded. The results for the Highland bridge were somewhat unexpected, given the uniformity of the diaphragm spacing, which was expected to improve the simplified analysis and translated well to the TAEG input parameters. A summary of the TAEG results, field values that were used for comparison, and the corresponding percent errors are shown in Table 4.5 for the short spacing of permanent lateral supports and in Table 4.6 for the longer spacing between permanent lateral supports.

**Table 4.5 Highland Bridge with Short Diaphragm Spacing**

	Rotation (°)	Percentage Error
Field Value	0.173	
Full or Equivalent Cross-Sectional Areas	0.085	-50.8
2 TT/TB	0.085	-50.8
No TB and Full TT	0.122	-29.4
No TT and Full TB	0.251	45.3
1 TB and 1 TT (Center)	0.111	-35.8
No TB or TT	0.368	113.0

**Table 4.6 Highland Bridge with Long Diaphragm Spacing**

	Rotation (°)	Percentage Error
Field Value	0.510	
Full or Equivalent Cross-Sectional Areas	0.160	-68.6
3 TT/TB	0.192	-62.4
2 TT/TB	0.240	-52.9
No TB and Full TT	0.452	-11.4
No TT and Full TB	0.447	-12.4
1 TB and 1 TT (Center)	0.300	-41.2



## 4.2 THE MODIFIED ANALYSIS METHOD (AVERAGE LATERAL SUPPORT SPACING)

Because the program limits the analysis to include only one spacing of the permanent lateral supports, an alternative was investigated by assuming a modified value for the spacing between the permanent lateral supports. Because all of the bridges analyzed during this project included varying spacing of the diaphragms or cross frames, this seemed to be a possible source of error for all of the analysis cases. For each of the bridges analyzed, an average spacing was calculated and then input into the program. For all cases where the average spacing was used, three cases were evaluated—including one, two, and three standard-size tie bars and timber blocks spaced evenly between the permanent lateral supports. Each of these scenarios was performed and compared with the field results to determine whether this method improved the accuracy.

The values used for the lateral support spacing are shown in Table 4.7. These values were calculated based on the actual average spacing of the diaphragms within the span being analyzed.

**Table 4.7 Average Lateral Support Spacing Used for Each Bridge**

	Lateral Support Spacing (in)
Highland	120
Carlyle	241
Lincoln	221
Bloomington	208
Greenup	208

Table 4.8 shows the results from the analysis when the three standard-size tie bars and timber blocks were placed evenly between the permanent lateral supports. The results for this setup were fairly inconsistent, with the Carlyle bridge having the most accurate output at a calculated value 19.6% below the corresponding field rotation value. Table 4.9 shows the results when two standard-size tie bars and timber blocks were placed evenly between the permanent lateral supports, which were spaced at the average lateral support spacing shown in Table 4.7. The results for this setup were better than those of the three tie bar and timber block setup, with two bridges being within 20% of the field value.

**Table 4.8 Rotations Using Average Lateral Support Spacing with Three Tie Bars and Timber Blocks Used**

	Rotation (°)	Percent Error (%)
Highland	0.058	-66.4
Carlyle	0.074	-19.6
Lincoln	0.158	-65.3
Bloomington	0.275	-38.0
Greenup	0.273	-48.5

**Table 4.9 Rotations Using Average Lateral Support Spacing with Two Tie Bars and Timber Blocks Used**

	Rotation (°)	Percent Error (%)
Highland	0.068	-60.6
Carlyle	0.08	-13.1
Lincoln	0.207	-4.5
Bloomington	0.366	-17.5
Greenup	0.375	-29.3

The results when one standard-size tie bar and timber block are centered between the permanent lateral supports are shown in Table 4.10. This assumed configuration improved the results compared with the previous two setups, with three bridges being within approximately 10% of the field value.

The results from the cases where the number and spacing of temporary lateral supports were the same as the number and spacing arrangement used in the equivalent cross-sectional area method did not show overall improvement, with only two cases yielding error within 20% compared with the field value. These results are shown in Table 4.11.

**Table 4.10 Rotations Using Average Lateral Support Spacing with One Tie Bar and Timber Block Used**

	Rotation (°)	Percent Error (%)
Highland	0.082	-52.5
Carlyle	0.087	-5.5
Lincoln	0.249	-45.3
Bloomington	0.458	3.2
Greenup	0.474	-10.6

**Table 4.11 Rotations Using Average Lateral Support Spacing When Lateral Support Configuration Was the Same as the Equivalent Cross-Sectional Area Method**

	Rotation (°)	Percent Error (%)
Highland	0.068	-60.6
Carlyle	0.074	-19.6
Lincoln	0.158	-65.3
Bloomington	0.366	-17.5
Greenup	0.375	-29.3

Using an average spacing of the permanent lateral supports did not seem to improve the ability of the TAEG program to accurately predict the rotation of the exterior girder during placement of the concrete deck. In most circumstances, the program continued to underestimate the rotation expected during construction. As in the previous analysis of bridges, this was likely due to the assumption that the tie bars and timber blocks are fully effective. Because this full engagement does not accurately represent what is experienced in the field, it could account for the program consistently underestimating the rotation of the exterior girders.

### 4.3 TREND ANALYSIS

Because the previous two analysis methods did not yield good agreement between the field data and the TAEG software, the next step in the evaluation of TAEG was assessing whether any trends existed among all bridges. The trend analysis might help to predict how accurate the program's results would be under certain circumstances. Multiple parameters were investigated and compared with the measured data. Assessing these trends was performed in two parts: first using the equivalent cross-sectional area method, and second, using the lateral support standard size, which resulted in the same number of tie bars and timber blocks when using the equivalent cross-sectional area.

Table 4.12 shows the results of parametric study based on the equivalent cross-sectional area and Table 4.13 shows the results of the rotational stiffness when the equivalent cross-sectional area was used. The flange thickness, flange width, girder depth, web thickness, girder cross-sectional area,

girder spacing, and rotational stiffness of the exterior girder were investigated as key factors. The difference in the calculation of the stiffnesses was based on  $L$ , the span length over which the rotation was measured. This length is shown in Equation 4.2 (see Section 4.4 of this report), which was used to calculate the rotational stiffness. The span stiffness  $K_{span}$  represents the torsional stiffness across the entire bridge span. The stiffness between diaphragms  $K_{middle}$  represents the torsional stiffness across the distance between diaphragms at the center spacing of the permanent lateral supports. The span distances for these two rotational stiffness values are shown in Figure 4.1.  $K_{average}$  represents the torsional stiffness with the average spacing for the permanent lateral support that was previously calculated. The equations for calculating the rotational stiffness and the polar moment of inertia for a steel I-shaped beam are shown in Equations 4.1 and 4.2 (see Section 4.4 of this report).

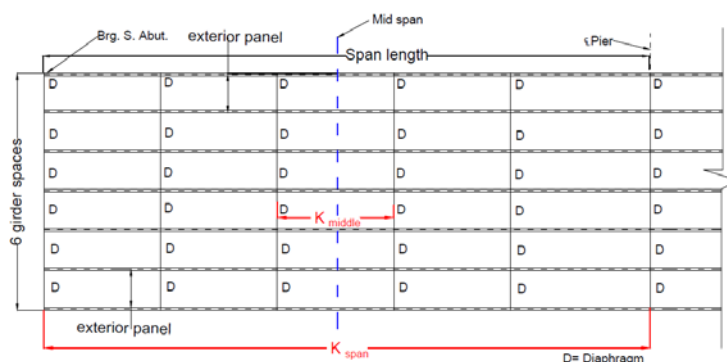


Figure 4.1 Procedure for calculating stiffness in a span.

Table 4.12 Results of Parametric Analysis Using Equivalent Cross-Sectional Area

Bridge Name	Percentage of Field Value	Flange Thickness (in.)	Flange Width (in.)	Girder Depth (in.)	Web Thickness (in.)	Girder Cross-Sectional Area (in. <sup>2</sup> )	Girder Spacing (in.)
Lincoln	-75.82	1.00	10.5	32.3	0.615	39.63	87
Greenup	-55.32	0.67	10.5	29.6	0.522	28.79	76
Highland	-50.80	0.75	16.0	49.5	0.500	48.00	88
Bloomington	-38.70	0.93	10.5	30.2	0.585	36.11	84
Carlyle	5.34	0.31	24.0	78.6	0.250	34.38	78

Table 4.13 Results of Rotational Stiffness Parametric Analysis Using Equivalent Cross-Sectional Area

Bridge Name	Percentage of Field Value	Span Length (in.)	$K_{span}$ (kip-in.)	$K_{middle}$ (kip-in.)	$K_{weighted}$ (kip-in.)
Lincoln	-75.82	642	174.13	414.05	505.22
Greenup	-55.32	621	63.71	191.14	190.34
Highland	-50.80	1398	53.97	579.83	626.28
Bloomington	-38.70	972	94.54	389.39	441.98
Carlyle	5.34	1200	8.53	43.75	42.43

Using the equivalent cross-sectional area method, none of the parameters investigated predicted reasonable results, meaning that there was no correlation between the magnitude of any parameter and the percentage error of the TAEG results compared with the field value. The only parameter that did seem to nearly predict the close value of the girder rotation was the stiffness of the girder over the span, with the Bloomington bridge being the only bridge lying outside of the trend. Overall, the stiffness of the exterior beam did not seem to have a significant effect on the accuracy of these results. For the case of the standard-size temporary bracing, the results of the girder key factors are shown in Table 4.14, and the results from assessing the rotational stiffness of the bridges compared with measured values from the field are shown in Table 4.15.

**Table 4.14 Results of Parametric Analysis Using Standard-Size Temporary Lateral Support**

Bridge Name	Percentage of Field Value	Flange Thickness (in.)	Flange Width (in.)	Girder Depth (in.)	Web Thickness (in.)	Girder Area (in <sup>2</sup> )	Girder Spacing (in.)
Highland	-73.95	0.75	16.0	49.5	0.500	48.00	88
Lincoln	-64.61	1.00	10.5	32.3	0.615	39.63	87
Carlyle	-64.16	0.31	24.0	78.62	0.250	34.38	78
Greenup	-33.26	0.67	10.5	29.64	0.522	28.79	76
Bloomington	-3.54	0.93	10.5	30.2	0.585	36.11	84

**Table 4.15 Results of Rotational Stiffness Parametric Analysis Using Standard-Size Temporary Lateral Support**

Bridge Name	Percentage of Field Value	Span Length (in.)	K <sub>span</sub> (kip-in)	K <sub>middle</sub> (kip-in)	K <sub>weighted</sub> (kip-in)
Highland	-73.95	1398	53.97	579.83	626.28
Lincoln	-64.61	642	174.13	414.05	505.22
Carlyle	-64.16	1200	8.53	43.75	42.43
Greenup	-33.26	621	63.71	191.14	190.34
Bloomington	-3.54	972	94.54	389.39	441.98

As was the case with the equivalent cross-sectional area, the key parameters that were considered did not have a significant effect in the prediction of exterior girder rotation. The cross-sectional area of the exterior girder seemed to demonstrate a trend as it was varied, though the Bloomington bridge once again lay outside of this particular trend.

#### 4.4 PARAMETRIC ANALYSIS

For all five bridges, six variables were investigated. For two of the bridges (Bloomington and Greenup), additional variables were investigated, and some of the variables were investigated in greater depth. Each parameter was investigated by fixing all other parameters, with the exception of variables that had to be modified to preserve the geometry of the overhang bracket. For the Highland bridge, only the side with the shorter diaphragm spacing was investigated.

For example, because the overhang width was modified, the angle of the overhang bracket had to be adjusted. The standard method in the analysis was using the permanent lateral support spacing that existed at the midspan of the bridge and the arrangement of the temporary lateral supports. For the temporary lateral supports, the cross-sectional area was modified until the program yielded a rotation that was the same as the value experienced in the field. All parameters were varied to a similar extent.

For all five bridges, six parameters were investigated:

- Width of the overhang
- Depth of the exterior girder web
- Width of the flange of the exterior girder
- Thickness of the flange of the exterior girder
- Girder spacing
- Permanent lateral support spacing

In some cases, through the parametric study, the results were compared with the variance of the rotational stiffness. The equation of the polar moment of inertia is shown in Equation 4.1, where  $b$  is half the width of the tension or compression flange or the depth of the web, and  $t$  is the thickness of the tension or compression flange or the web.

$$J = \sum \frac{b't^3}{3} \tag{4.1}$$

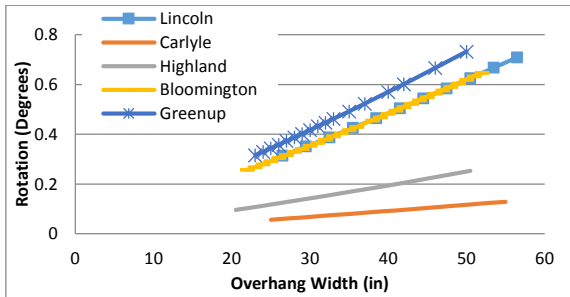
The equation for the rotational stiffness is shown in Equation 4.2, where  $G$  is the shear modulus of elasticity and  $L$  is the span length over which the rotation is being measured.

$$k = \frac{GJ}{L} \tag{4.2}$$

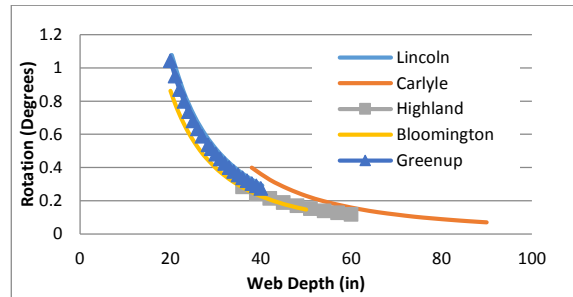
Figure 4.2 shows the results of the effect of overhang width on the exterior girder rotation. As the width was varied, the angle of the overhang bracket was modified accordingly to maintain the bracket resting 6 in. above the bottom flange of the exterior girder. The results remained consistent for all the five bridges because the rotation increased linearly because of the increase in the overhang width. Figure 4.2 shows consistency in the trend for all bridges, which indicates that the torsional moment imparted by the screed is linearly related to the width of the overhang.

Figure 4.3 shows the rotation of the exterior girder when the depth of the web of the exterior girder changed, assuming the flanges had constant thicknesses and widths. As the depth of the girder web increased, a number of other variables were modified to preserve the overall setup of the bridge. The overhang bracket was modified to keep the bottom of the overhang bracket resting 6 in. above the

bottom flange of the exterior girder. The top offset of the diaphragms was modified to keep them at the center of the exterior girder web, and the permanent lateral support height for the cross frames was modified to preserve its offset from the top flange as the girder web depth was adjusted. The results of this parameter also remained consistent, with the girder rotation decreasing in an exponential fashion as the depth of the girder web increased. This trend remained consistent among all bridges.



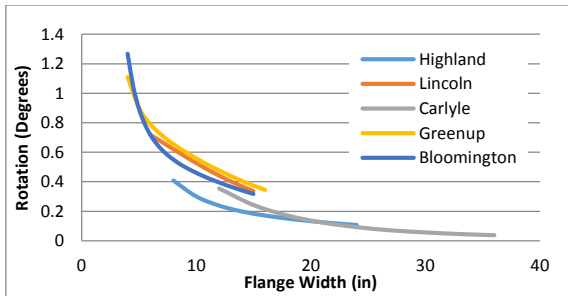
**Figure 4.2 Effect of overhang width on girder rotation.**



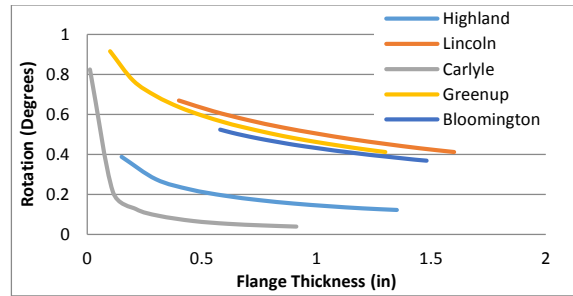
**Figure 4.3 Effect of web depth on girder rotation.**

Figure 4.4 shows the effect of variable widths of the top and bottom flanges of the exterior girder. The results as shown remained consistent for all five bridges, with the girder rotation decreasing exponentially as the flanges were made progressively wider. This could be expected because the width and thickness of the girder’s flanges contributed significantly to the rotational stiffness of the beam. The trend was somewhat different between the plate girder bridges and the W-section bridges. The decrease in the rotation was steeper in the case of the W-section bridges and was less significant with the plate girder bridges.

Figure 4.5 shows the results when the thicknesses of the top and bottom flanges were varied. It can be seen that the rotation of the girders decreased with an increase in the flange thickness in a consistent fashion for all five bridges. It can be observed that in the Carlyle bridge, the rotation decreased sharply initially and then decreased in a more linear fashion as the flanges became thicker. For the other four bridges, the girder rotation decreased in a semi-linear fashion as the flanges became thicker. The observed behavior was attributed to the thin web thickness, which demonstrated a decrease in rotation compared with the thicker web thicknesses, as can be seen in the two plate girder bridges. In conclusion, the thicknesses of the flanges were less important than in the other cases where the girder webs were thinner.



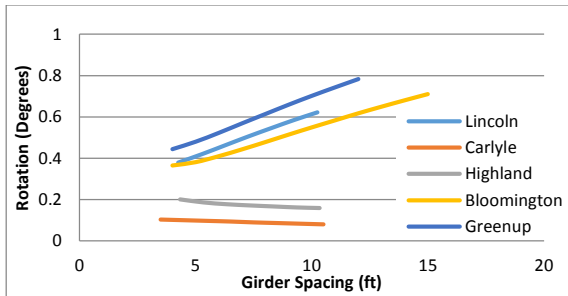
**Figure 4.4 Effect of flange width on girder rotation.**



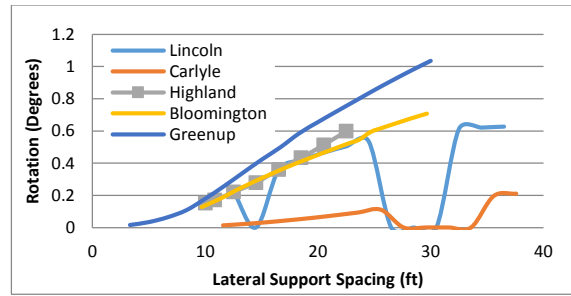
**Figure 4.5 Effect of flange thickness on girder rotation.**

Figure 4.6 shows the effect on exterior girder rotation of changing the spacing between the longitudinal girders. The trends for all five bridges were consistent. Three bridges experienced greater rotation as the girders were spaced farther apart, and two bridges experienced reduced rotation as the girders were spread farther apart. The one distinguishing characteristic between the two groups was the depth of the girders. The Greenup, Lincoln, and Bloomington bridges all had longitudinal girders that were approximately 30 in. in depth, whereas the Carlyle and Highland bridges had significantly deeper plate girders. The two plate girder bridges also had greater global bridge stiffness as a result of the increased number and decreased spacing of diaphragms (Highland) and the use of cross frames (Carlyle). Although the rotation decreased with these two bridges, it did not change by a significant amount as the girder spacing was increased.

Figure 4.7 shows the results when the spacing between the permanent lateral supports varied within all of the bridges. As the permanent spacing was varied, the spacing between the temporary lateral supports was also modified to keep them equally distributed between the permanent lateral supports. The cross-sectional area of these temporary lateral supports was kept constant through the spacing being modified for the permanent lateral supports. For three of the bridges, the results behaved as would be expected, with the girder rotation increasing as the spacing was increased. Closer spacing would result in the use of more permanent lateral supports and therefore greater overall global rotational stiffness, and a longer spacing would result in overall reduced global rotational stiffness and therefore more rotation. The results for the other two bridges were unexpected and did not seem to be logical because the trend was completely inconsistent with the increase of the lateral support spacing. With the Lincoln and Carlyle bridges, certain permanent lateral support spacing values resulted in a rotation value of 0°, with no lateral deflection of the exterior girder or rotation. In both cases, further increasing the spacing eventually resulted in resumed rotation values being calculated by the program. For these two bridges, the rotation values (excluding zero values) followed a consistent behavior with the other three bridges. However, these zero value cases were unexpected, and it is unclear why the program produced those results.



**Figure 4.6 Effect of girder spacing on girder rotation.**



**Figure 4.7 Effect of lateral support spacing on girder rotation.**

## 4.5 PROGRAM CONCLUSIONS

On the basis of the overall results, it was found that the TAEG program did not yield consistent and accurate results in assessing the rotation experienced during deck placement for the five bridges that were analyzed as part of this study. As was found in the previous research by Roddis et al. (1999), much of the uncertainty was due to differences between field conditions and modeling conditions. The primary reason for this discrepancy was the program's inability to account for certain situations and conditions, such as gaps in engagement for tie bars or timber blocks, inability to include all temporary lateral supports, or inconsistent spacing for permanent lateral supports. Because inconsistent spacing for diaphragms and cross frames is a common practice within bridge design, this limitation is a significant one. These limitations, in addition to the program's inability to account for other bracing methods and systems, restrict the program's usability. Because the program consistently underestimated the rotation measured during construction, a cross check of the program results must be conducted. If the rotation of exterior girders is a concern and additional analysis is considered necessary, then FE modeling is a better option for assessing a bracing system or estimating rotations that should be expected for a particular bracing system.

Certain limitations of the TAEG program must be improved to make the program more useable and to be more accommodating of various field and bridge configurations. Suggested improvements are as follows:

- The program should include multiple spacing distances between diaphragms or cross frames.
- The program should include a gap option for tie bars and timber blocks in addition to allowing more flexibility in terms of the number of temporary lateral supports.
- The program should include alternative bracing systems, including steel pipes, intermediate diaphragms, and cross frames and be able to adjust the stiffness of the connections.
- The program should provide a visual representation of the bridge setup being analyzed.
- The program should have a comprehensive user's manual that explains the intricacies of the program, specifically describing the inputs and methods necessary to properly use the program.
- The program should provide more flexibility with loading conditions.



- The program should properly consider the behavior of the girders—that is, it should be able to analyze multiple types of girders, in addition to considering a girder’s ability to distort locally instead of using an assumed rigid body motion and deformation of the girder.

# CHAPTER 5: EXPERIMENTAL PROGRAM

## 5.1 OVERVIEW

The primary objective of the experimental program was to evaluate the traditional girder rotation prevention systems used by IDOT contractors to prevent exterior girder rotation during bridge deck construction. The evaluation included an analysis of the main factors that influence effectiveness (e.g., tie bar sagging and field-installation quality control, the compression capacity of timber blocks, and improper shimming of timber blocks). The evaluation included the traditional block-and-tie systems described in Article 503.06(b)(2) of the IDOT Standard Specifications for Road & Bridge Construction (IDOT 2012), as well as proposed bracing systems to minimize girder rotation.

## 5.2 DESIGN OF THE LABORATORY BRIDGE SCALED MODEL

The test setup included two W21×44 steel girders 15-ft. long and supported at each end on 3-ft. W14×82 sections. The support girders (W14×82) were connected to a strong floor using threaded anchors. A single bracket was mounted at midspan of one of the W21×44 girders and was used to apply an unbalanced load to simulate eccentric field loads leading to exterior girder rotation. A preliminary FEA was conducted that led to the design of the system and to calculate all section strengths, as described in Appendix D. The setup also included permanent cross frames at both ends of the girders simulating those used in actual structures, as shown in Figure 5.1. A detailed description of the scaled model can be found in Appendix D.



Figure 5.1 Test setup.

The possibility of testing concrete girders was considered; however, no testing was performed because only small rotations had been measured in the field during construction of the Belleville-I bridge. The design was driven by the following lab constraints: (1) limited space of 16 × 10 ft available at the SIUE laboratory (Figure 5.2), (2) the need for a simple and quick assembly of the setup to conduct a large number of tests, and (3) the need to maintain setup safety.

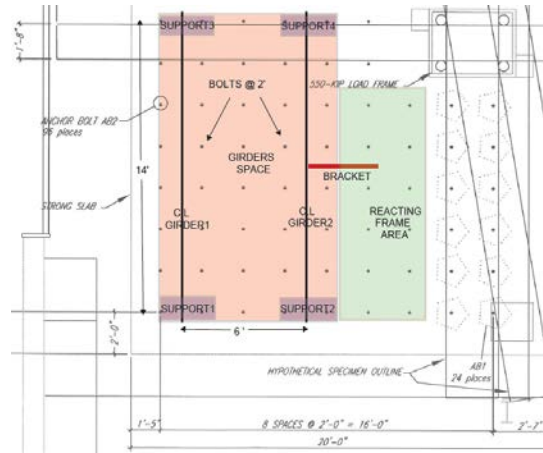


Figure 5.2 Scaled bridge model location at the SIUE Structural Engineering Laboratory.

### 5.3 ELEMENTS OF THE EXPERIMENTAL SETUP

The primary aspects of the setup are described in Table 5.1. All elements, geometry, materials, and assembly specifications are provided in Appendix D.

Table 5.1 Setup Configuration Parameters

	Elements	Characteristics
Main Girders	Type	W21x44
	Length	15 ft.
	Effective length (between supports)	14 ft.
	Distance between main girders	6 ft.
Support Girders	Type	W14x82
	Length	3 ft.
Cross Frames	Cross bracing	L 2x2x1/4 section
	Top angle iron	L 2x2x1/8 section
	Connecting plate to girder	L 3x3x1/4 section
Compression Struts	Timber blocks	4 x 4 in. cross section
	Horizontal pipes	1-1/2 in. diameter
	Diagonal pipes	2-3/8 in. diameter
Connections	Between support and main girders	Bolts 1-3/8 in. diameter x 6 TPI
	Support girder to floor	Bolts 1-3/8 in. diameter x 6 TPI
	Cross frame to connecting plate	Bolts 1/2 in. diameter
	Connecting plate to main girder web	Bolts 3/4 in. diameter
	Top angle to main girder top flange	Bolts 1/2 in. diameter
Load Application System	Applied vertical load	2.5 kips at 2.5 in. from tip of bracket
	Location	Midspan
	Load dispositive	Hydraulic jack
Bracket	Type	Dayton Superior C49 JR
	Location	Midspan
	Connection to main girder hanger	Coil rod 0.5 in. diameter
Hangers	Conventional and New*	Dayton Superior
	Safe working load (SWL)	3 kips

\*Custom made hanger not commercially available (see Appendix D).

## 5.4 INSTRUMENTATION

### 5.4.1 Data Acquisition System

Data were collected using an NI data acquisition system (multiplexor) connected to a data logger (CR3000 Micro-logger) and laptop with data collection using LabVIEW. The data acquisition system required loading to be applied manually in five steps of 500 lb each to obtain adequate readings. It was necessary to wait approximately 30 seconds between each loading step. The load reading system and data logger are shown in Figure 5.3.



Figure 5.3 Load reading device (left) and data logger (right).

### 5.4.2 Tilt Sensors

Twelve dual-axis (CXTLA02) tilt sensors were attached to the scaled bridge model at several locations to measure girder rotation. Three tilt sensors were located on the support girders to measure the rotation at the supports and to ensure that rotation was minimal. The remaining sensors were installed at different locations at midspan in both exterior faces of the main girders, as shown in Table 5.2 and in Figures 5.4 and 5.5.

Table 5.2 Marking of Tilt Sensors at Midspan

Location Tilt Sensor	Loaded Girder	Non-Loaded Girder
Top Flange	Tilt sensor No. 4	Tilt sensor No. 1
Bottom Flange	Tilt sensor No. 6	Tilt sensor No. 3
Top Web	Tilt sensor No. 12	Tilt sensor No. 10
Middle Web	Tilt sensor No. 5	Tilt sensor No. 2
Bottom Web	Tilt sensor No. 8	No tilt sensor installed

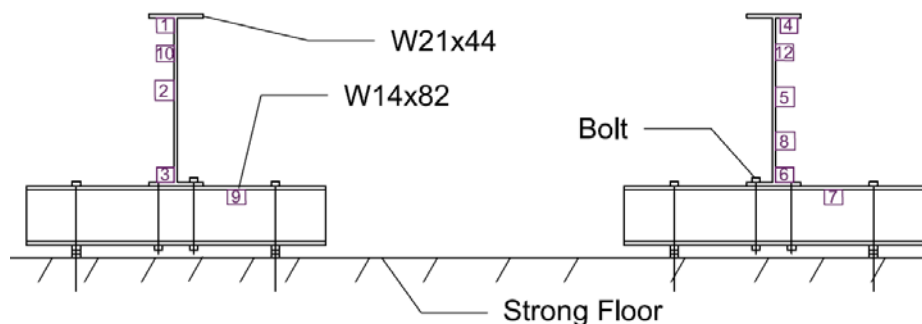


Figure 5.4 Marking and location of the tilt sensors in the girders.



**Figure 5.5 Tilt sensors at loaded girder at midspan.**

## 5.5 TESTING PROGRAM

### 5.5.1 Bracing Elements

As shown in Table 5.3, every bracing element needs to be considered with the goal of combining them to propose all possible test cases and to build the testing matrix. Depending on the test case, certain elements are tested individually or in combination with others, as shown in Tables 5.4 through 5.6.

**Table 5.3 Individual Bracing Elements to Be Considered for Testing Purposes**

Elements		Number of elements installed
Ties	Transverse (TT)	No ties, two, three, and four
	Adjusted Diagonal (ADT)	
	Unadjusted Diagonal (UDT)	
Intermediate Cross Frames (CF)		No cross frames, one, and two
Timber Blocks (TB)		Three, and four
Horizontal Steel Pipes (HP)		Three, and four
Diagonal Pipes (DP)		Two, three, and four

### 5.5.2 Testing Matrix

Forty-five cases were tested at the SIUE laboratory. The tests were divided into nine groups (families) identified by the main bracing element (primary element) being evaluated. Every group included all cases that corresponded to the same family (combination of the main element with other selected elements). This distribution in groups enabled a consistent comparison of cases, as shown in Tables 5.4 through 5.6.

**Table 5.4 Cases in Groups 1, 2, 3, and 4 (see Appendix D for details)**

Group 1	Group 2: Four transverse ties (TT) combined with other elements		Group 3: Three transverse ties (TT) combined with other elements		Group 4: Four adjusted diagonal ties (ADT) combined with other elements	
No bracing system	4-TT	Only	3-TT	Only	4-ADT	Only
		4-TB		3-TB		4-TB
		4-HP		3-HP		4-HP
		4-DP		3-DP		4-DP
		1-DP				1-DP
		2-DP				2-DP

**Table 5.5 Cases in Groups 5, 6, and 7 (see Appendix D for details)**

Group 5: Three adjusted diagonal ties (ADT) combined with other elements		Group 6: Four unadjusted diagonal ties (UDT) combined with other elements		Group 7: Three unadjusted diagonal ties (UDT) combined with other elements	
3-ADT	Only	4-UDT	Only	3-UDT	Only
	3-TB		4-TT		3-TB
	3-HP		4-HP		3-HP
	3-DP		4-DP		3-DP

**Table 5.6 Cases in Groups 8 and 9 (see Appendix D for details)**

Group 8: One cross frame combined with other elements			Group 9: Two cross frames combined with other elements			
1-Cross frame (CF) @ midspan (@MS)	Only	One cross frame (CF) not at midspan (N@MS @ 3.5 ft. from midspan)	Only	Two cross frames (CF) not at midspan (N@MS @ 3.5 ft. from midspan)	Only	
	4-TT				4-TT	
	3-TT				3-TT	
	2-TT		2-DP		2-DP	4-ADT
	2-DP					
	2DP+3-TT					
	2-ADT					3-ADT
	2-DP+3-TT					

### 5.5.3 Data Analysis Procedure

The rotation measured at the top of the web (at the top flange–web intersection) of the loaded girder was the most relevant rotation measured for this study. This girder rotation was measured using a tilt sensor, and it corresponds to the difference between the initial rotation of the girder (when tightening of the ties is applied) and the final rotation of the girder (just before the load is released at 2.5 kips). Owing to initial loading, the initial rotation was negative (inward) but transitioned to positive (outward) rotation as the load was applied (Figure 5.6). The calculated rotation simulates the rotation that occurs in the field under actual loading, which is measured prior to placement of concrete for the deck to the point when the deck has been placed and the overhang receives the maximum construction load.

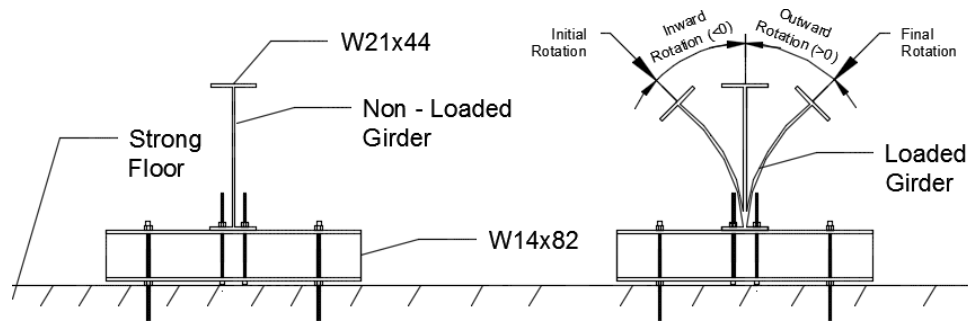


Figure 5.6 Rotation sign criteria for loaded girder.

To obtain the initial and final rotation values from the measured data, the regression to the mean method was applied to find the average starting and final rotation values, as shown in Figure 5.7. and described as follows: (1) the starting rotation is the average of the rotations between point A and point B (B is the point where the rotation starts to increase), and (2) the final rotation is the average of the values at the summit of the graph between points C and D (D is the point when the load is released and the rotation drops).

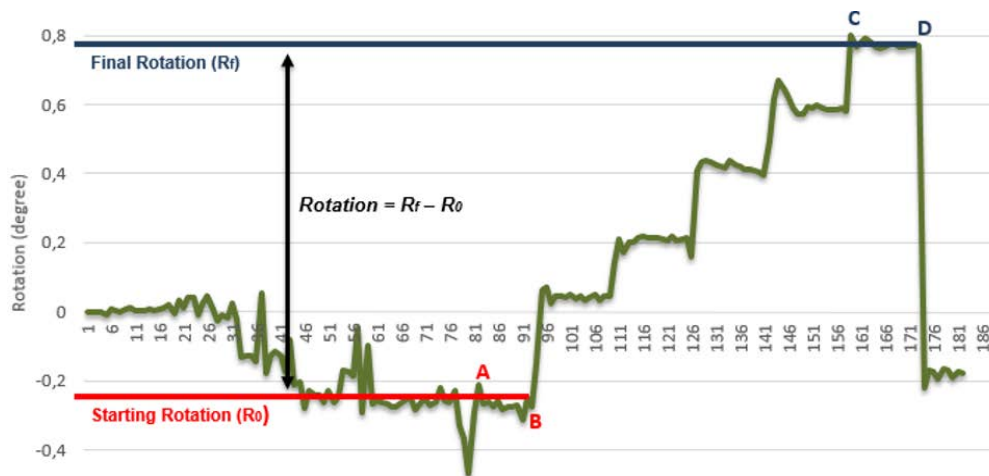


Figure 5.7 Example of the methodology to calculate the initial and final rotation (3-TT + 3-DP).

### 5.5.4 Experimental Results

The various bracing systems considered in the experimental testing study are described in this section. The experimental girder rotation measured from the top of the web of the loaded girder is presented for each case, as shown in Figures 5.8 through 5.16. Loading was applied to one girder to simulate exterior girder rotation occurring in actual bridges. Rotation of the top flange of the girder was also analyzed; however, this option was dismissed because, in each case, the rotation at the top flange was larger than the rotation at the top of the web by an average of 10% to 15%. Consequently, the same conclusions were reached when analyzing either the top flange rotation or the web rotation. In addition, rotations of the support girders were checked for each case to ensure that such rotations were minimal and not included in the rotation of the girders being evaluated. The effectiveness of each bracing system depends on the combination of ties and compression struts.

Both elements act together to resist rotation; however, the effectiveness of these elements depends on their configuration and spacing. The best system is the one that maximizes the tensile forces in the ties and compression of the struts while minimizing rotation.

#### 5.5.4.1 Group 1: No Bracing System

As shown in Figure 5.8, the measured web rotation for this case was 2.73°, which was the largest rotation observed in testing. This case was the most critical configuration for the loaded girder because there was no bracing system to prevent rotation. In this test, the hanger carried the maximum load without failure. Therefore, the safety of the system was ensured for the other tested cases which included additional bracing. Furthermore, no rotation was observed at the supports, which indicated that the supports were properly designed and constructed.

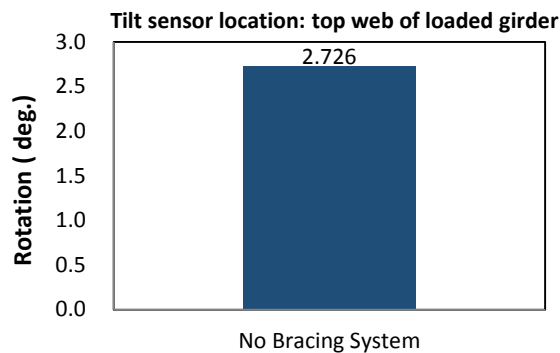


Figure 5.8 Group 1: No bracing system.

#### 5.5.4.2 Group 2: 4-TT + Other Element

As shown in Figure 5.9, rotation for the 4-TT and for the 4-TT + 4-TB / 4-HP were nearly the same. This tends to indicate that the transverse ties were the only elements acting properly to prevent rotation and that timber blocks and horizontal pipes did not have a large influence on rotation prevention. The installation procedure used for both the timber blocks and horizontal pipes was similar. In both situations, there was no direct contact between the end of the struts and the girder webs, which provided a gap that reduced the effectiveness (see Figure 3.26) of this system.

Alternatively, diagonal pipes resulted in better behavior compared with the system containing either timber blocks or horizontal pipes, preventing rotation much more effectively (55% to 60% reduction compared with using only transverse ties). For this group, the two cases with the lowest rotation were 4-TT + 4-DP (0.87°) and 4-TT + 1-DP (0.87°). For the 4-TT + 2-DP case, the rotation was about 0.3° higher than the cases with four or with one diagonal pipe because with the 4-TT + 2-DP case, the two pipes were located 3.5 ft. from midspan, where no pipes were placed where the load was applied.

#### 5.5.4.3 Group 3: 3-TT + Other Element

Group 3 rotations are shown in Figure 5.10, where it is seen that the horizontal timber blocks and pipes behaved similarly, with rotations of 1.77° and 1.70°, respectively. As was the case with Group 2,



the diagonal pipes performed much better than timber blocks and the horizontal pipes, with a rotation of only 0.76°. However, there are some interesting comparisons to be made between Groups 2 and 3:

- The rotation for 3-TT was 0.20° higher than the 4-TT. This was true despite the fact that one of the ties for the 3-TT configuration was placed 6 in. from the midspan.
- When 3-TB and 3-HP were added to the three transverse ties, the system rotated about 0.40° less than the 4-TT + 4-TB/HP, which showed that the location of the timber blocks and the horizontal pipes was more relevant than how many were installed. In the case of Group 2, 4-TB/HP were installed 2 ft. and 4 ft. away from midspan (shown in Figure B.23). However, for Group 3, one of the three TB/HP was 6 in. from the midspan section, which showed that using three compression struts prevented more rotation than the four struts case.
- In addition, the last case in the group (3-TT + 3-DP) showed the least rotation (0.76°) of any system evaluated in Groups 2 and 3. In this case, one of the three transverse ties and one of the diagonal pipes were installed 6 in. from midspan. The location of both elements made this alternative more efficient than any of the alternatives with TT + DP compared with Group 2.

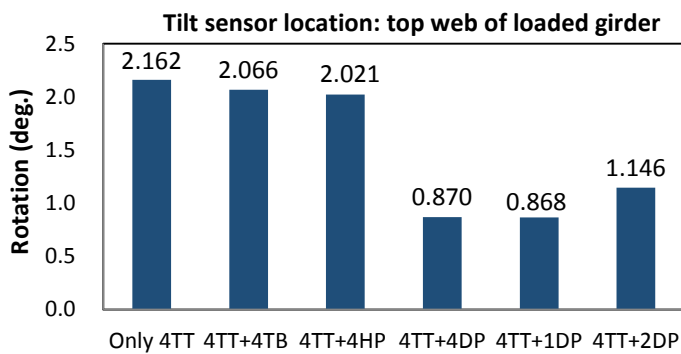


Figure 5.9 Group 2: 4-TT + other element.

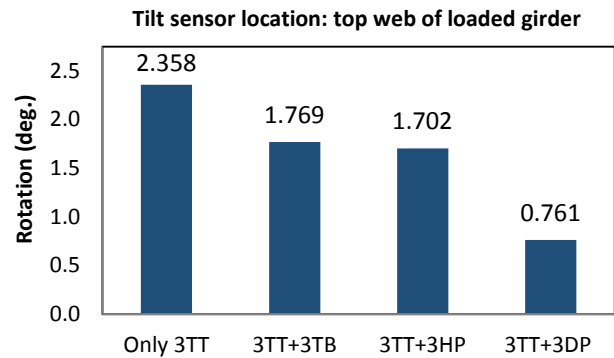


Figure 5.10 Group 3: 3-TT + other element.

#### 5.5.4.4 Group 4: 4-ADT + Other Element

This group shows that timber blocks and horizontal steel pipes perform better when they are combined with diagonal ties rather than transverse ties. As shown in Figure 5.11, the 4-ADT system is much better at limiting rotation than the 4-TT system. In Group 4, the rotation reduction from using only 4-ADT to 4-ADT + 4-TB/HP was nearly 35%, while in Group 2, the percentage difference in rotation between 4-TT and 4-TT + 4-TB/HP was considerably smaller (5%). The most efficient case in this group was achieved by using 4-ADT + 4-TB, which had a rotation value of only 1.17°. Regarding the systems with diagonal pipes, the cases of 4-ADT combined with 4-DP (1.41°) and 1-DP (1.58°) were slightly less effective than the case that included 2-DP (1.68°). The same situation occurred in Group 2 in comparing 4-TT + 2-DP (1.15°) with 4-TT + 1-DP (0.87°) and 4-TT + 4-DP (0.87°). However, when comparing DP with TB or HP, diagonal pipes behaved differently. The three cases with DP in this

group (4-ADT + 4-DP / 2-DP / 1-DP) presented larger rotations than the cases with TB or HP (4-ADT + 4-TB / 4-HP). This behavior occurred because of the configuration of the tie rods that were installed from the top flange of the loaded girder to the bottom flange of the non-loaded girder. That configuration made the non-loaded girder rotate outward when the load was applied, leading to the diagonal pipes to lose some compression force with the addition of HP or TB.

Hence, diagonal pipes behave more efficiently as an exterior girder prevention system when they are combined with transverse ties rather than with adjusted diagonal ties. Comparing the rotations from only 4-ADT with the case of only 4-TT, it was also shown that adjusted diagonal ties acting as the only bracing system (1.78° for only 4-ADT) were more efficient than transverse ties only (2.16° for only 4-TT).

#### 5.5.4.5 Group 5: 3-ADT + Other Element

With this group, similar conclusions to those identified in Group 4 were made: timber blocks and horizontal steel pipes perform better when they are combined with diagonal ties rather than transverse ties, and diagonal pipes behave more efficiently as an exterior girder prevention system when they are combined with the transverse ties rather than adjusted diagonal ties. Other observations can be made about Group 4 (Figure 5.11) and Group 5 (Figure 5.12) bridges:

- Compared with 4-ADT, the rotation of 3-ADT was higher by 0.20°. This showed that the global behavior of 4-ADT was slightly better than the case with 3-ADT, despite one of the ties having placed 6 in. from the midspan.
- When 3-TB and 3-HP were added to the 3-ADT system, the rotation was reduced by 0.80° to 0.90° compared with the case of 4-ADT + 4-TB/HP (see cases 4-ADT + 4-TB/HP vs. 3-ADT + 3-TB/HP). It showed that the timber blocks and horizontal pipes worked more effectively with 3-ADT than with 4-ADT because the location of one of the ties and the compression struts was 6 in. from midspan, not 2 ft. from midspan.
- The lowest rotation value from this group was 1.00° for the 3-ADT + 3-HP system. This value represented a reduction of 50% compared with the 3-ADT case.

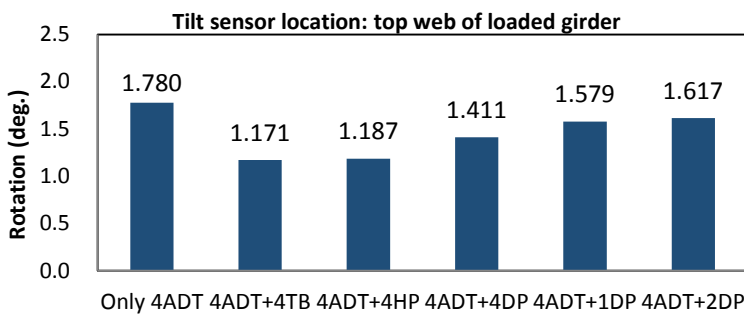


Figure 5.11 Group 4: 4-ADT + other element.

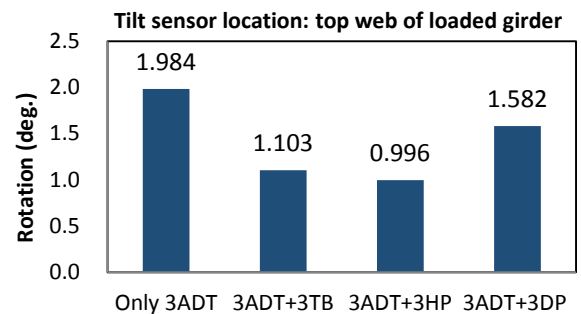


Figure 5.12 Group 5: 3-ADT + other element.

#### 5.5.4.6 Group 6: 4-UDT + Other Element

It is also relevant to point out the difference between the adjusted diagonal ties (ADT) and the unadjusted diagonal ties (UDT) in comparing Figures 5.11 and 5.13. The UDT were difficult to install, which would also likely be the case in the field. The UDT lost efficacy because of the initial bending that was required to adjust the ties to fit between the top flange of the exterior girder and the bottom flange of the first interior girder. In contrast, the adjusted ties were placed straight and were directly connected to the hangers. Accordingly, all cases in Group 6 had higher rotation values than the analogous cases in Group 4 using 4-ADT instead of 4-UDT.

#### 5.5.4.7 Group 7: 3-UDT + Other Element

The same conclusions can be established for this group to the analogous Group 5 systems by comparing Figures 5.12 and 5.14. Even though the rotation measured for one case (3-UDT) was slightly less than the corresponding value using adjusted ties (3-ADT) ( $1.805^\circ$ ) than the obtained value from using the 3-ADT ( $1.984^\circ$ ). This difference might be attributed to the application of greater torque to install the 3-UDT in the hangers. For the remaining cases (3-UDT + 3-TB / 3-HP / 3-DP), the rotations shown in Figure 5.14 are larger than those obtained in Figure 5.12 for the analogous cases. On the basis of this comparison, the adjusted diagonal ties were found to be more effective than the unadjusted diagonal ties.

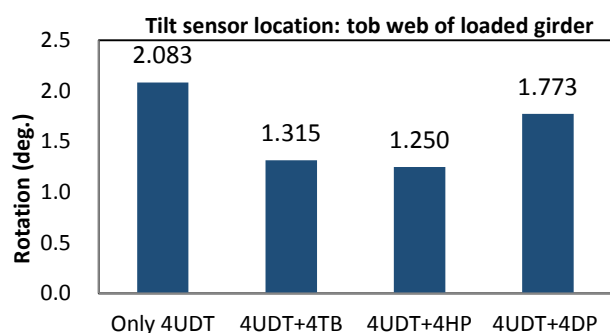


Figure 5.13 Group 6: 4-UDT + other element.

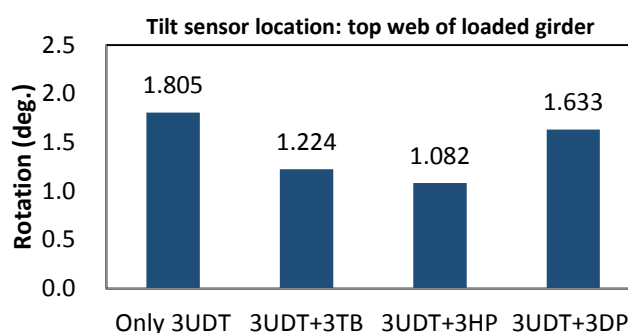


Figure 5.14 Group 7: 3-UDT + other element.

#### 5.5.4.8 Group 8: One Cross Frame + Other Element

This group (Figure 5.15) was tested to identify the performance of intermediate cross frames. The intermediate cross frames used in the tests were installed without top- or bottom-angle sections—only cross-bracing members and connecting plates were used (see Figure D.39 of Appendix D) for assembling the cross frame. The cross frames were tested alone or in combination with different elements (TT, ADT, and DP). Several cases were tested in this group to ensure a complete understanding of the efficiency of the intermediate cross frames in preventing exterior girder rotation. The cross frames were located either at midspan or were offset from midspan by 3.5 ft. on either side. Rotations for these two cases were  $2.05^\circ$  when the cross frame was not at midspan and were  $1.72^\circ$  when placed at midspan. The resulting midspan rotation was reduced by approximately 20%. When 1-CF was combined with 3 or 4 TT, a 50% reduction in the rotation was observed compared with the system containing only one cross frame ( $1.72^\circ$  with 1-CF at midspan to  $0.86^\circ$  with

1-CF at midspan + 3-TT or 0.94° with 1-CF at midspan + 4-TT). These results demonstrate that the combination of 1-CF at midspan plus TT is an extremely effective method to decrease rotation.

A comparison of the effectiveness of TT with ADT is also shown in Figure 5.15. The combination of 1-CF at midspan + 4-TT (0.94°) provided less rotation than the case of using 1-CF at midspan + 4-ADT (1.29°), which presented a 28% reduction. Also, when comparing 1-CF at midspan plus 2-TT (1.46°) with 1-CF + 2-ADT (1.48°), the case with 2-TT showed almost the same results as the case with 2-ADT. Therefore, transverse ties performed better than the adjusted diagonal ties. It was noticed that the distance between the ties from the loading point, has a significant impact on girder rotation.

The influence of DP can also be observed in Figure 5.15. When the DP were combined with 1-CF (1-CF at midspan + 2-DP and 1-CF not at midspan + 2-DP), the rotation values (1.56° for 1-CF at midspan + 2-DP and 1.92° for 1-CF not at midspan + 2-DP) were not as small as the ones observed when the DP were combined with TT (0.84° for 1-CF at midspan + 2-DP + 3-TT and 0.88° for 1-CF not located at midspan + 2-DP + 3-TT). Consequently, when combined with 1-CF, diagonal pipes act more efficiently when they are also used in combination with TT. However, if 1-CF is combined with TT only, the values were very similar to the case of using 1-CF using both DP and TT. Therefore, when TT and one intermediate CF were used, diagonal pipes did not influence the girder rotation reduction as much as the transverse ties. The combination with the smallest rotation was 1-CF at midspan + 2-DP + 3-TT (0.84°).

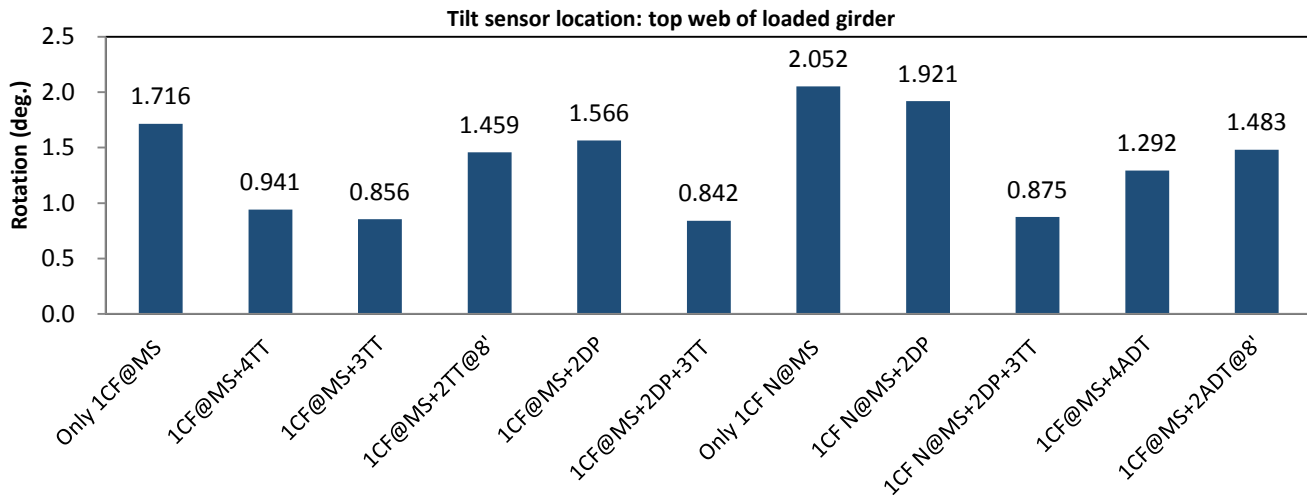


**Figure 5.15 Group 8: 1-CF + other element.**

#### 5.5.4.9 Group 9: Two Cross Frames + Other Element

In this group, the cross frames were located 3.5 ft. from midspan. As shown in Figure 5.16, the measured rotation when using only 2-CF was 1.68°, while the rotation for only 1-CF is 1.72°. With a load applied at midspan, this indicated that the torsional stiffness of the two systems was similar. A different behavior was observed, however, when the systems containing TT are analyzed. The rotation for 2-CF + 4-TT (1.08°) and 2-CF + 3-TT (1.25°) was found to be larger than for the 1-CF + 3-TT (0.86°) and 1-CF + 4-TT (0.94°) systems. For 1-CF combined with TT, the rotation was reduced by 25%

compared with the case using 2-CF + TT. It is evident that the transverse ties improved the system considerably. The 2-CF + 4-ADT (1.32°) and 1-CF + 4-ADT (1.29°) systems had nearly the same rotation. Hence, ADT did not influence how the system behaved when 1 or 2 cross frames were used. The best case for this group was 2-CF + 4-ATT, which, compared with the other systems, was not one of the best.

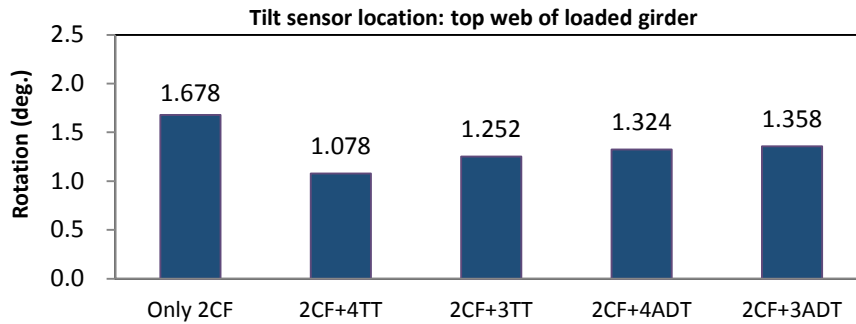


**Figure 5.16 Group 9: 2-CF + other element.**

### 5.5.5 Best Experimental Cases

The rotation results for the most effective cases obtained from the experimental investigation are presented in Table 5.7. The results show that the lowest rotation values were in the range of 0.7° to 0.9°, corresponding to combinations of either using one intermediate cross frame at midspan in addition to transverse ties or combining transverse ties and diagonal pipes.

**Table 5.7 Four Best Combinations from All Experimental Cases**

Configuration	Loaded Girder Top Web Rotation (°)
3-TT+3-DP	0.761
1-CF@MS+2-DP+3-TT	0.842
1-CF@MS + 3-TT	0.856
4-TT+1-DP	0.868

### 5.5.6 Comparison of Conventional and New Dayton Superior Hangers

Five cases were tested (Figure 5.17) to compare the conventional hangers and a new type of hanger supplied by Dayton Superior. The conventional C68 4AB and C67 hangers and the new C137 tie bar beam clip pre-stress hanger and C134 4AB pre-stress ty-down half hangers are presented in Section D.1.4 of Appendix D. The tests results indicated that both types of hanger perform very similarly under load.

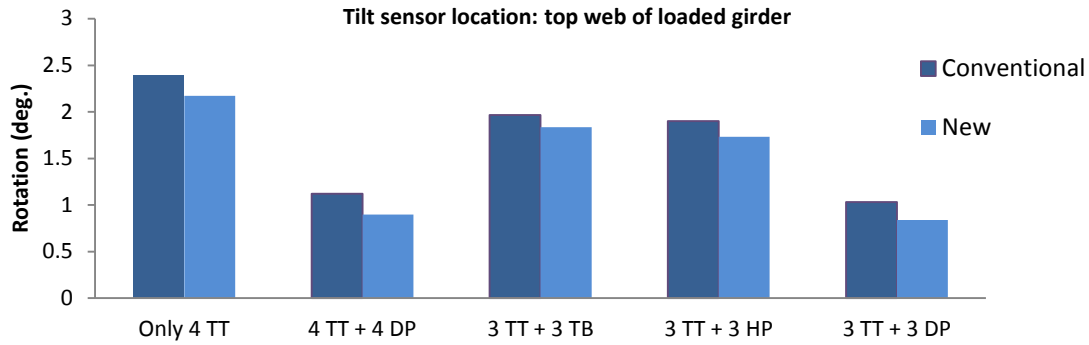


**Figure 5.17 Comparison of conventional and new Dayton Superior hangers.**

## 5.6 FINITE ELEMENT ANALYSIS

Once the experimental work was finalized, the next step was to develop an FEA model for each group tested experimentally. The commercial software Abaqus was used to conduct the analysis, with following goals: (1) validating the experimental results, and (2) running additional cases beyond the testing matrix to obtain broader knowledge and develop conclusions.

### 5.6.1 Abaqus Model

In the FE model, all parts of the experimental setup (girders, bolts, cross frames, hangers, brackets, tie bars, and compression struts) were included, simulated, and connected. The connection details were difficult to model, and as a result, several alternatives were investigated and analyzed until reasonable and consistent results were obtained with the experimental tests. Example models are shown in Figures 5.18 and 5.19. The load was modeled as a point load located 2.5 in. from the tip of the bracket and was applied in one step.

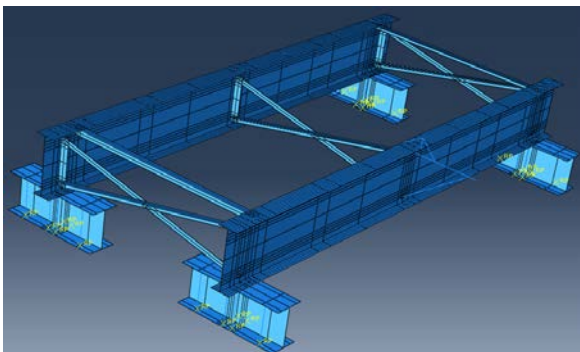


**Figure 5.18 Full-scale Abaqus model (only 1-CF at midspan).**

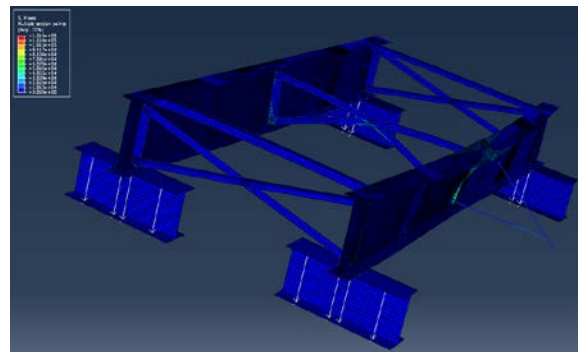


**Figure 5.19 Deformed shape of Abaqus model (only 1-CF at midspan).**

#### 5.6.1.1 FE Element Selection and Material Properties

Different three-dimensional element types were assigned to sections, as shown in Table 5.8. Three element types were selected, and each element was modeled using the same geometry and material properties (shown in Table 5.9) as those used in the experimental testing.

**Table 5.8 Abaqus Element Selection**

Part of Scaled Model	Type of Abaqus Element
Girders (main and supports)	Shell
Connecting bolts at supports	Wire (rigid body)
Cross frames (permanent and intermediate)	Shell
Hangers	Truss
Coil rod	Truss
Bracket	Beam
Compression struts	Truss
Tie bars	Truss

**Table 5.9 Steel and Wood Material Properties**

Property	Steel	Wood
Modulus of elasticity (ksi)	29000	1300
Poisson's ratio	0.3	0.37

### 5.6.1.2 Mesh Size and Model Partitioning

A mesh size of 0.5 × 0.5 in. was selected for both the main and support girders. The parts that were modeled using truss elements did not require a mesh size definition because they were assigned one element. Several partitions were defined to break the parts to facilitate assembling and connecting the parts, depending on the case under consideration, as shown in Figures 5.20 and 5.21.

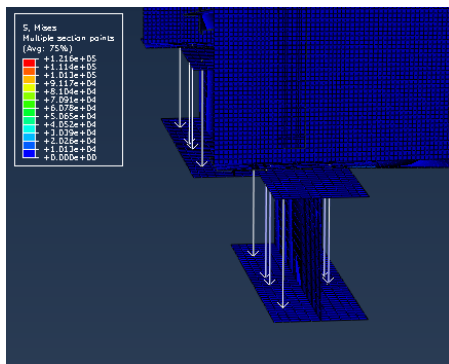


**Figure 5.20 Connection detail showing the bolts and the selected mesh.**

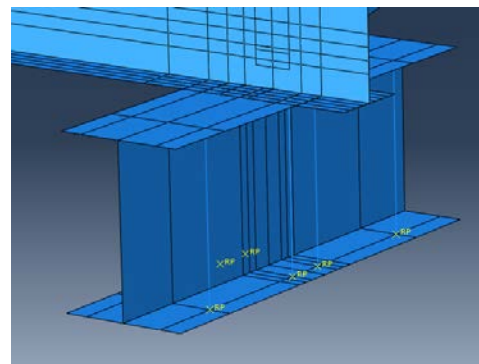


**Figure 5.21 Corner detail showing different partitions in main and support girders.**

### 5.6.1.3 Analysis of the Connections

The definition of consistent connection conditions was the most difficult and challenging step in the construction of the model. The model had many connections that needed to be defined and modeled to match the boundary conditions in the laboratory. Because of the level of detail provided by Abaqus, small changes in the connection conditions can result in large changes to the analysis results. Therefore, two types of connections were used and analyzed (node-to-node connections and surface-to-surface connection), as shown in Table 5.10. Both connections represented different boundary conditions that could be defined and allowed to assign stiffness to the connection.

In addition, the following concepts were considered: (1) definition of different coordinate systems and their orientation relative to the connection model (shown in Figure 5.22); (2) definition of the

initial (before loading) bending in the ties for the cases with unadjusted diagonal ties (UDT)—this effect was modeled by assigning an equivalent gap of 0.2 in., as shown in Figure 5.23; and (3) application of torque to tie the tie bars to the hangers using a node-to-node connection with axial rigidity in the direction of the reinforcement. The definition of appropriate connections between the main and support girders was also a key point considered.

The connection was modeled using surface-to-surface type connections on the four bolt-connection points between the main and the support girders, providing zero rotation and displacement at the supports in all tests.

**Table 5.10 Type of Connections Used to Model the Experimental Setup**

Parts Connected	Type of Connection
Tie bar to Hanger	Pinned connection (node-to-node translator link element) with axial rigidity in the direction of the tie—connection used for tests with TT and ADT
	Pinned connection (node-to-node translator link element) with assigned gap of 0.2 in.—connection used for tests with UDT
Hanger to girder	Pinned connection (node-to-node translator link element)
Main girder to support girder	Surface-to-surface tie connection
Horizontal leg of the bracket to web of loaded girder	Pinned connection (node-to-node bushing link element)
Diagonal leg of the bracket to web of loaded girder	Pinned connection (surface-to-surface) tie connection used for tests with TT
	Pinned connection (node-to-node bushing link element)—connection used for tests with ADT and UDT
Timber blocks to girder	Pinned connection (node-to-node bushing link element)
Horizontal pipes to girder	Pinned connection (node-to-node bushing link element)
Diagonal pipes to girder	Pinned connection (node-to-node bushing link element)
Cross bracing to connecting plate	Fixed connection (node-to-node bushing link element)
Top angle to top flange of girder	Fixed connection (node to node bushing link element)
Connecting plate to girder	Fixed connection (node-to-node bushing link element)



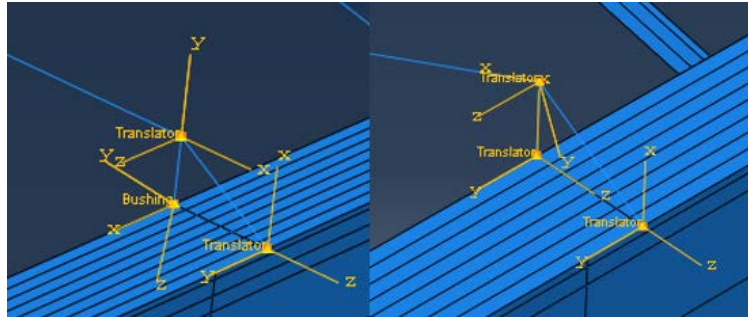


**Figure 5.22 Coordinate system orientation for transverse ties (left) and diagonal ties (right).**

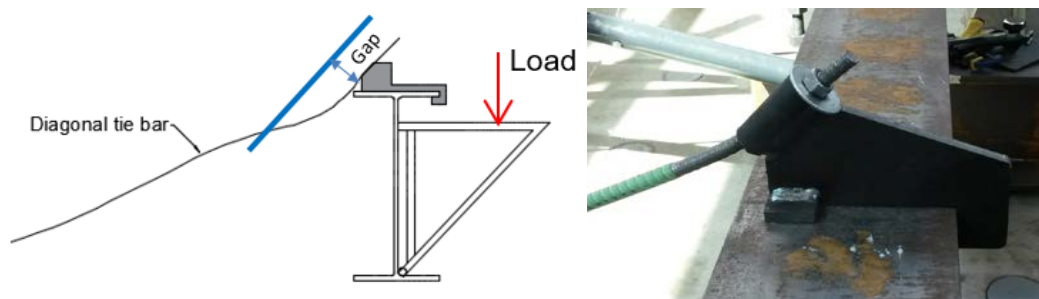


**Figure 5.23. Assigned gap (left) in FE for modeling of unadjusted diagonal ties to hangers (right).**

## 5.6.2 Test Results and Comparison with Finite Element Analysis Results

This section presents a comparison of the rotations obtained from the FE and the experimental results (Figures 5.24 through 5.32). Both sets of results correspond to the rotation at the top of the web of the loaded girder. As shown in Figure 5.24, the results for both experimental and FE with no bracing system were nearly the same (3% difference), which shows that the assumed connection type used for girders and cross frames was accurate.

In Figures 5.23 through 5.26, it is shown that the cases with no compression struts, or ties combined with TB or HP, showed less rotation compared with the experimental results (7 % on average). On the other hand, the FEA results for the cases with DP indicated rotations that were on average 13% higher than the corresponding cases tested experimentally. For the other groups, the cases with diagonal pipes also showed higher results (Figures 5.27 through 5.30 ) compared with the corresponding experiments. The diagonal pipes were connected to the girders using pinned connections. However, on the basis of these results, it may be necessary for future FE studies to assume stiffer connections for models with DP.

For the two groups containing UDT, as shown in Figures 5.29 and 5.30 (4-UDT + other element and 3-UDT + other element), the FE analysis results are higher than the results from the laboratory—on average, by 16%. The cause for those results is the initial bending in the ties when they were connected to the hangers. To model this situation, a gap of 0.2 in. was assumed, as shown in Figure

5.23. The equivalent gap was selected because it provided results similar to those of the experimental tests. The internal moment created in the actual connection could not be determined in the laboratory and was very difficult to simulate using the FE model. For the two last groups (Figures 5.31 and 5.32), the FEA results were 9% larger than the corresponding experimental cases. The maximum percentage difference (21%) between the experimental and FEA results occurred in Group 7 when using 3 UDT + 3 HP, whereas the FE showed 1.32° and the experimental was 1.08°.

On average, the results from the FE and the experimental tests were within 10% of each other. This difference was assumed to be reasonable for modeling purposes.

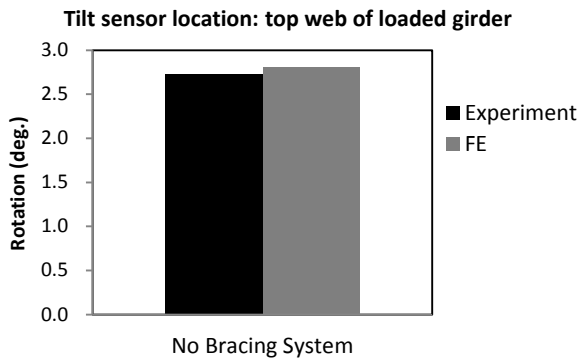


**Figure 5.24 Group 1**  
laboratory vs. FEA results.

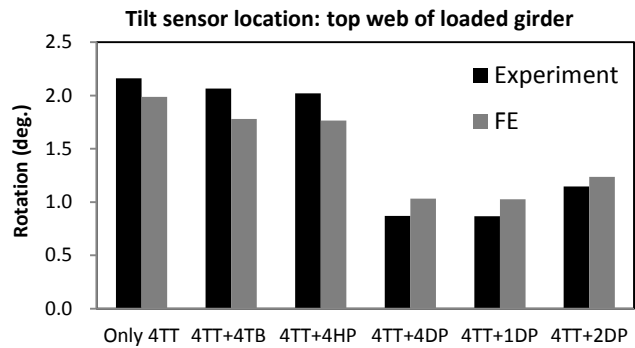


**Figure 5.25 Group 2**  
laboratory vs. FEA results.

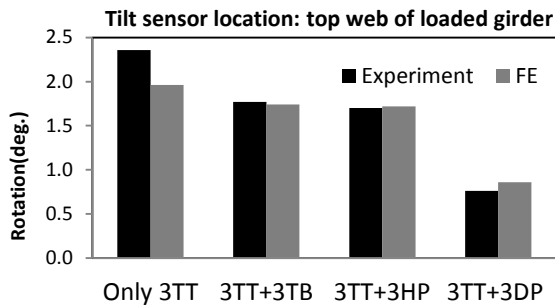


**Figure 5.26 Group 3**  
experimental vs. FEA results.

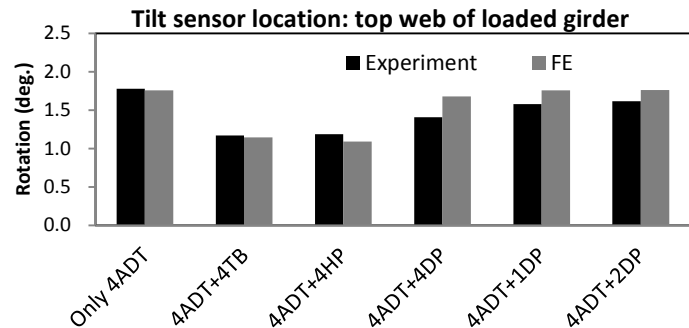


**Figure 5.27 Group 4**  
experimental vs. FEA results.

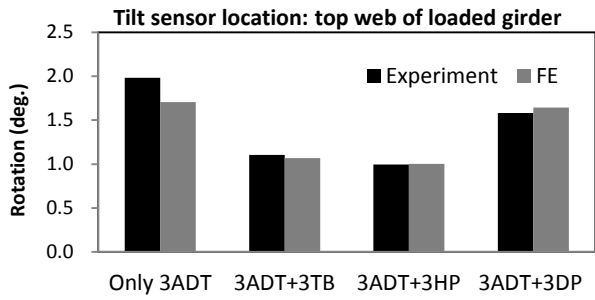


**Figure 5.28 Group 5**  
experimental vs. FEA results.

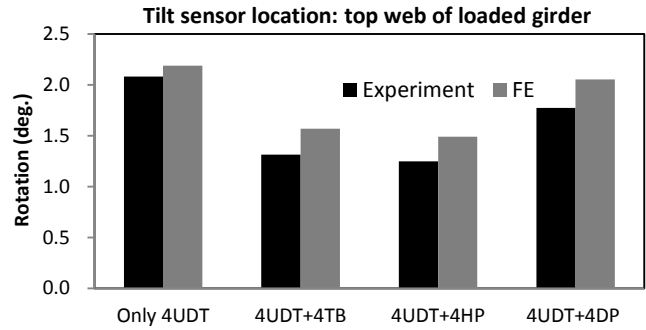


**Figure 5.29 Group 6**  
experimental vs. FEA results.

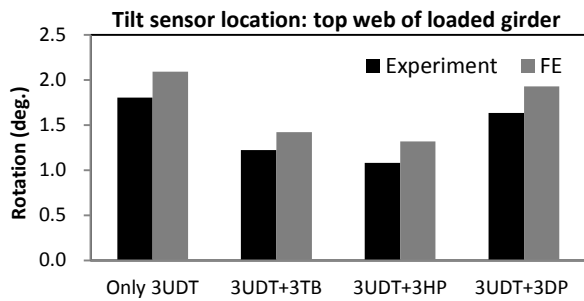


**Figure 5.30 Group 7**  
experimental vs. FEA results.

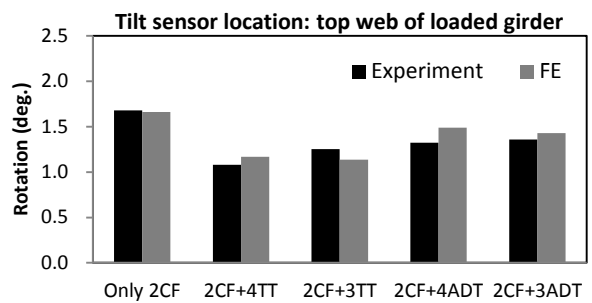


**Figure 5.31 Group 9**  
experimental vs. FEA results.

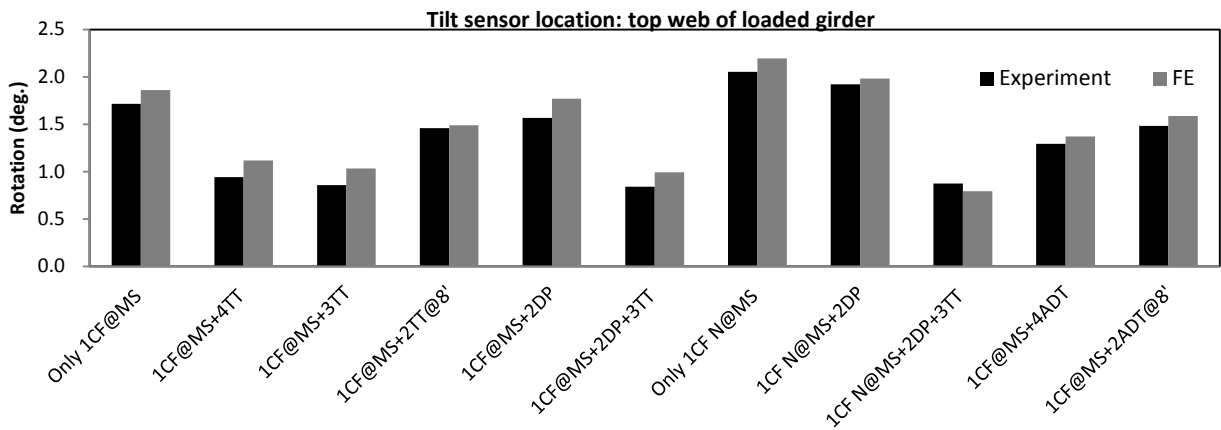


**Figure 5.32 Group 8** experimental vs. FEA results.

### 5.6.3 Additional Cases Evaluated Using FEA

Once the FEA was validated by the experimental study, additional cases were analyzed in Abaqus to expand the results beyond the studied parameters by removing the tie bars and using intermediate cross frames with top and bottom angles, as shown in Figures 5.33 and 5.34.

The objective of this additional FE work was to investigate the implementation of cross frames with top and bottom angles and to ensure their effectiveness in preventing rotation. Instead of including the transverse tie bars, cross frames were modeled with a top and bottom angles placed at the same location as in the laboratory (midspan for 1-CF and 3.5 ft. from midspan for 2-CF). The top and bottom angles were the same size (L 2x2x1/8) as the angles used in the permanent cross frames at both ends of the model. In this case, the load of 2.5 kips was not statically applied at midspan; instead, it was run along the span of the scaled model to simulate the effect of the screed moving across the bridge as expected during construction. The goal was to assess the efficiency of the cross frames when a moving load is applied to the system.

As expected, the rotation results at the midspan of the loaded girder when the load was at the midspan were in the range of 0.7° to 0.9°, as shown in Table 5.11. Comparing these values with the best experimental results (Table 5.7), it is apparent that all are in good agreement and within the same range of rotation (0.7° to 0.9°).

**Table 5.11 Rotation Results for Loaded Girder at Midspan with Moving Load**

<b>Configuration</b>	<b>Loaded Girder, Top Web Rotation (°)</b>
1-CF @ MS + Top and Bottom Angle	0.799
1-CF @ MS + Top Angle	0.868
2-CF @ MS + Top and Bottom Angle	0.847
2-CF @ MS + Top Angle	0.905

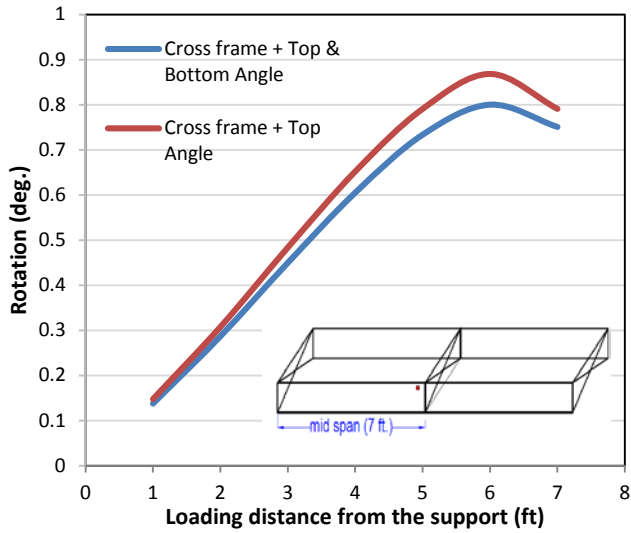


**Figure 5.33** Rotation at top of the web of the loaded girder for one intermediate cross frame with top and bottom angles.

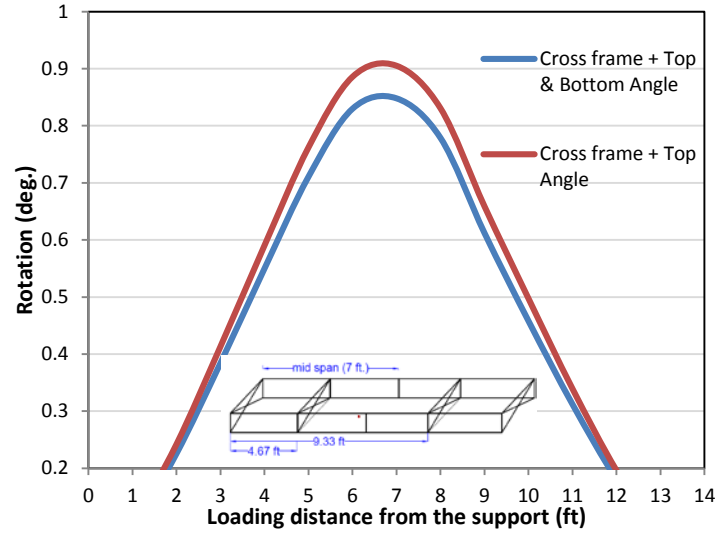


**Figure 5.34** Rotation at top of the web of the loaded girder for two intermediate cross frames with top and bottom angles.

## 5.7 COST-EFFECTIVE ASSESSMENT

An economic comparison of the proposed alternatives and the current block-and-tie methods is presented in Table 5.12 for a 20-ft. long one-bay steel bridge assuming two W21×44 girders at a 6-ft. spacing. The materials cost per unit was based on the approximate purchase cost of the materials when the experimental program was designed. Two cross frame options were evaluated:

- Option 1: placement of one intermediate cross frame (not including the two permanent CF at both ends of the bay)
- Option 2: placement of two intermediate cross braces (not including the two permanent CF at both ends of the bay).

The following assumptions were used in the cost effective assessment:

- Tie bars, timber blocks, and steel pipe were always placed between the two permanent cross frames
- Cost of pipes: diagonal pipe (\$60), horizontal pipe (\$50)
- The use of transverse ties and timber blocks (TT + TB) is the current methodology implemented in the field by IDOT contractors and was therefore used as the baseline to estimate percentile increases or decreases in cost.

**Table 5.12 Cost of Materials for Alternatives in a 20 Ft. Steel Bridge Bay**

Items		Tie Bar (#4)	Timber Block (TB)	Steel Pipe	Cross Frame (CF), Cross Braces Only	Cross Frame (CF) with Top or Bottom Angle	Cross Frame (CF) with Top and Bottom Angle	Tie Bar Hanger	Total Cost (\$)	Percentile increase (+) or decrease (-) related to TT + TB	
Cost/unit (\$)		10	7	60/50	160	200	250	40	582		
<b>ALTERNATIVES</b>	TT+TB	6	6					12	582		
	TT+CF (braces only)	Option 1	6			1			12	700	+20.27%
		Option 2	6			2			12	860	+47.47%
	CF with top or bottom angle	Option 1					1			200	-65.63%
		Option 2					2			400	-31.27%
	CF with top and bottom angle	Option 1						1		250	-57.04%
		Option 2						2		500	-14.09%
	TT+DP	6		4				12	780	+34.02%	
	ADT + HP	6		4				12	740	+27.14%	

## 5.8 SUMMARY

From the experimental program, FE analysis, and the economical assessment, the following conclusions are offered:

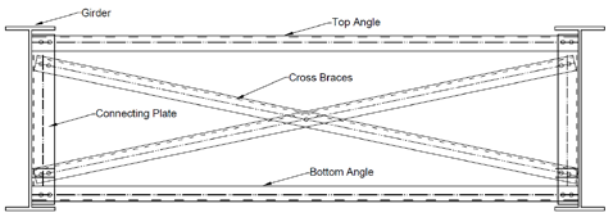
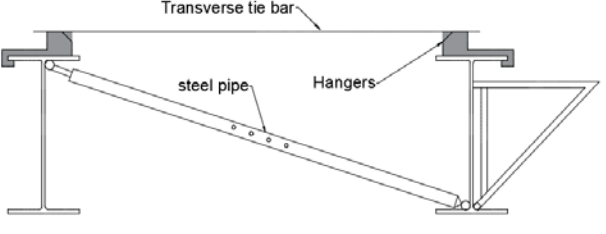
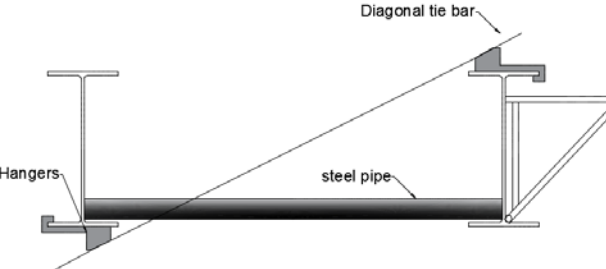
- Improper shimming and poor workmanship can make timber blocks ineffective during construction.
- Misalignment of diagonal ties makes the ties ineffective as a result of the initial bending produced by the forced adjustment to correct the diagonal angle before the bridge is loaded.
- It is comparatively better to use transverse ties instead of diagonal ties when they are connected from the exterior girder to the first interior girder.
- Timber blocks and horizontal steel pipes can be efficient when they are combined with diagonal ties.
- Diagonal pipes can prevent exterior girder rotation efficiently when they are combined with transverse ties.
- Dayton Superior conventional and new hangers perform similarly.
- Intermediate cross frames can be more effective as a rotation prevention method than the installation of bracing tie bars when the cross frames include top or bottom angles or both. If

the cross frames do not include top or bottom angles, it is necessary to include transverse ties to achieve a similar reduction in the exterior girder rotation.

- The FE model presented many challenges regarding the definition of appropriate connections to match the laboratory model, even though it was executed in a controlled environment. Despite this limitation, the results between the FE and the experimental results were similar (10% difference on average for all cases).

Therefore, the three configurations presented in Table 5.13 are recommended to reduce exterior girder rotation.

**Table 5.13 Three Configurations Recommendation for Implementation**

Recommended Options for Field Implementation	Detailing of the Bracing System	Remarks
1. Intermediate cross frames with top- and bottom-angle section		<ul style="list-style-type: none"> <li>• Avoids the need for ties, tie bars, and quality control.</li> <li>• No close observation required in the field to maintain quality control.</li> <li>• Economically efficient.</li> </ul>
2. Transverse ties (exterior girder to first interior girder) + diagonal pipe		<ul style="list-style-type: none"> <li>• Diagonal pipes are reusable but heavy and difficult to install.</li> <li>• Does not eliminate need for quality control for ties and pipes</li> <li>• Not as economically efficient.</li> </ul>
3. Adjusted diagonal ties + horizontal pipe		<ul style="list-style-type: none"> <li>• Diagonal ties require modification of the hangers to proper angle.</li> <li>• Does not eliminate the need quality control for ties and steel pipes.</li> <li>• Steel pipes are reusable.</li> <li>• Not as economically efficient.</li> </ul>

## **CHAPTER 6: EVALUATION AND ASSESSMENT OF IMPROVED ROTATION PREVENTION SYSTEMS**

The recommended rotation prevention systems presented in Chapter 5 were evaluated based on measured and calculated rotations and current IDOT requirements. The three systems were selected based on the experimental testing, which included a traditional cross frame with top and bottom chords and diagonal pipes accompanied by transverse or diagonal ties. The systems were numerically integrated into FE models of the Greenup, Bloomington, and Lincoln bridges using SAP2000. Field rotations measured during construction of these bridges exceeded the maximum rotation permitted by IDOT.

In general, the current rotation prevention system used in Illinois includes transverse ties connecting the top flanges of exterior girders along with timber blocks between the exterior girders and the first interior girders. Observations in the field during construction, however, indicate that these systems are frequently installed improperly. Transverse tie bars are difficult to tighten properly and often interfere with the deck reinforcement and timber blocks are often too short to prevent inward rotation of the exterior girder. Improved rotation prevention systems based on experimental testing are described in Chapter 5. These systems include cross frames between permanent bracing systems or combinations of adjustable steel pipes and transverse ties. These permanent or adjustable systems are selected based on their ability to prevent rotation and the ability to properly install or adjust the bracing as needed. This chapter includes the results from a suite of FE models created to assess the effectiveness of those systems with different spacing and member sizes.

### **6.1 FINITE ELEMENT ANALYSIS**

The FE models include full-scale bridge models including bracing systems, girders, supports, connections, and loads to accurately represent the actual bridge. Three-dimensional shell elements were used to create the girder flanges, webs and diaphragms, while frame elements were used for the brackets and bracing systems. Loads were simplified to represent actual bridge loads including the plastic concrete weight and finishing machine. Validation of the FE models was implemented by comparing the experimental field and FEA results with traditional rotation prevention systems (transverse ties with timber blocks). The improved systems were integrated into these models providing a model with an improved bracing system for comparison. Figure 6.1 shows one of the SAP2000 models incorporating the intermediate cross frames.

#### **6.1.1 Evaluation of Intermediate Cross Frames**

Cross frames or diaphragms are structural elements that distribute loads transversely across the bridge width between longitudinal girders. In this case, the purpose of using additional intermediate cross frames in the exterior panels is to prevent rotation of the exterior girder by bracing against the first interior girder. The shop fabricated connections also ensures proper installation and minimizes the possibility of ineffective bracing.



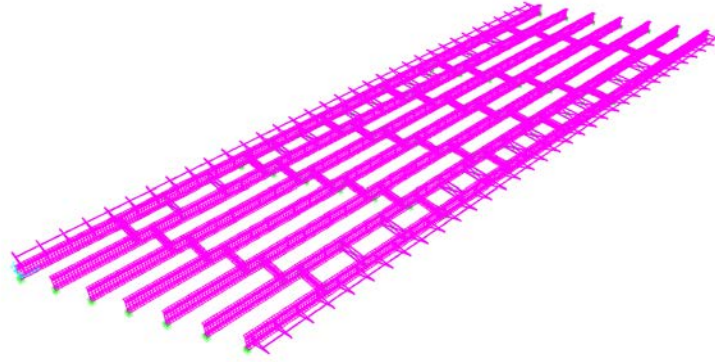


**Figure 6.1 Finite element model (using SAP2000).**

Six different cross-frame arrangements are evaluated for each bridge, as shown in Table 6.1. For the three bridges evaluated in this portion of the analysis, two intermediate cross-frame spacings and three angle sections are evaluated. The intermediate cross frames consist of one or two equally spaced frames located between permanent cross frames. The three angle sections evaluated include L2x2x¼, L4x4x¾, and L6x6x½.

**Table 6.1 Intermediate Cross Frames**

Bridge Name	Number of Intermediate Cross Frames	Spacing of Intermediate Cross Frames (in.)	Cross Section of Intermediate Cross Frames	B/D
Greenup Bridge	1	112.2	L2x2x¼	3.74
			L4x4x¾	
			L6x6x½	
	2	74.8	L2x2x¼	2.49
			L4x4x¾	
			L6x6x½	
Bloomington Bridge	1	118	L2x2x¼	3.94
			L4x4x¾	
			L6x6x½	
	2	78.7	L2x2x¼	2.62
			L4x4x¾	
			L6x6x½	
Lincoln Bridge	1	135	L2x2x¼	4.50
			L4x4x¾	
			L6x6x½	
	2	90	L2x2x¼	3.00
			L4x4x¾	
			L6x6x½	

The results of the analysis are shown in Figure 6.2 through Figure 6.4 for the Greenup bridge, Bloomington bridge, and Lincoln bridge, respectively. In general, exterior girder rotations are significantly reduced to below the IDOT allowable limit in each case through the use of intermediate cross frames without ties and with different cross-frame sections and spacing. Rotation was reduced by 30% or more compared with bridges with traditional rotation prevention systems and by more than 50% compared to the same bridges without bracing. Increasing the number of intermediate cross frames (and the corresponding decrease in B/D ratios) decreases the calculated rotation, but the biggest reduction occurs with the addition of a single cross frame. The angle section selected had a limited effect on girder rotation and therefore should be selected based on stability. The proposed section was able to provide enough stiffness to prevent exterior girders from rotating. However, using a section of L4x4x3/8 was considered the most efficient and effective for economic and safety reasons.

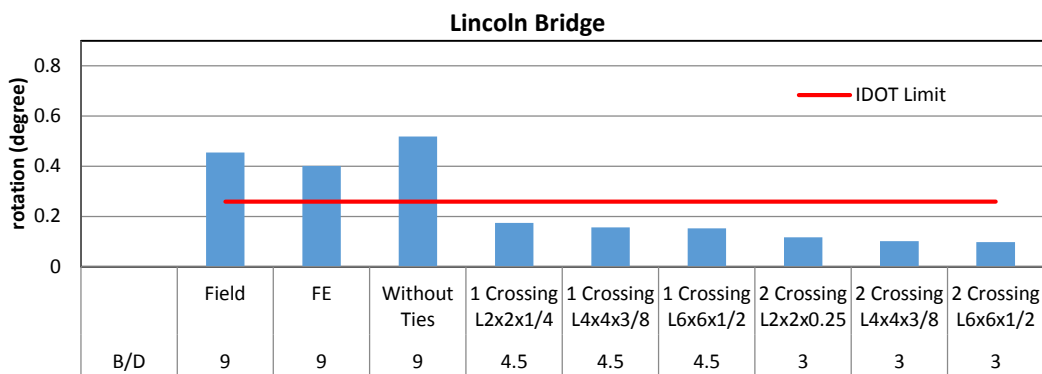


Figure 6.2 Maximum rotations in Lincoln bridge for different types of intermediate cross frames.

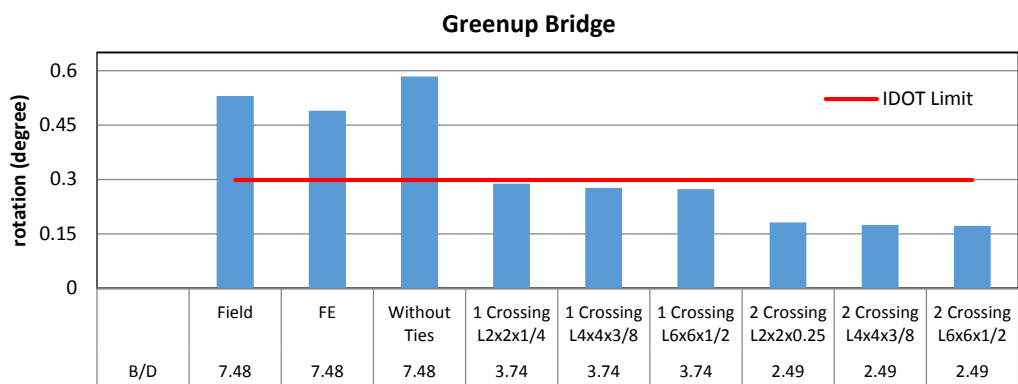
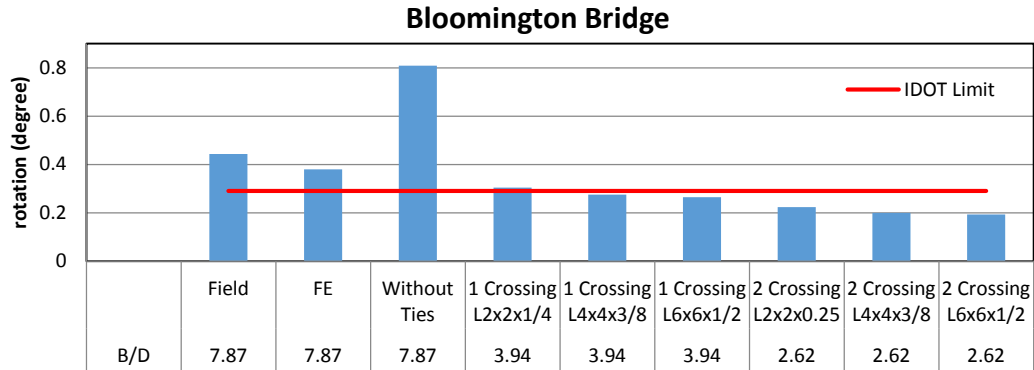


Figure 6.3 Maximum rotations in Greenup bridge for different types of intermediate cross frames.



**Figure 6.4 Maximum rotations in Bloomington Bridge for different types of intermediate cross frames.**

### 6.1.2 Evaluation of Diagonal Pipes (DP) Combined with Transverse Ties (TT)

In this system, transverse ties connect the top flange of the exterior girder and the first interior girder to resist rotation due to unbalanced construction loads. The diagonal steel pipes are placed between the bottom web of the exterior girder and top web of the first interior girder (as shown in Table 5.13, Chapter 5) to prevent the bottom web from rotating inward.

To evaluate this rotation prevention system and to recommend the appropriate spacing, diagonal pipes and transverse ties were placed at two spacings, 4 ft. and 8 ft. and at the mid-distance between permanent bracings for each bridge. As shown in Figures 6.5 through 6.7, one diagonal pipe with a transverse tie placed at the middle of the existing diaphragms reduced the B/D ratio in half and was sufficient to reduce the rotation to meet the allowable vertical deflection limit of all three bridges. A further reduction in the B/D ratio achieved by adding additional pipes and ties resulted in a further reduction of the calculated rotation.

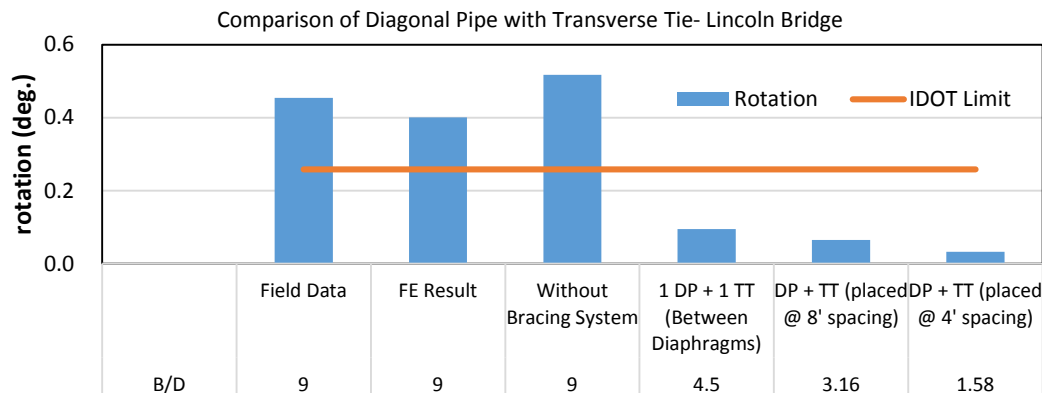


**Figure 6.5 Maximum rotation in Lincoln Bridge for different spacing of pipes and ties.**

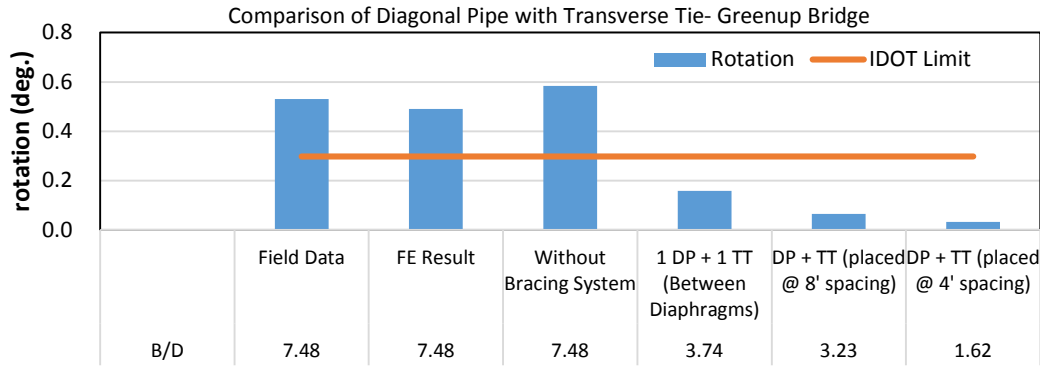


Figure 6.6 Maximum rotation in Greenup Bridge for different spacing of pipes and ties.

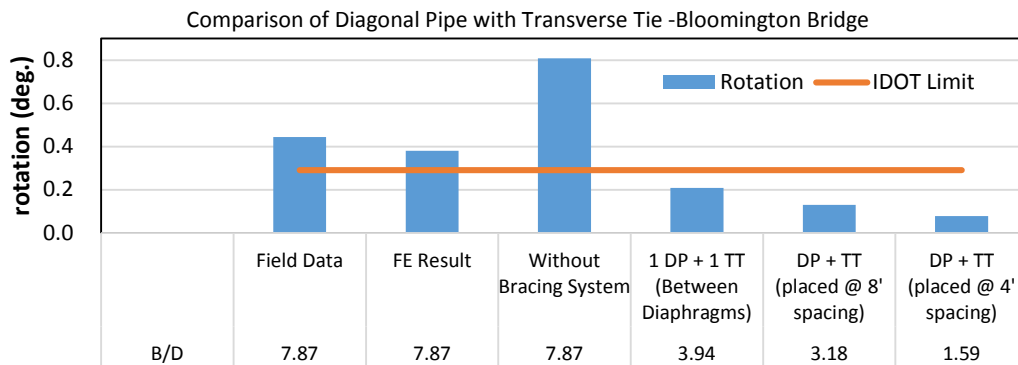


Figure 6.7 Maximum rotation in Bloomington Bridge for different spacing of pipes and ties.

Although the effectiveness of this rotation prevention system was assessed using FEA, the transverse ties and diagonal pipes are still subject to proper field implementation. Adjustable pipes should improve installation compared with the timber blocking currently in use; however, evaluation of field implementation should be conducted to ensure the bracing system is properly applied and effective.

### 6.1.3 Assessment of Adjusted Diagonal Ties (ADT) Combined with Horizontal Pipes (HP)

Diagonal ties connecting the top flange of the exterior girder to the bottom flange of the first interior girder are recommended based on the experimental lab work. When properly oriented, these ties pull the top flange of the exterior girder inwards. In addition, adjustable horizontal pipes have a larger stiffness compared with timber blocks and can be easily adjusted. This system was evaluated at three different spacing including 4 ft., 8 ft. and centered between the existing permanent diaphragms using FEA. The results are shown in Figure 6.8 through Figure 6.10. One horizontal pipe and diagonal ties centered between diaphragms reduced the B/D ratio by 50% but was not effective compared with the previous improved rotation prevention systems evaluated (cross frames or DP + TT). For this system, smaller B/D ratios were required in order to limit rotations to acceptable levels. Improper installation is a potential issue with this system.

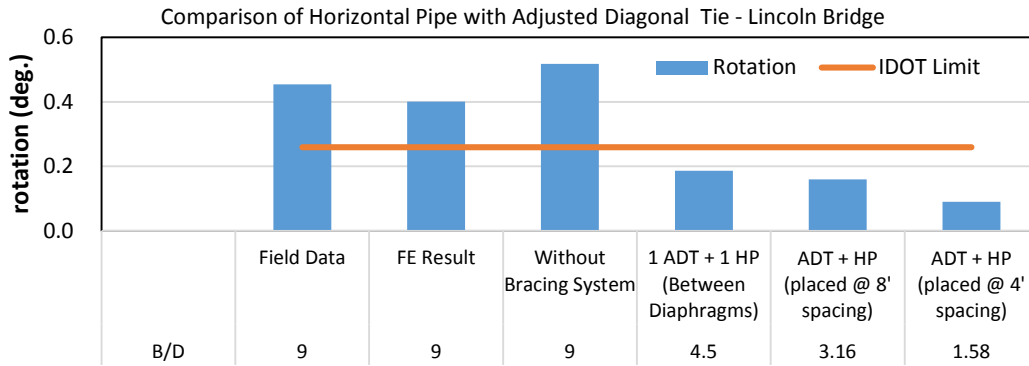


Figure 6.8 Maximum rotation in Lincoln Bridge for different spacing of pipes and ties.

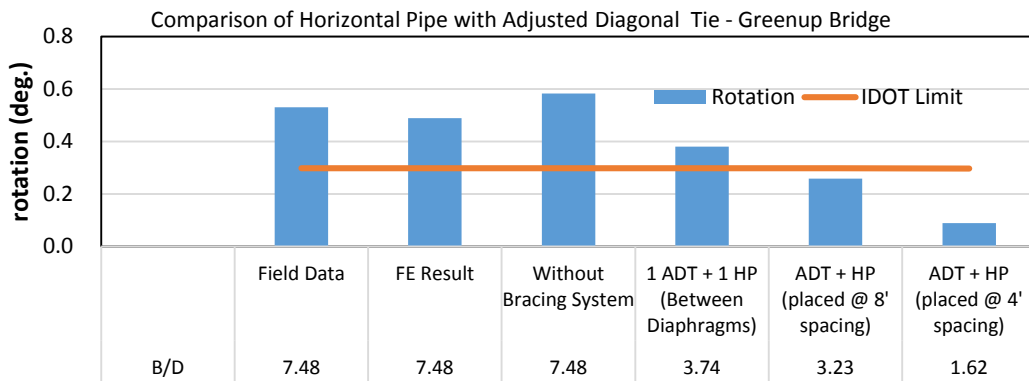


Figure 6.9 Maximum rotation in Greenup Bridge for different spacing of pipes and ties.

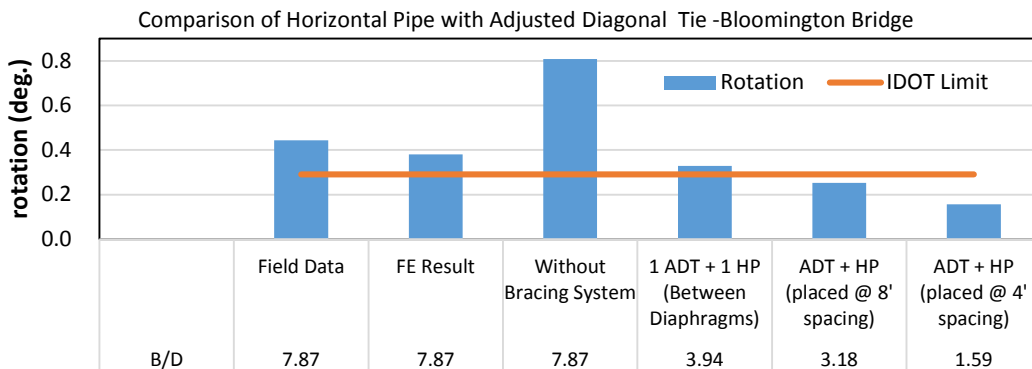


Figure 6.10 Maximum rotation in Bloomington Bridge for different spacing of pipes and ties.

## 6.2 MAXIMUM ALLOWABLE B/D RATIO

Exterior girder rotation depends on the B/D ratio and the bracing system selected. Rotations of exterior girders increases with increases in the B/D ratio—a simple ratio defining the depth of the section compared with the spacing of permanent diaphragms. The B/D ratio also provides a practical way for engineers to determine whether a rotation prevention system is needed and the maximum spacing of the system. To determine the maximum allowable B/D ratio, exponential regression analysis was applied based on five bridges selected from the field study. As a result of the nonlinear regression analysis of these five bridges, a critical ratio is recommended, as shown in Figure 6.11. To take the varied overhang length of the bridges into consideration, the vertical axis represents the difference between exterior girder rotations without bracing systems and relative limits due to the deflection of the overhang of 3/16 in. The horizontal axis shows the B/D ratios. In this case, the critical B/D ratio occurs at the location where the net rotation is zero, which is 3.94. This B/D ratio was determined based upon the five bridges that were monitored in the field during construction. From the field monitored bridges, the maximum and minimum bridge width was 20.17 ft. and 50.67 ft., respectively. The maximum and minimum skew was 0° and 24°, and the maximum and minimum girder depth was 30 in. and 78 in., respectively. The screed load depends on the width of the deck and was calculated using the procedure recommended by the manufacturer (GOMACO, Bidwell, etc.).

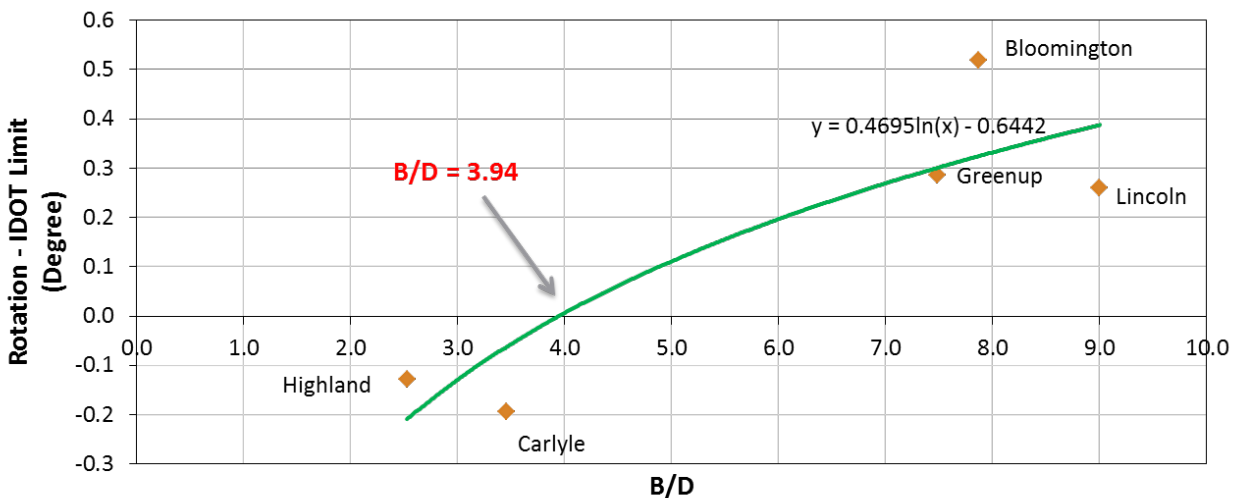


Figure 6.11 Finding allowable B/D ratio.

## 6.3 SUMMARY

The following conclusions can be made from the FEA:

- The improved bridge rotation prevention systems can reduce the rotation to satisfy the IDOT requirement that limits the overhang deflection to 3/16 in.
- Intermediate cross frames are recommended and should be compared with other rotation prevention systems since these effectively reduce or eliminate variability problems associated with tie and bracing systems installed in the field.
- Using intermediate cross frames can reduce rotation by a range of 30% to 70%, depending on the number of intermediate cross frames and bridge dimensions.
- The maximum allowable B/D ratio is 3.94, which can be used to determine whether bracing systems are required for bridges and the number of bracing systems when bracing systems are required.

## CHAPTER 7: CONCLUSIONS AND RECOMMENDATIONS

### 7.1 CONCLUSIONS

The conclusions of this research study are summarized in this section and are based on the data and analysis presented. The study resulted in a substantial improvement in the understanding of bridge deck overhang construction and on the structural behavior of bridge girder systems during construction. The identification of critical overhang geometries was achieved along with the development of design recommendations for overhang construction. The conclusions are provided in the following three subsections.

### 7.2 FIELD-MONITORED DATA

On the basis of the results of the field instrumentation of seven bridges (six steel girders and one concrete girder), the following conclusions can be drawn:

- In general, for steel girder bridges, the maximum rotation of the exterior girder can be expected to occur near the midspan section.
- For bridges with W30 sections or similar size, the maximum exterior girder rotation was between  $0.45^\circ$  and  $0.53^\circ$ . The observed rotation was considered significant compared to the IDOT limit rotation induced from overhang vertical deflection.
- For the medium plate girder cross sections, the maximum measured rotation was  $0.17^\circ$ .
- For bridges with deep plate girders, the maximum rotation was between  $0.098^\circ$  and  $0.16^\circ$ .
- For the concrete girder bridge, a maximum rotation of between  $0.065^\circ$  and  $0.08^\circ$  was measured in the field.
- The rotation in the exterior girder depended on deck overhang width and the diaphragm or cross-frame spacing -to-girder-depth ratio (B/D). Test results showed that as the ratio of the diaphragm or cross-frame spacing to bridge girder depth increases, the rotation of the exterior girder increases. In addition, as the B/D increases, the vertical deflection ( $\Delta$ ) of the overhang also exceeded the current IDOT limit.
- Based on the limited data points for skewed bridges in this study; the skew angle of the bridge played a significant role in affecting rotation of the exterior girder. The rotation increased on the side of the bridge, which was farther from the piers, and as the angle of the skew increased.
- Timber blocks are not an effective temporary bracing technique because of improper shimming and poor installation. With transverse tie bars, improper or inadequate tightening was observed frequently. For diagonal tie bars, bending occurred as a result of the unadjusted angle of those bars. Lack of quality control of these systems was a recurring issue for the seven bridges monitored.



### 7.3 TAEG ASSESSMENT

On the basis of the results of the TAEG program assessment, it was determined that the software did not yield consistent results when calculating the expected rotation of exterior girders during deck construction. The TAEG program consistently underestimated rotations of the exterior girder compared with the field-measured rotations and the detailed FEA. Much of this uncertainty was based on construction issues that occurred in the field that were not possible to model using TAEG—specifically, poor quality control during tie rod and timber block installation resulted in a less effective bracing system. In addition, the program cannot model inconsistent spacing of diaphragms and cross frames. Because the spacing of these permanent lateral supports and the effectiveness of the temporary bracing play a significant role in preventing rotation of exterior girders, these are significant limitations regarding the applicability of the program.

### 7.4 EXPERIMENTAL RESULTS

In the experimental portion of this study, 45 cases were tested and analyzed based on a scaled bridge model and representing different bracing methods and arrangements. On the basis of the results of this study, it was observed that careful attention is required to ensure the correct installation of timber blocks and diagonal tie rods. Improper shimming of timber blocks made them ineffective in resisting rotation of the exterior girder. Misalignment of diagonal tie rods made them ineffective as a result of the initial bending that was produced by the force adjustment required to correct the diagonal angle before loading could begin.

### 7.5 RECOMMENDATIONS

On the basis of the results of this project, the following recommendations are made regarding bracing of exterior girders in to resist rotation during placement of the concrete deck.

#### 7.5.1 WF Beams and Shallow Plate Girders

The following rotation prevention systems are recommended during bridge deck construction:

1. Structural cross-frames or diaphragms as construction bracing. Install intermediate diaphragms or cross frames with both a top- and bottom-angle section in addition to the cross-angle sections in the exterior beam panels to provide exterior beam bracing in lieu of contractor installed transverse tie assemblies. Install the intermediate cross frames so that the B/D ratio is  $\leq 3.94$ . If  $B/D > 3.94$ , install one cross frame, as shown in Figure 7.1. This recommendation is based on the results of FEA and has a number of advantages:
  - a. It allows the designer to avoid the use of tie rods and timber blocks, and it reduces concerns about construction variability and quality control.
  - b. It is economically efficient.
2. Transverse Ties with Diagonal Pipe Struts. Place transverse ties (tied between the exterior girder and first interior girder) plus diagonal pipes in the exterior beam panels. During placement of this type of bracing system, it is recommended to maintain a B/D ratio below 3.94. It is suggested that the transverse ties and diagonal pipes (TT + DP) be placed at a

spacing of 4 to 8 ft. This recommendation is based on the results of both the experimental results and the FEA and based on the recommended B/D ratio of 3.94. Key points to consider when selecting this bracing system are as follows:

- a. Diagonal pipes are reusable but relatively heavy and more difficult to install than typical timber blocking.
  - b. Their use does not omit the need for quality control relating to tie rods and diagonal pipes.
  - c. This system is not as economically efficient. The use of intermediate cross frames may be necessary for bridges where permanent cross frame's are not possible or feasible and contractor installed tie systems may be required. For example, in the case of re-decking existing bridges, it is not be feasible or economical to fabricate and field install additional permanent cross frames.
3. Adjustable Diagonal Ties with Horizontal Pipe Struts. Adjustable diagonal tie rods and horizontal pipes in the exterior panels could be another solution to minimize rotation. It is recommended that the ADT+ HP be placed at a spacing of 4 to 8 ft. This recommendation is also based on the results of both the experimental and FE studies. The following points should be considered when selecting this system:
- a. Diagonal tie rods require modification of the hangers to achieve the proper angle for each structure.
  - b. This system does not eliminate the need for quality control relating to tie rods and steel pipes.
  - c. Steel pipes are reusable.
  - d. This system is not as economically efficient as the use of intermediate cross frames and contractors should determine the optimal case.

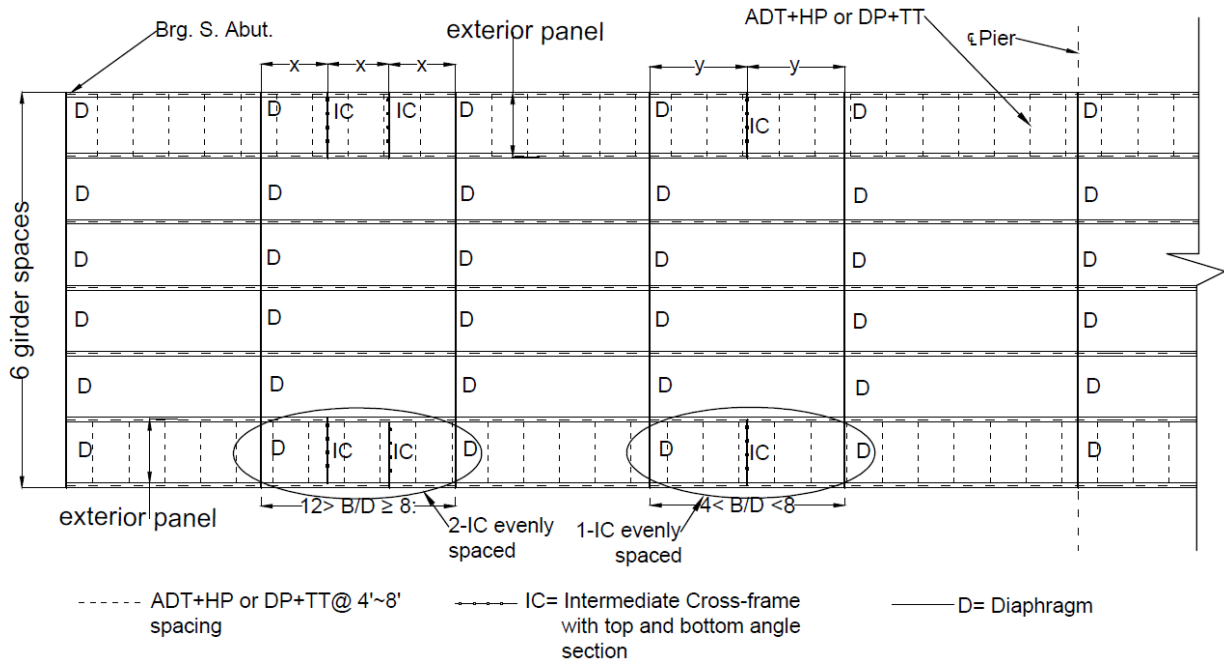


**Figure 7.1. Example of recommended bracing system.**

The following additional recommendations are made to alleviate concerns about rotation of exterior bridge girders.

1. Improved bridge rotation prevention systems can reduce rotation to satisfy the IDOT requirement that limits overhang deflection to 3/16 in.
2. Intermediate cross frames are recommended and should be compared with other rotation prevention systems since these effectively reduce or eliminate variability problems associated with tie and bracing systems installed in the field. Using intermediate cross frames can reduce rotation by a range of 30% to 70%, depending on the number of intermediate cross frames and the bridge dimensions.
3. The maximum allowable recommended B/D ratio is 3.94, which can be used to determine whether bracing systems are required for bridges and the number of bracing systems when bracing is necessary.

### 7.5.2 Medium and Deep Steel Plate Girders

It was seen from the field results and FEA that the rotations with and without a rotation prevention system were much smaller than the IDOT limit. However, it is still recommended to use transverse ties (tied between the exterior girder and first interior girder) plus diagonal pipes or timber blocks. It is also important to keep the B/D ratio within 3.94 (generally not an issue for these girders); otherwise, it is recommended that intermediate cross frames be used to reduce the B/D ratio.

### 7.5.3 Concrete Girders

Only one concrete bridge was monitored in the field, and the rotation was very small compared with the other steel girder bridges and also much smaller than the IDOT specification limit. Therefore, the

current bracing system [transverse ties (tied between the exterior girder and first interior girder) plus timber blocks] is adequate as a rotation prevention system.

## **7.6 FUTURE STUDIES**

A future study is recommended to evaluate and refine the bracing systems that are recommended in this research to limit exterior girder rotation. A future study would further evaluate and validate the effectiveness of any policies, standards, specifications, and details related to these systems. The study would develop specific policy recommendations for B/D requirements for typical beam depths and develop specific language for the IDOT Bridge Design Manual. The study would also determine whether transverse tie bars and timber blocking can be omitted for deep girders or in other situations. Finite element analyses will continue to be used for modeling; however, new software may be developed as an alternative to TAEG to analyze and verify the previously described scenarios and overcome current software limitations. The results of this project are considered a proof of concept and more investigations and parametric studies are needed before a specification could be developed.

## REFERENCES

- AASHTO (2010). LRFD Bridge Design Specifications, Third Edition, American Association of State Highway and Transportation Officials, Washington, D.C.
- Ariyasajjakorn, D. (2006). Full Scale Testing of Overhang Falsework Hanger on NCDOT Modified Bulb Tee (MBT) Girders, Thesis, North Carolina State University.
- Bradford, M. A. (1992). Lateral-Distortional buckling of steel I—Section members. *Journal of Constructional Steel Research*, 23(1), 97-116.
- Brown, R. G., and Meyer, R. F. (1961). The fundamental theorem of exponential smoothing. *Operations Research*, 9(5), 673-685.
- CEN, 1995. Eurocode SS-EN 1993-1-1, S.I.: European Committee for Standardization, Swedish Standards Institute.
- Clifton, S. (2008). Bridge Deck Overhang Construction, Thesis, University of Texas at Austin.
- Dayton Superior Corporation. (2015). Bridge Deck Handbook.
- Fasl, J. (2008). The Influence of Overhang Construction on Girder Design, Thesis, University of Texas at Austin.
- Grubb, M. (1990). Design for Concrete Deck Overhang Loads, Final Report, AISC Marketing Inc.
- Gupta, V. K., Okui, Y., and Nagai, M. (2006). Development of web slenderness limits for composite I-girders accounting for initial bending moment. *Structural Engineering/Earthquake Engineering*; 23(2): 229S-239S.
- Haskett, M., Oehlers, D. J., Ali, M. M., and Wu, C. (2009). Rigid body moment–rotation mechanism for reinforced concrete beam hinges. *Engineering Structures*; 31(5): 1032-1041.
- IDOT (2012). Standard specifications for road and bridge construction, Illinois Department of Transportation, Springfield, IL, USA
- Jones, J., and LaTorella, T. M. (1990). Torsional Analysis of Exterior Girders Subjected to Construction Loading (TAOEGSTCL), Version 1.3, KDOT, Topeka, December, revised December, 1994.
- Kala, Z., Kala, J., Melcher, J., Skaloud, M., and Omishore. A. (2009). Imperfections in steel plated structures—should we straighten their plate elements? Nordic Steel Construction Conference
- Kemp, A. R. (1996). Inelastic local and lateral buckling in design codes. *Journal of Structural Engineering*, 122(4), 374-382.
- Kemp, A. R., and Dekker, N. W. (1991). Available rotation capacity in steel and composite beams. *Structural Engineer*, 69, 88-97.
- Lay, M. G., and Galambos, T. V. (1967). Inelastic beams under moment gradient. *Journal of the Structural Division*, 93(1), 381-399.
- Meadow Burke. Corporate 2835 Overpass Rd. Tampa, FL.

- Mehri, H., and Crocetti, R. (2012). Bracing of steel-concrete composite bridge during casting of the deck. In Nordic Steel Construction Conference.
- Phillips, B., Raju, S., and Webb, S. (1992). Bracing of steel beams in bridges. Center for Transportation Research, Bureau of Engineering Research, University of Texas at Austin.
- Roddis, K., Kriesten, M., and Liu, Z. (1999). Torsional Analysis of Exterior Girders, Report for Kansas Department of Transportation, the University of Kansas.
- Roddis, K., Kriesten, M., and Liu, Z. (2006), TAEG 2.0, Report for Kansas Department of Transportation, the University of Kansas.
- Sayed-Ahmed, E. Y. (2005). Lateral torsion-flexure buckling of corrugated web steel girders. *Proceedings of the ICE-Structures and Buildings*; 158(1): 53-69.
- Shokouhian, M., and Shi, Y. (2015). Flexural strength of hybrid steel I-beams based on slenderness. *Engineering Structures*; 93: 114-128.
- Stanton, J., Roeder, C., Mackenzie-Helnwein, P., White, C., Kuester, C., and Craig, B. (2006). Rotation Limits for Elastomeric Bearings, Final Report for NCHRP, University of Washington.
- Suprenant, B. (1994). Setting Screed Rails for Bridge Deck Paving, Concrete Construction, the Aberdeen Group.
- Winge, A. (2014). Temporary formworks as torsional bracing system for steel-concrete composite bridges during concreting of the deck. LUTVDG/TVBK.
- Yang, S., Helwig, T., Klingner, R., Engelhardt, M., and Fasl, J. (2010). Impact of overhang construction of girder design. Technical Report No. FHWA/TX-10/0-5706-1. Texas, U.S.A.: Texas Department of Transportation.

## APPENDIX A: STATE DEPARTMENTS OF TRANSPORTATION OVERHANG DESIGN GUIDELINES (FASL 2008)

State	Specifications		
California	For Composite Box Girders, 60 percent of the average distance center-to-center of flanges of adjacent boxes, but shall in no case exceed 6 feet (2004).		
Colorado	For Precast concrete and Steel I-Girders, use maximum of center-to-center spacing/3 or flange/web distance + 12" For Steel Box Girders, use center-to-center spacing/3 Overhang criteria may be exceeded with approval from Staff Bridge Engineer (1991).		
Connecticut	Minimum of four feet or depth of the member (2003).		
Delaware	Normal overhang is 2'-6." Maximum overhang is half the beam spacing or 4'-0," whichever is less (2005).		
Florida	Use empirical design method for overhangs less than 6'-0" and traditional design method for total deck overhang is less than 6'-0" (2008)		
Kansas	Use TAEG software to determine torsional loads (2006).		
Maine	Type of Beam	Beam Spacing	Maximum Deck Overhang
	Structural Steel	Less than 9'-0"	3'-0" or depth of beam
		9'-0" to 10'-6"	1/3 of the beam spacing or depth of beam
		Greater than 10'-6"	3'-6" or depth of beam
	Concrete	All	2'-0"
Michigan	Follow typical details, maximum overhang = 2'-6"		
Montana	For steel girders, the overhang width restrictions (more strict of): 1. Not more than 0.30 to 0.35 times the beam spacing to balance moments in interior and ext. beams 2. Not more than the depth of the beam, or 3. Not more than 1200 mm For prestressed concrete beams, the overhang dimensions are standardized (2002)		
Nebraska	Max overhang = 4'-6" For up to 5-girder bridges, minimize overhang and if the exterior girder controls, use exterior girder design for all girders. For more than 5-girder bridges, minimize the overhang and use the interior girder design for the entire bridge (2006).		
Nevada	Deck overhangs shall be considered as falsework and designed as such (2001)		
New York	The recommended maximum overhang of a concrete deck slab beyond the centerline of the steel fascia I-girder is 4 ft. In addition, the maximum overhang for steel fascia I-girders less than 5 ft in depth should be limited to 3 ft. The use of an overhang greater than 3 ft. with steel fascia I-girders less than 5 ft. in depth requires a detailed analysis (2008).		
Ohio	In order to facilitate forming, deck slab overhangs should not exceed 4'-0" (2004).		
Oregon	Deck overhangs should be no more than one-half the span length (2004)		
South Carolina	Deck overhang shall be designed in accordance with Section 13 of the LRFD Specifications.		
Texas	Maximum overhang is lesser of 3'-11" or 1.3 times depth of girder from centerline of beam (2001).		
West Virginia	For bridges with structurally continuous concrete barriers, the minimum total overhang width shall be 3.0 times the depth of the deck, measured from the center of the exterior girder (AASHTO 9.7.2.4). The maximum total overhang width shall be the smaller of 0.625 times the girder spacing and 6 feet (2004).		

## APPENDIX B: DETAILS OF THE BRIDGES

### B.1 FUNDAMENTAL INFORMATION OF THE MONITORED BRIDGES

**Table B. 1 Basic Information for All Field-Monitored Bridges**

	Lincoln Bridge	Greenup Bridge	Bloomington Bridge	Highland Bridge	Belleville-II Bridge	Carlyle Bridge	Belleville-I Bridge	
Contract No	72E11	74466	70570	76836	76884	76479	76884	
Beam Type	W30x132	W30x99	W30x124	48" PLG	64" PLG	78" PLG	72" Bulb-T	
Skewed?	None	24°	3.8°	None	30°	None	30°	
Staged?	Yes	No	Yes	No	yes	No	No	
No of Spans	3	7	3	2	2	2	1	
Span length	54'	52'	81'	116'	145'	200'	126'-4"	
Overhang Width	3'-5.5"	3'-0"	3'-1"	2'-11.5"	3'-5"	3'-4"	2'-11"	
Girder Spacing	7'-3"	6'-4"	7'-0"	7'-4"	9'-1"	6'-6"	5'-4"	
Tie Type	Diagonal (ext. girder top to first int. girder bottom )	Transverse (ext. girder to furthest ext. girder)	Transverse (ext. girder to furthest ext. girder)	Transverse (ext. girder to furthest ext. girder)	Transverse (ext. girder to furthest ext. girder)	Transverse (ext. girder to furthest ext. girder)	Transverse (ext. girder to first int. girder)	
Screed Type	Vibrating Paver	Screed machine	Screed machine	Screed machine	Screed machine	Screed machine	Screed machine	
Screed Rail Support Location	On overhang deck	On overhang deck	On Overhang deck	On overhang deck	On overhang deck	On overhang deck	On overhang deck	
Diaphragm spacing	Span-1	15.2'	17.1', 24v	19.4', 11'	W:10.8', 8.7' E:21.7', 8.7'	21.5', 25' 23.4'	19.5', 23.6'	
	Span-2	15.5', 22.5'	15.8', 17.3', 18.7'	11', 19.7'	W:10.8', 8.7' E:21.7', 8.7'	22.6', 25' 16.1'	22.4', 23.6' 19.5'	32.5', 31.6', 29.4'
	Span-3	15.2'	23.6', 16.7'	19.4', 11'				

### B.2 PLAN VIEW OF GROUP 1 BRIDGES

**Table B. 2 Sensor Locations on the Bridges**

	Location of tilt sensors		
	Lincoln Bridge	Greenup Bridge	Bloomington Bridge
<b>Section S1: at midspan with no diaphragm</b>	<i>Exterior girder:</i> bottom flange and the web	<i>Exterior girder:</i> bottom flange	<i>Exterior girder:</i> bottom flange and the web
	<i>First interior girder:</i> bottom flange	<i>First interior girder:</i> bottom flange	<i>First interior girder:</i> bottom flange
<b>Section S2: at diaphragm location</b>	<i>Exterior girder:</i> bottom flange and the web	<i>Exterior girder:</i> bottom flange	<i>Exterior girder:</i> bottom flange
<b>Section S3: with no diaphragm</b>	<i>Exterior girder:</i> bottom flange and the web	<i>Exterior girder:</i> bottom flange	<i>Exterior girder:</i> bottom flange



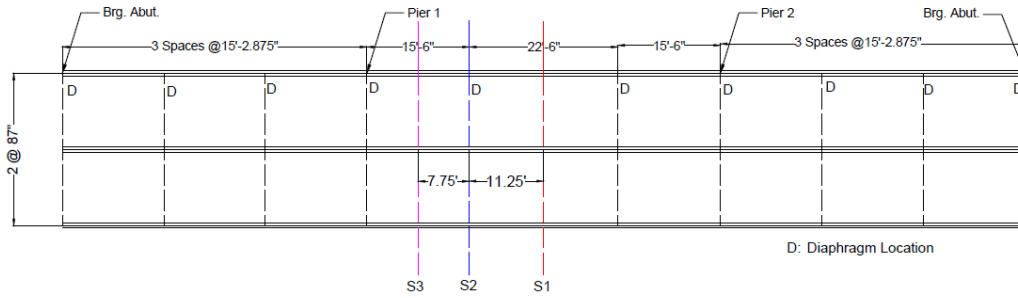


**Figure B.1 Plan of the Lincoln bridge and the chosen sections for instrumentation.**

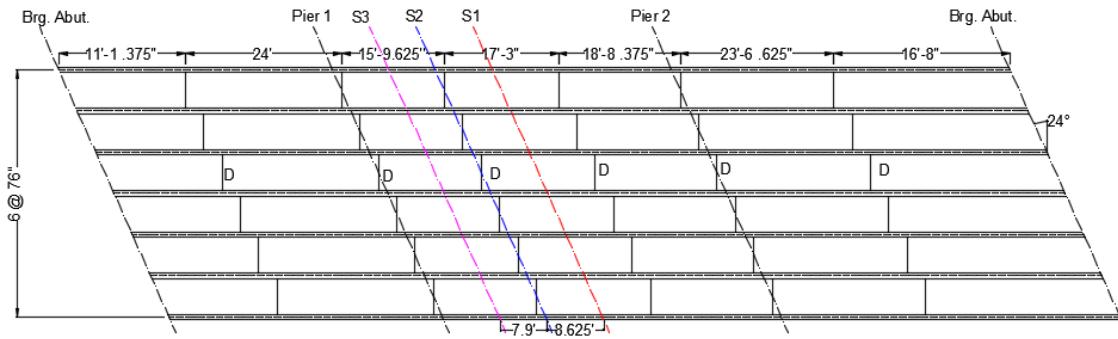


**Figure B.2 Plan of the Greenup bridge and the chosen sections for instrumentation.**

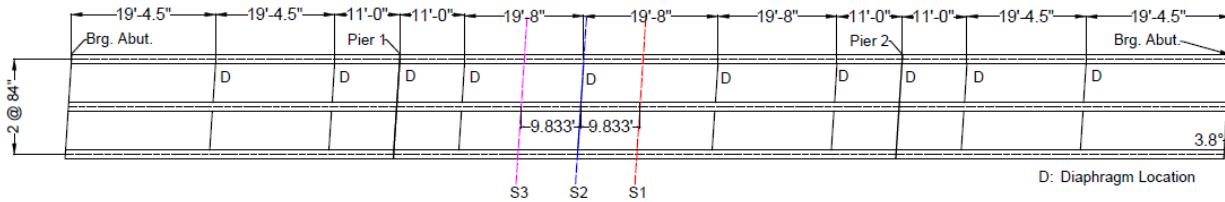
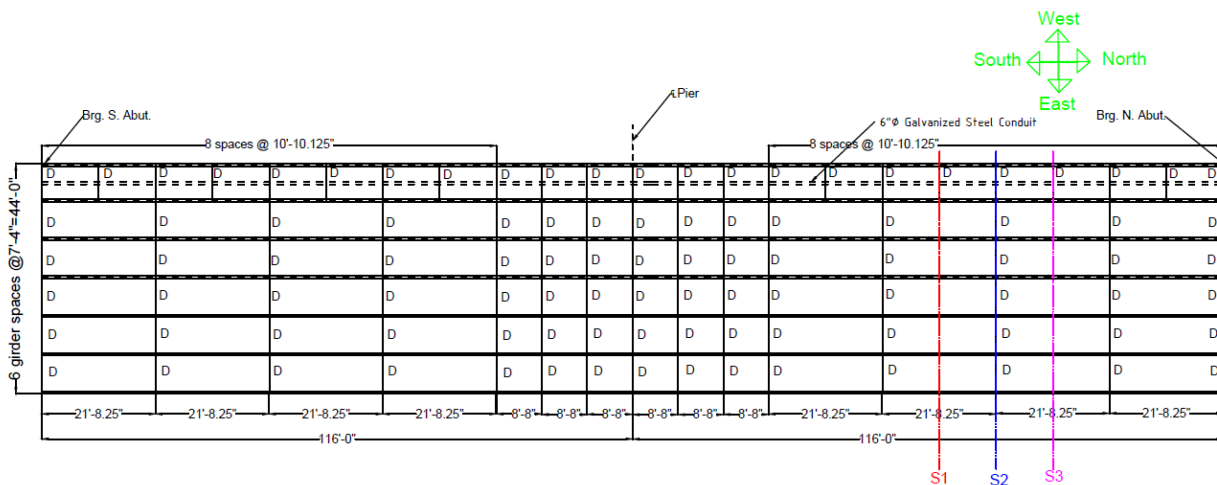


**Figure B.3 Plan of the Bloomington bridge and the chosen sections for instrumentation.**

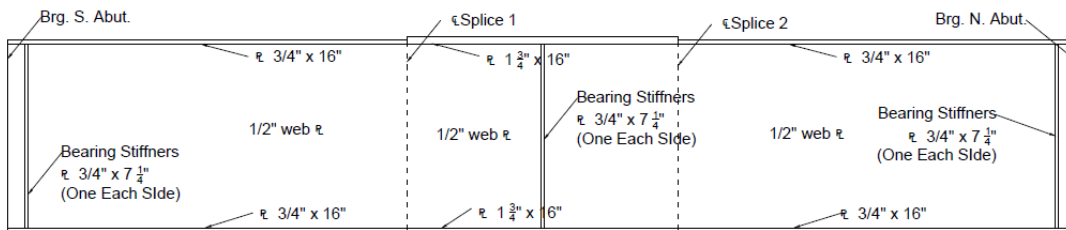
### B.3 PLAN VIEW OF GROUP 2 BRIDGES

**Table B.3 Location of Tilt Sensors on Group 2 Bridges**

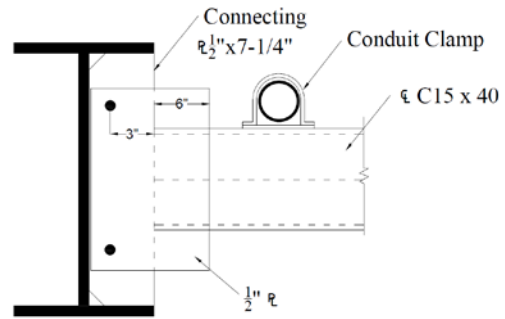
	Location of tilt sensors			
	West end		East end	
	Exterior girder	First interior girder	Exterior girder	First interior girder
<b>Section S1</b>	<i>Location:</i> bottom flange and the web <i>Presence of diaphragm:</i> Yes	<i>Location:</i> bottom flange	<i>Location:</i> bottom flange and the web <i>Presence of diaphragm:</i> No	<i>Location:</i> bottom flange
<b>Section S2</b>	<i>Location:</i> bottom flange and the web <i>Presence of diaphragm:</i> Yes	--	<i>Location:</i> bottom flange and the web <i>Presence of diaphragm:</i> Yes	--
<b>Section S3</b>	<i>Location:</i> bottom flange and the web <i>Presence of diaphragm:</i> Yes	--	<i>Location:</i> bottom flange and the web <i>Presence of diaphragm:</i> No	--



(a)



(b)



(c)

**Figure B.4 Detail of the Highland bridge: (a) Plan of the bridge with sections instrumented, (b) Elevation of the exterior plate girders, and (c) Detailing of the west side diaphragms.**

## B.4 PLAN VIEW OF GROUP 3 BRIDGES

Table B.4 Location of Sensors on the Bridge

	Location of tilt sensors	
	Carlyle Bridge	Belleville-II Bridge
<b>Section S1: with no diaphragm</b>	<i>Exterior girder: bottom flange and the web</i>	<i>Exterior girder: bottom flange and the web</i>
<b>Section S2: at diaphragm location</b>	<i>Exterior girder: bottom flange and the web</i>	<i>Exterior girder: bottom flange</i>
<b>Section S3: no diaphragm</b>	<i>Exterior girder: bottom flange and the web</i>	<i>Exterior girder: the web</i>

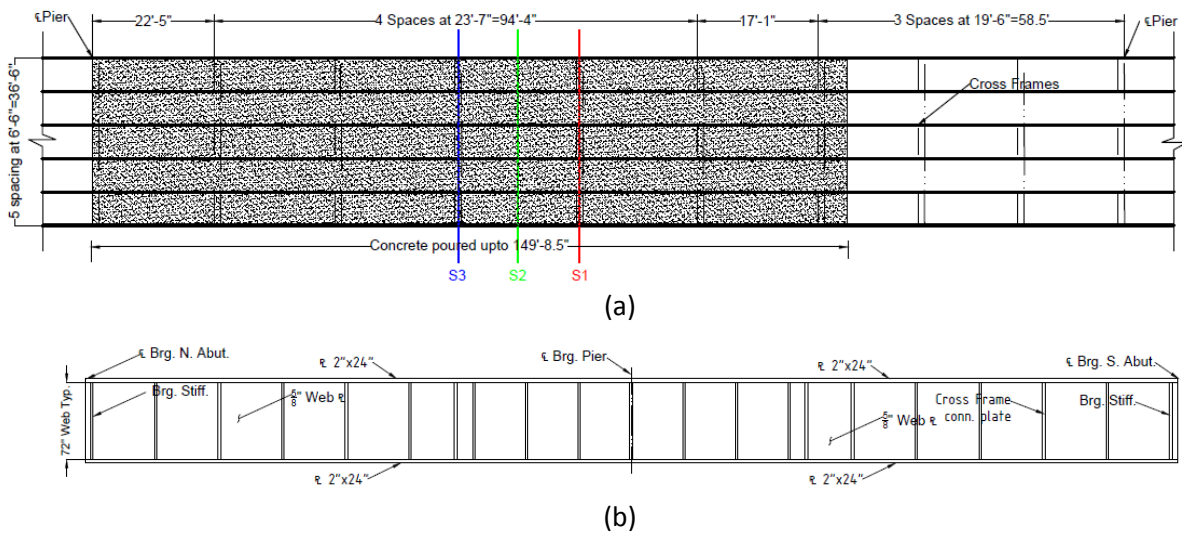
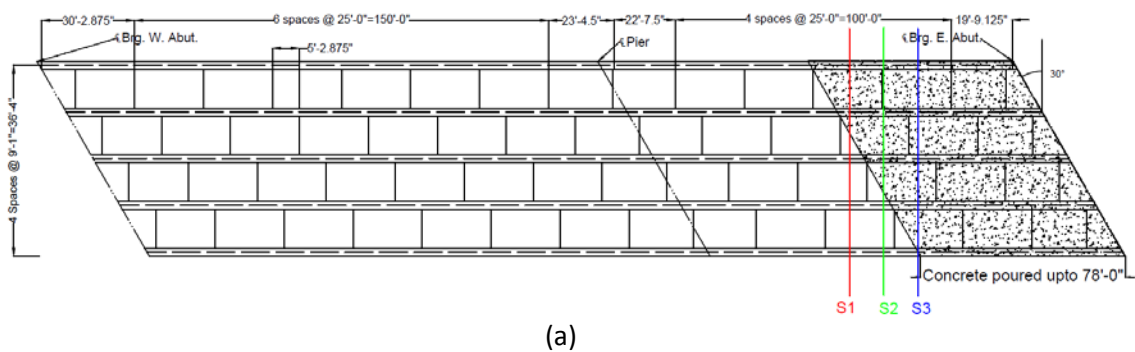
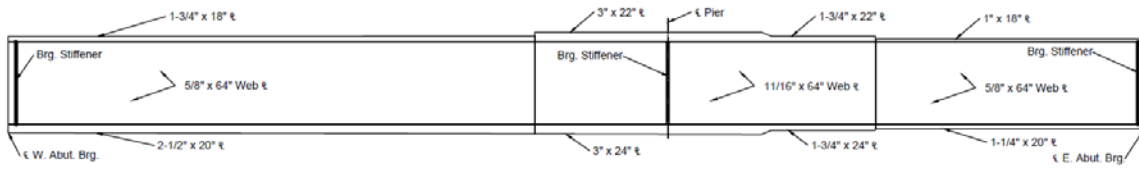


Figure B.5 Carlyle bridge. (a) Plan of the bridge, (b) Elevation of the exterior girders.





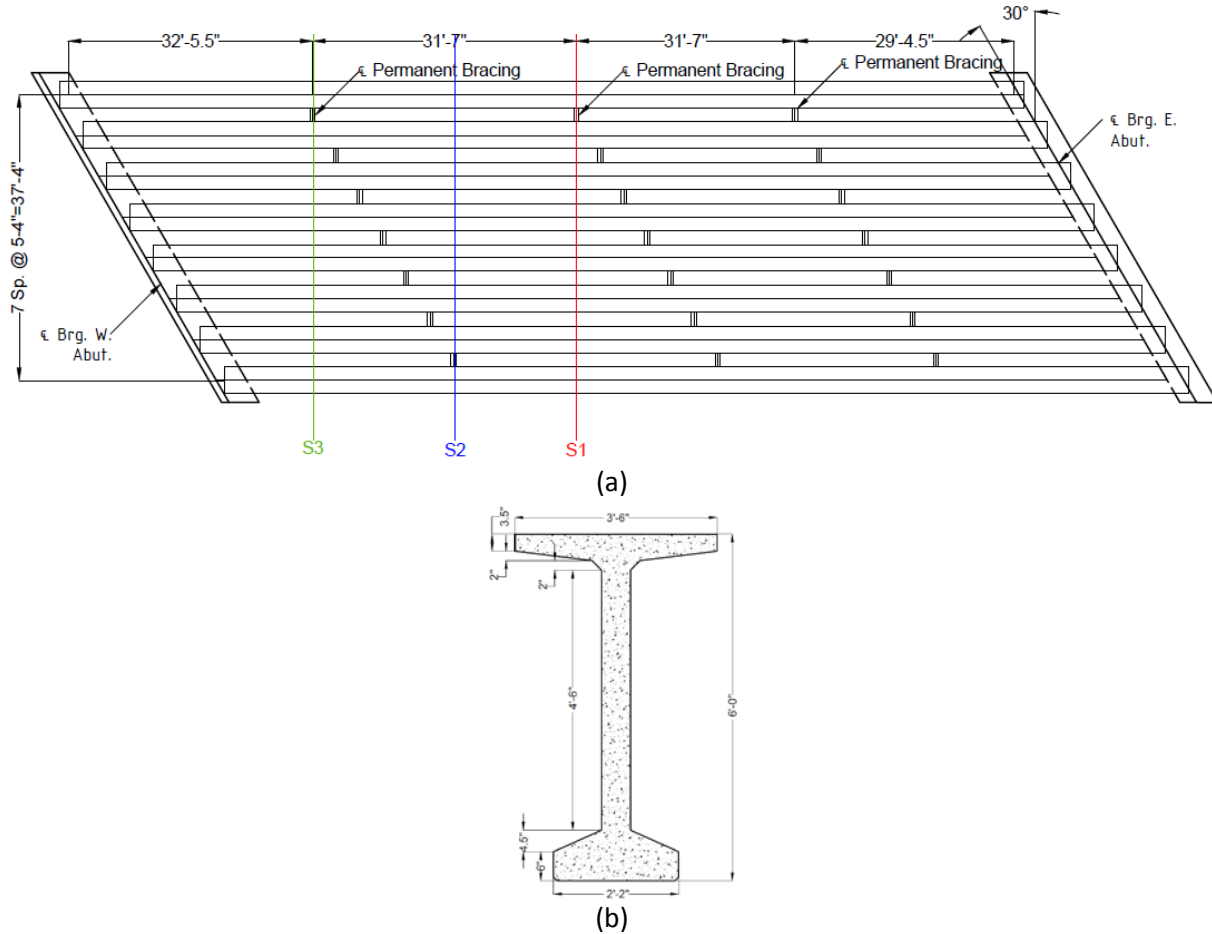
(b)

Figure B.6 Belleville-II bridge. (a) Plan of the bridge, (b) Elevation of the exterior girders.

## B.5 PLAN VIEW OF GROUP 4 BRIDGES

**Table B.5 Location of Tilt Sensors on the Bridge**

Location of tilt sensors	
<b>Section S1</b>	<i>Exterior girder: bottom flange and mid of the web</i>
<b>Section S2</b>	<i>Exterior girder: bottom flange and mid of web</i>
<b>Section S3</b>	<i>Exterior girder: bottom flange and mid of web</i>



**Figure B.7 Detail of Belleville-I bridge (concrete girder bridge).**

**(a) Plan of the bridge with sections for instrumentation, (b) Cross section of the girder.**

# APPENDIX C: TORSIONAL ANALYSIS OF EXTERIOR GIRDERS (TAEG)

## C.1 DESCRIPTION OF ANALYSIS ASSUMPTIONS

A number of assumptions are implemented in the TAEG program for the purpose of simplicity including the conditions described in the sections that follow.

### C.1.1 Description of Loading Conditions

The TAEG program assumes that the weight of the plastic concrete is only placed on the exterior tributary area of the exterior girder. In reality, this weight should be placed on both the exterior and interior of longitudinal girders. This simplification is done in order to attain a conservative estimate of the concrete weight acting to rotate the exterior girder.

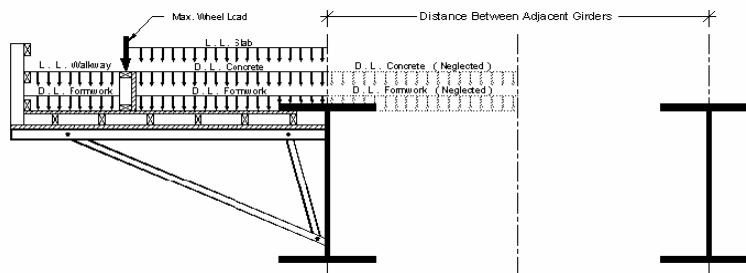


Figure C.1 Placement of loads in the TAEG program (TAEG 2.1 User's Manual 2005).

The program also assumes that the entire span of the bridge is placed, meaning that the exterior girder's bay is entirely loaded by the weight of the wet concrete. The distribution of these loads is shown in Figure C. 1.

### C.1.2 Location of Maximum Rotation

The program assumes that the maximum rotation occurs at the mid-span of the longest span of a bridge, as this would constitute the point furthest from the piers or abutments, where rotation is assumed to be negligible. Therefore, the program only reports the results of the rotation of the exterior girder at mid-span.

### C.1.3 Diaphragm Spacing

The TAEG program only permits input for uniformly spaced diaphragms. When the spacing was not uniform throughout the bridge span, as was the case for the bridges analyzed in this study, the diaphragm spacing at mid-span was input into the program as the spacing between permanent lateral supports. This was also the recommended method given by the TAEG contact at KDOT (Paul Kenseth, personal communication, January 16, 2015).

### C.1.4 Overhang Width

The width of the worker's walkway along the exterior girder was assumed to be 24 inches for all bridges analyzed based on observations from the field. The live loads for the walkway and for the slab were assumed to be 15 psf each as was recommended by the Indiana Department of Transportation Design Manual (INDOT, 2013). All overhang brackets were assumed to be placed such that the bottom of the bracket was 6 inches from the bottom flange of the exterior girder based on observations in the field.

### C.1.5 Temporary Lateral Supports

Temporary lateral supports, including transverse tie bars and timber blocks, were assumed to be spaced at 48 inches. Transverse tie bars were considered to be #4 bars, with a cross sectional area of 0.196 in<sup>2</sup>. Timber blocks were considered to be 4 in. x 4 in. timber pieces. These assumptions and inputs were done to meet IDOT specifications for the case when screed rails are used (IDOT 2012). However, the TAEG program limits the number of temporary lateral supports between permanent lateral supports to three or less. If the number of temporary lateral supports exceeded three, then an equivalent cross-sectional area of the temporary lateral supports must be utilized and these larger temporary lateral supports are placed in such a manner as to most accurately reflect the placement of the supports in the real bridge. If an odd number of temporary lateral supports are used, then three temporary lateral supports were input with an equivalent cross-sectional area that would satisfy the spacing requirement. If the number of temporary lateral supports exceeded three with an even number, then two temporary lateral supports were input. Temporary lateral supports were evenly distributed between the permanent lateral supports. The setup of the tie bars and timber blocks is shown in Figure C. 2, demonstrating how these are placed between the exterior girder and the first interior girder. The program assumes full engagement of these tie bars and timber blocks, meaning that the timber blocks are assumed to be in full contact with the bottom of the exterior girder and there is no slack in the tie bars.

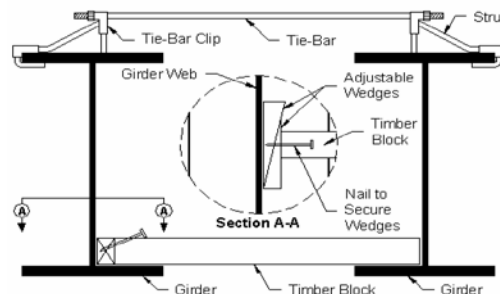


**Figure C.2 Tie bar and timber block setup (TAEG 2.1 User's Manual 2005).**

For this research study, seven bridges were inspected and monitored in the field, with only five bridges analyzed using TAEG. The Belleville I and Belleville II bridges were not included in the analysis. The Belleville I bridge is a concrete girder bridge, which cannot be analyzed using the TAEG program. The Belleville II bridge had a deck placing sequence which was different than the other bridges, and the TAEG does not have an option to simulate such situations. The Highland bridge was analyzed twice due to the inconsistency of the bracing system on the two exterior panels of the bridges. For



each of the bridges, multiple cases were considered for the placement of the temporary lateral supports and the data was recorded for each of these cases in order to compare it with the field results. For these different cases, the arrangements and placement of the tie bars and timber blocks were varied to help account for the uncertainty within the temporary lateral supports in the field. These arrangements included a full or equivalent cross sectional area for both the tie bars and timber blocks spaced at even intervals between the permanent lateral supports, placement of two and three tie bars and timber blocks spaced at even intervals between permanent lateral supports, exclusion of the tie bars and exclusion of the timber blocks, inclusion of only one tie bar and timber block placed at the center between the permanent lateral supports, and a final case where tie bars and timber blocks were neglected.

## **C.2 UNIFORM BRIDGE ANALYSIS**

In order to perform a final evaluation of the TAEG program, a finite element model was created of a fully uniform bridge. The same bridge was also modelled using TAEG in order to see how well the program results matched the results from the finite element model.

The bridge had a span length of 80 ft. Permanent lateral supports were diaphragms, spaced evenly at 16 ft. Because the spacing was 16 ft., temporary lateral supports could be properly placed, with three tie bars and timber blocks placed between the permanent diaphragms and spaced at 4 ft. Diaphragms were C12×25 sections. Longitudinal girders were spaced at 7 ft. and were W30×124 Grade 50 beams. The bridge did not have skew. This bridge was also modeled in Abaqus with the same parameters and both models were evaluated. The finite element model is shown below in Figure C. 3. Within this finite element analysis, temporary lateral supports were included and were assumed to be attached to the girders and were therefore fully engaged.

The TAEG program yielded a rotation of  $0.40^\circ$  at midspan. As the bridge closely resembled the Bloomington Bridge, the girder rotation was consistent with the previous data obtained from running the Bloomington Bridge. The Abaqus model yielded rotation results of  $0.43^\circ$  at the bottom flange of the exterior girder and  $0.45^\circ$  at the web.

A second analysis was also done on a uniform bridge which had noticeable skew. The bridge configuration shown in Figure 4.10 was modified to have a skew angle of  $30^\circ$ . In order to make the arrangement of the diaphragms function properly in the Abaqus model, the spacing between diaphragms was changed to 15 feet. Within the TAEG program, the skew was adjusted to its setting of greater than  $20^\circ$  and asymmetric loading. The Abaqus model of the skewed bridge is shown below in Figure C. 4.

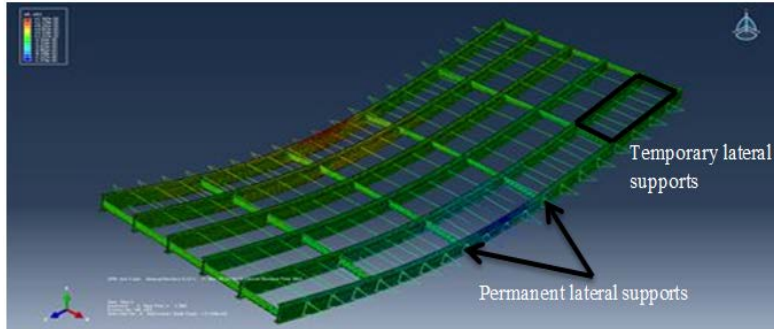


**Figure C.3 Finite element model of a uniform bridge in Abaqus.**

The results of this model were in much less agreement between the TAEG and Abaqus models. The TAEG program calculated a rotation of  $0.00^\circ$ , with no deflection of either the top or the bottom flanges. The Abaqus model calculated a rotation of  $0.17^\circ$  on the side, which was closer to the pier and  $0.63^\circ$  on the side, which was further from the pier. The TAEG program experienced further unexpected behavior by giving no rotation in a circumstance when this did not seem to make sense as the model was very similar to the previous model performed in the previous section when the bridge did not have skew.

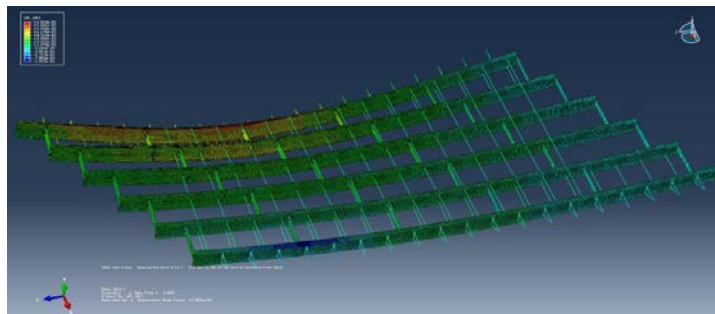


**Figure C.4 Finite element model of a bridge with skew angle of  $30^\circ$  in Abaqus.**

Based on this comparison, the TAEG program yielded results, which were fairly consistent with the results of the finite element program when the bridge did not have skew. Significant conclusions can be drawn from this study including the significance of engagement and effectiveness of the temporary lateral supports and the significance of bridge skew. When the finite element included full engagement for the temporary lateral supports and when the modeled bridge was not skewed, the results for the finite element program were fairly consistent with the results from TAEG.

### **C.3 PROGRAM LIMITATIONS**

Based upon the results of this overall study, the TAEG program contains a number of limitations which affect its overall accuracy. These limitations include the following:

- The program assumes full engagement of temporary lateral supports (tie bars and timber blocks) and does not allow for the inclusion of gaps in the onsite installation
- The program only allows for one input for the spacing of permanent lateral supports

- The program is not able to account for local distortions in the bridge girders
- The program cannot account for intermediate diaphragms or other alternatives like the temporary lateral supports, including pipes or different materials
- The program does not properly consider the effects of skew
- The program provides no visual representation of the bridge assembled, resulting in difficulty verifying that inputs are correctly being included
- Unable to account for unique construction conditions

The spacing of permanent lateral supports is also significant as the arrangement of these supports plays a significant role in affecting the global stiffness of the exterior girder. As the program is unable to include multiple spacing distances for the permanent lateral supports, the program is unable to properly model bridges with irregularly spaced supports. As was shown earlier, this variable within the program also demonstrated a certain amount of inconsistency, with its modification yielding seemingly unexplainable results. As the diaphragms and cross frames represent an essential parameter in assessing the rotational stiffness of the bridge, and therefore have a considerable effect on the rotation which can take place, uncertainty with this parameter represents a noticeable limitation.

Another significant limitation of the program is its inability to account for unique construction conditions. Within the Lincoln Bridge, there were a number of other construction circumstances which were possible to include in finite element modeling and not using the TAEG program. The TAEG program is unable to properly account for this circumstance other than including loading on only one side of the bridge. As other unique circumstances exist, such as alternative bracing methods, the program's inability to account for these conditions represents a significant limitation.

# APPENDIX D: ADDITIONAL INFORMATION FROM THE EXPERIMENTAL PROGRAM

## D.1 DESCRIPTION OF THE SETUP ELEMENTS

### D.1.1 Girders

To finalize the twin girder system, two W21×44 girders 15 ft. in length within one span are selected for this experimental program as shown in Figure D.1. These girders are smaller and lighter than the most common girder sections used in actual bridge design. However, this girder type was considered to have minimum rigidity that would permit consistent results and enable differentiation between bracing systems. This criterion was based on the relation between the girder length and the minimum rotation needed to overcome the sensitivity of the tilt sensors. The lateral distance between the two girders was required to be an even value since the embedded anchoring points were located on 2 ft. × 2 ft. centers. Taking this into consideration and the distance between girders in the instrumented bridges (6.33 ft. minimum distance, 7.33 ft. maximum distance), the adopted distance was 6 ft.

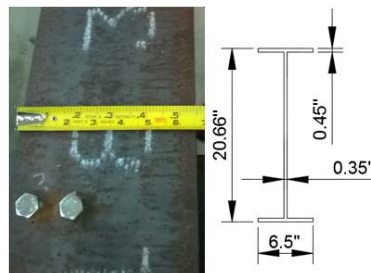


Figure D.1 W21x44 dimensions.

### D.1.2 Tie Bars

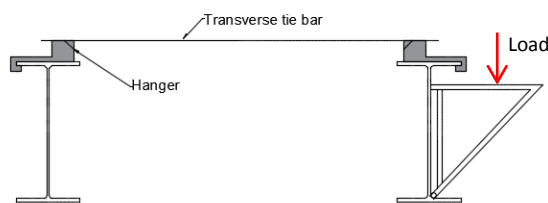
Tie bars are the current bracing system used in the field to control exterior girder rotation; therefore, different configurations with 2, 3 and 4 tie bars were proposed and tested to evaluate performance. Grade 60 epoxy-coated #4 reinforcement was used, depending on the test case. Threaded connections were used to connect the tie bars to the girder hangers using nuts and washers as shown in Figure D.2. The torque in the connection was applied using a manual controlled electronic torque wrench that permitted to apply a constant torque between 5.5 and 6 ft-lb for all cases.



Figure D.2 Transverse tie connected to Dayton Superior C137 tie bar beam clip pre-stress hanger.

Three tie bar configurations are tested within the testing matrix:

- Transverse Ties (TT): Connected from the top flange of the non-loaded girder to the top flange of the loaded girder. This configuration is the most commonly used in the field (Figure D.3).
- Unadjusted Diagonal Ties (UDT): Connected from the top flange of the loaded girder to the bottom flange of the non-loaded girder. The bars are lightly bended before the load is applied due to its installation method. This configuration is currently used in the field as an alternative to the transverse tie configuration (Figure D.4).
- Adjusted Diagonal Ties (ADT): Connected from the top flange of the loaded girder to the bottom flange of the non-loaded girder. The ties are placed diagonally with a straight shape. This option was tested as an alternative of the two previous cases (Figure D.5).



**Figure D.3 Transverse tie configuration.**

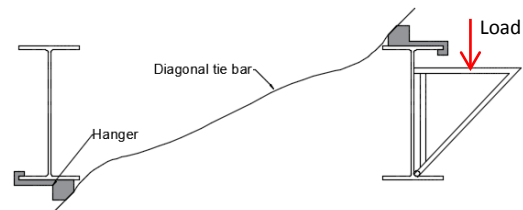


**Figure D.4 Unadjusted diagonal tie configuration.**

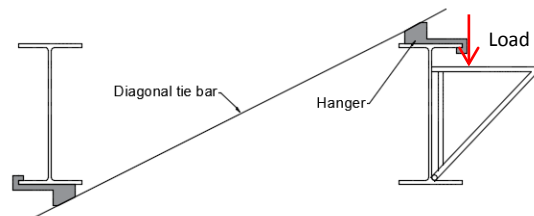


**Figure D.5 Adjusted diagonal tie configuration.**

### D.1.3 Bracket

One bracket is installed at mid span of the exterior girder to simulate the bridge overhang load. The bracket has to be consistent with the girder type that is being tested. Therefore, based on its horizontal and vertical adjustment range ratio, the C49JR Bridge Overhang Bracket (Figure D.6) is selected from the four options that Dayton Superior provides as shown in Table D.1. Dayton Superior was selected as the bracket supplier following recommendations from IDOT representatives. This bracket is normally used when there is limited space between twin girders. This bracket allows for a coil rod angle of 45 degrees. The coil rod (#4 rebar) is the element that connects the girder flange with the hanger clip. Threaded connections with a nut and a washer are used in each end of the coil rod. The B12 Continuous Coil Threaded Rod has a 0.5-in. diameter and a SWL of 9 kips. The B13 Coil Nuts are adapted for the coil rod threading.

**Table D.1 Bracket Types (Dayton Superior)**

	Vertical Adjustment Range (in.)	Horizontal Length (in.)
C49	30-50	54
C49D	50-70	54
C49S	16-28	54
C49JR	16-28	27

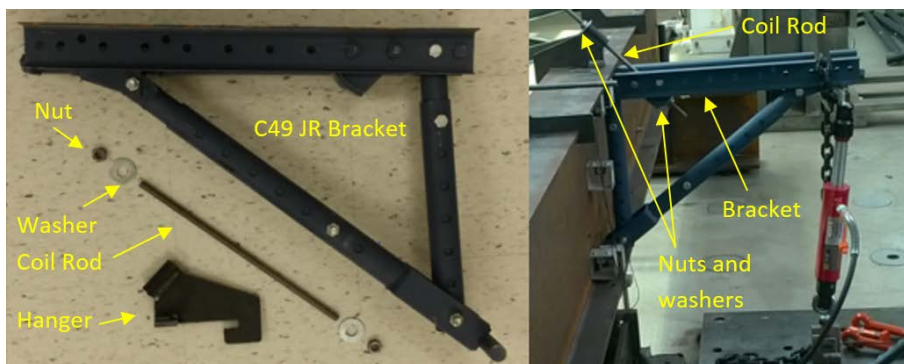


**Figure D.6 Bracket C49 JR installed in loaded girder.**

## D.1.4 Hangers

### D.1.4.1 Dayton Superior C68 4 AB Pre-Stress Hanger

The Dayton Superior C68 4 AB pre-stress hanger (shown in Figure D.7) is a “J” shape hanger adequate for supporting overhang formwork when stay-in-place metal decking is used on the interior bays of a bridge deck. The hanger is engaged to the flange, without the necessity of any welding. This hanger has a 45 degrees end clip that allows for a 0.5 in diameter coil rod. This hanger type is commonly used on the field.

### D.1.4.2 Dayton Superior C67 Tie Bar Beam Clip Pre-Stress Hanger

The C67 tie bar beam clip pre-stress hanger (Figure D.8) is a half hanger that attached to the edge of the top flange to his “J” shape. No welding is required. This type is also widely used in the field for supporting overhang formwork over stay-in-place decking. It allows for a 0.5 in diameter coil rod.

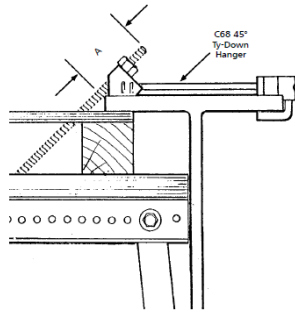


**Figure D.7 C68 4 AB pre-stress hanger.**

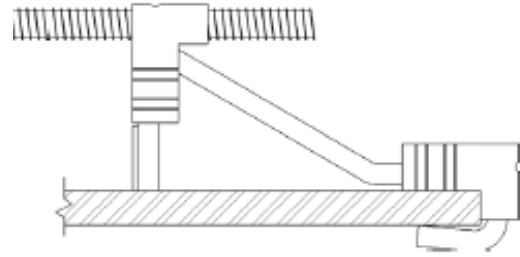


**Figure D.8 C67 tie bar hanger.**

#### *D.1.4.3 Modified Conventional Combined C68 4 AB Pre-Stress Hanger and C 67 Tie Bar Beam Clip Pre-Stress Hanger*

In the field, the C68 4 AB and C67 hanger types are mounted together in a reversible hanger that can be used for both types. However, this type of hangers that is used for actual construction did not fit the experimental girders because of the reduced flange thickness. Because of that, as shown in Figure D.9, the front part of the hanger was removed and a small metal support plate was welded to the body of the hanger. Also, for engaging the hanger to the girder flange, it was necessary to weld a customized small C-channel section that allowed the hanger to fit into the flanges of the W21×44 girder. The mechanical properties of the hanger remained the same after the modifications.

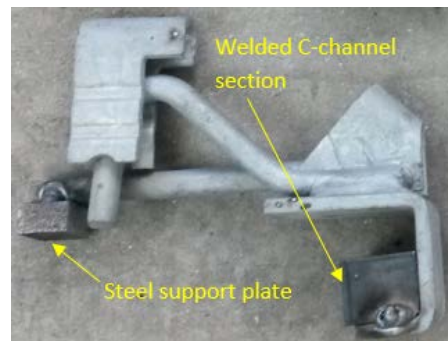


**Figure D.9 Modified combined C68 4AB and C67 hanger.**

#### *D.1.4.4 Dayton Superior C134 4 AB Pre-Stress Ty-Down Half Hanger*

According to Dayton Superior, this hanger can be substituted for the C68 4 AB pre-stress. The new C134 4AB (Figure D.10) is being progressively introduced in the market; therefore, testing them in this research will permit us to compare behavior between current hangers and those proposed by the supplier. This hanger can be used for two purposes:

- The first purpose is the connection of the bracket to the girder, holding in place the coil rod that is connected at both the hanger and the bracket.

- Also, the hanger can be used for connecting the ties to the girders for the case that was previously denominated as unadjusted diagonal tie (UDT). In both cases the hanger is not modified and the connection clip angle between the coil rod and the tie is 45 degrees.

#### *D.1.4.5 Dayton Superior C137 Tie Bar Beam Clip Pre-Stress Hanger*

According to Dayton Superior, the C137 hanger will substitute the C67 tie bar beam clip pre-stress hanger and it is being progressively introduced in the market. Testing the new C137 type in this study will permit us to compare the new C137 with the conventional C67. This hanger is the only one used for the transverse ties cases as Figure D.11 shows.

#### *D.1.4.6 Modified C137 Tie Bar Beam Clip Pre-Stress Hanger*

This type of hanger is slightly different from the new C137. This type of hanger is a special type of hanger and not readily available since it was custom made. As can be seen in Figure D.12, this type has been modified and tailored to the specific test set up characteristics in order to be able to test the adjusted diagonal cases (ADT) where the ties are installed straight. The mechanical properties of the hanger have not been changed. The adjusted angle is approximately 21°.



**Figure D.10 C134 4AB pre-stress ty-down half hanger (Dayton Superior).**



**Figure D.11 C137 tie bar beam clip pre-stress hanger (Dayton Superior).**



**Figure D.12 Modified C137 tie bar beam clip pre-stress hanger.**



### D.1.5 Load Application System

The vertical load is applied from a manually operated jack that hooks to the bracket with a steel chain as shown in Figure D.14. The use of a U-bolt was considered as an alternative to the chain but dismissed because the chain didn't introduce any relevant eccentricity. The hydraulic jack is connected to a load cell, which is bolted to a reaction frame. The reaction frame is bolted to the floor using four bolts. A maximum load of 2.5 kips is applied gradually at the horizontal leg of the bracket at a distance of 2.5 in. from the tip to maximize the rotation values as shown in Figure D.13.

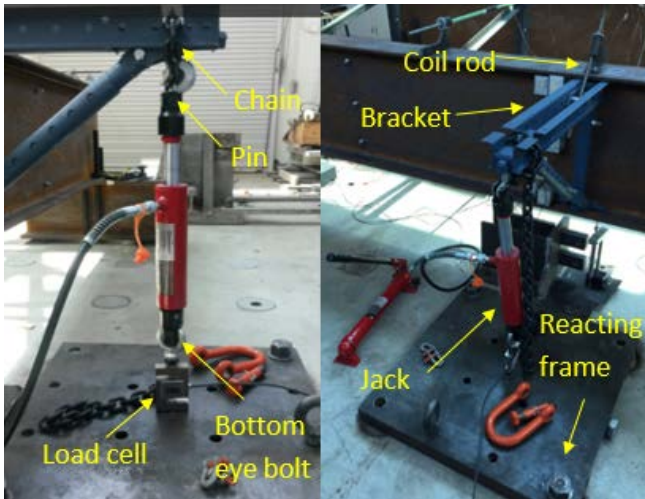


Figure D.13 Hydraulic jack and bracket.

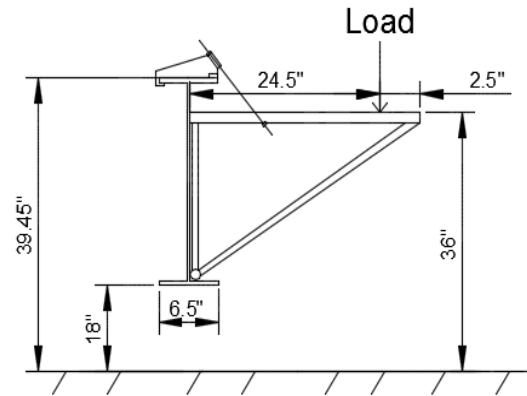


Figure D.14 Attachment of bracket to the girder.

### D.1.6 Girder Supports

Design of the girders supports was one of the critical issues for two reasons:

- The rotation and displacements at the supports needed to be null. It was necessary to assure null rotation and displacement at the supports to avoid issues at the time of interpreting the data and model the scaled bridge bay using finite elements.
- No overturning movement was permitted for the girders because of safety reasons.

To assure zero rotation and displacement at the supports it was a key to take into account the uncertainties of the threaded anchors embedded in the strong floor (depth and +/- 0.5 in. error on the distance from center to center). Because of that, an extra rigid and conservative bolted connection type was designed as shown in Figure D.15 and Figure D.16. Four A36 W14x82 girders three feet long are used as girder supports. Those W14x82 girders are connected from the top flange to the floor using bolted connections with long bolts type A325 1 3/8 in x 6 TPI with an allowable tension of 55 kips. The distance between them is 2 ft. A nut and a washer are used both at the bottom and top flange of the support girders to tighten the girders to the floor and adjust the connection.

To connect the main girders to the support girders, in each of the four girder supports there are four more holes in both flanges in order to accommodate the bolts that connect the support and the main

girders. The W21x44 girders have 4 holes located at the bottom flange where the same type of long A325 bolts are used to connect them to the support girders. In this occasion the bolts go through both flanges of the support girders and the head of the bolts are placed below the bottom flange of the support girders.

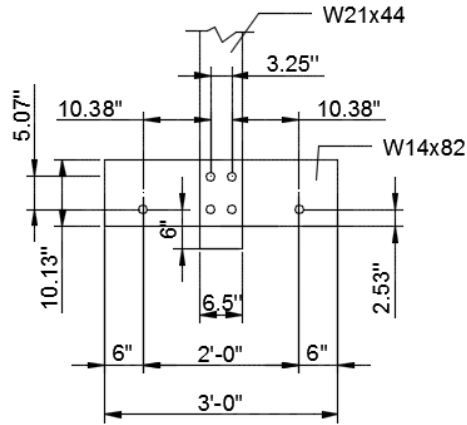


Figure D.15 Connection detailing between girders and floor.

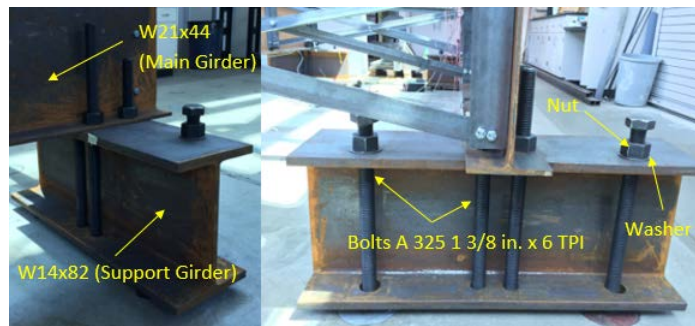


Figure D.16 W14x82 girder support and connecting bolts.

### D.1.7 Cross Frames

Two permanent cross frames (CF) are placed at both ends of the scaled model between the main girders to simulate the effect of the cross frames in the real bridges as it is shown in Figure D.17. Consequently, only rotation at the mid span is allowed. The distance between the two permanent cross frames is 14 ft. The cross bracings are L2x2x1/4 sections, and the connecting plates are L3x3x1/4 sections. Bolts of diameter 0.75 in. were used to bolt the connecting plates to the girder webs, and bolts of diameter 0.5 in. were used to connect the cross bracings to the connecting plates. Furthermore, two top angle L 2x2x1/8 sections were placed at the same level of the cross frames and bolted to the top flanges of the W21x44 girders.

Two additional cross frames were assembled with the goal of testing several combinations that included intermediate cross frames. The intermediate cross frames were placed between the two permanent ones at different locations depending upon the test case. The two removable cross

frames were built using the same sections and bolts used for the permanent cross frames, but in this case no top angle was added to the cross bracing.

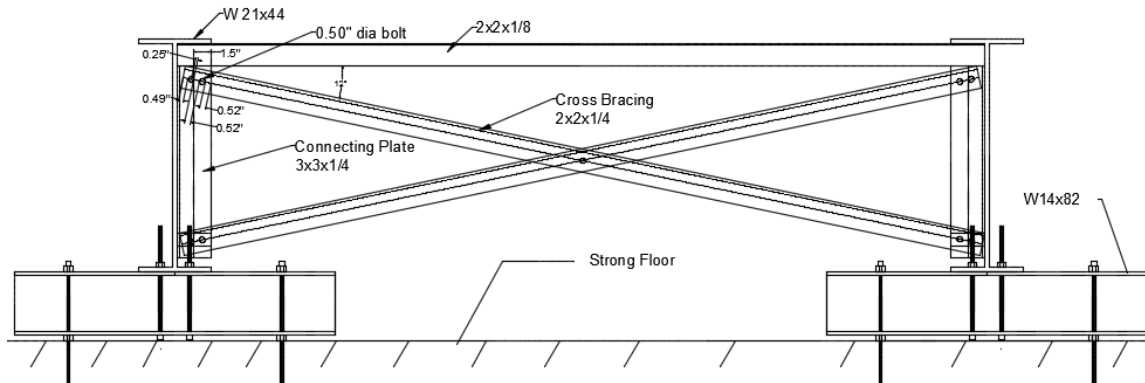


**Figure D.17 Cross section at permanent cross frame location.**

## **D.1.8 Compression Struts**

### *D.1.8.1 Timber Blocks (TB)*

Timber blocks with a 6 ft. length and a cross section of 4 in. x 4 in. were installed at the bottom flange-web intersection using wood shims to adjust the timber ends as shown in Figure D.18. This procedure is similar to the one that is used in the field by contractors. The timber blocks were added when three and four ties were tested. One timber block per tie is used and they were placed approximately at the same location of the tie bar.

### *D.1.8.2 Horizontal Steel Pipes (HP)*

Horizontal steel pipes with diameter of 1.5 in was Installed horizontally at the top surface of the bottom flanges of the main girders as shown in Figure D.19. The pipes were cut in 6 ft. length and a thin metal plate was welded in one of the ends of every pipe in order to create a larger surface contact between the pipe and the girder web. The other end of the pipes was threaded so an appropriate pipe coupler was used to adjust the pipe to the required position as shown in Figure 3.20. The pipes were placed at the lower part of the web and they were tested together with the ties for the 3 and 4 ties cases. One pipe was used per tie and both of them were used at the same location.

### *D.1.8.3 Diagonal Steel Pipes (DP)*

Steel pipes with a diameter of 2-3/8 in were placed diagonally from the bottom of the web of loaded girder to the top of the web of non-loaded girder as shown in Figure D.20. The diagonal pipes were created from the modification of four floor jack posts, which are commonly used in building construction. Depending on the test case, one, two, three or four DP were combined with the cross bracing and / or the tie bars. In order to determine the most effective pipe size, a detailed parametric study will be needed.



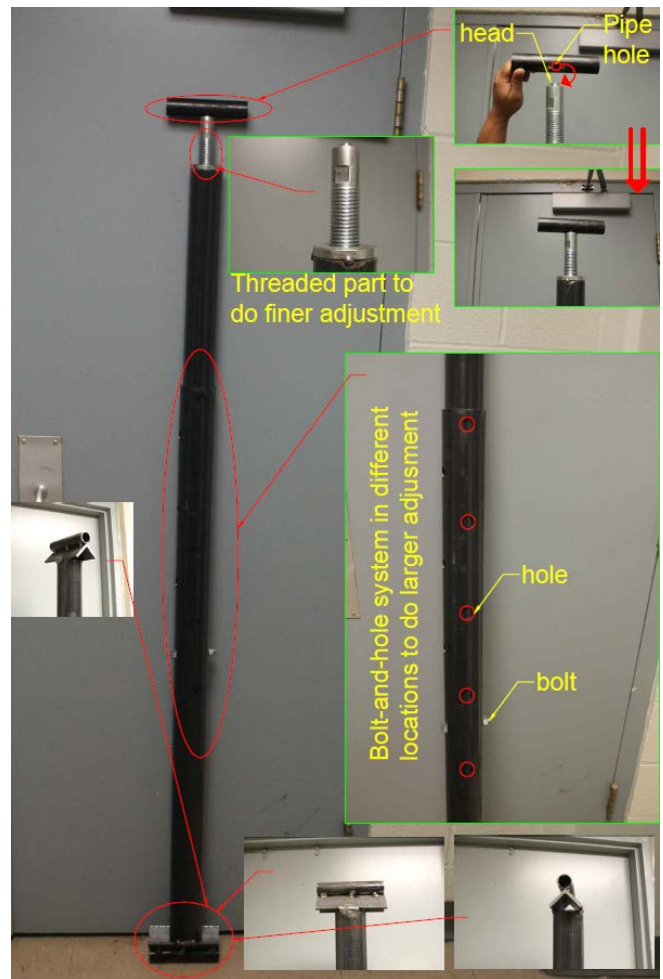
Figure D.18 Timber blocks at scaled model.



Figure D.19 Horizontal steel pipes at scaled model.



(a)



(b)

Figure D.20 Diagonal steel pipes at scaled model.

## D.2 LABORATORY LAYOUTS AND MOST RELEVANT CROSS-SECTIONS FROM THE TESTED CASES IN THE EXPERIMENTAL PROGRAM

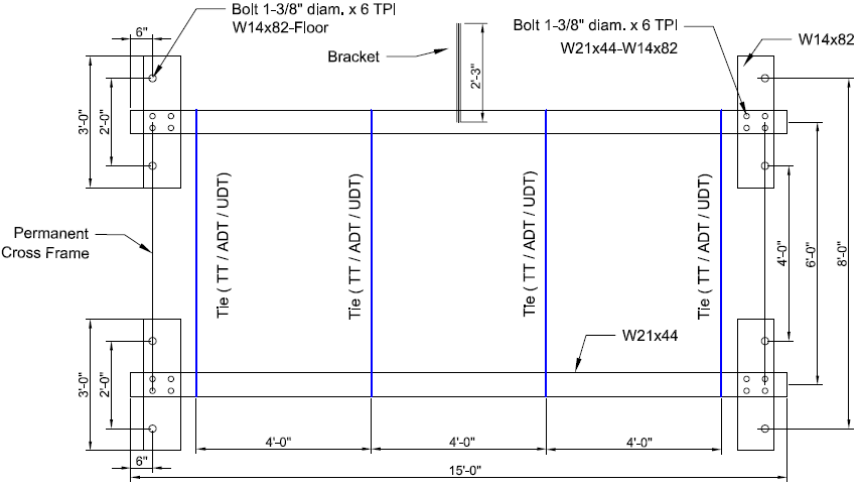


Figure D.21 Plan view for configurations with 4 ties (TT / ADT / UDT).

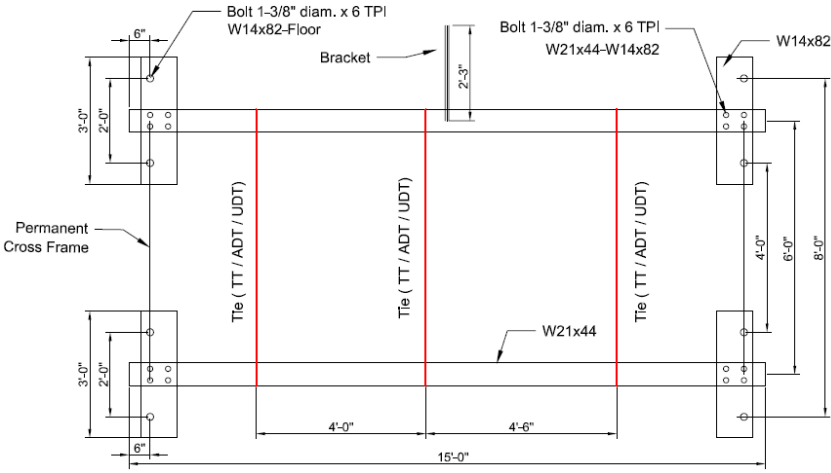


Figure D.22 Plan view for configurations with 3 ties (TT / ADT / UDT).

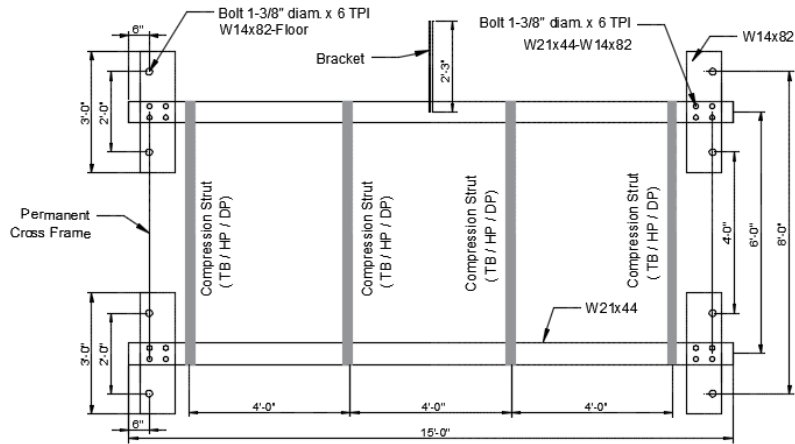


Figure D.23 Plan view for configurations with 4 compression struts (TB / HP / DP).

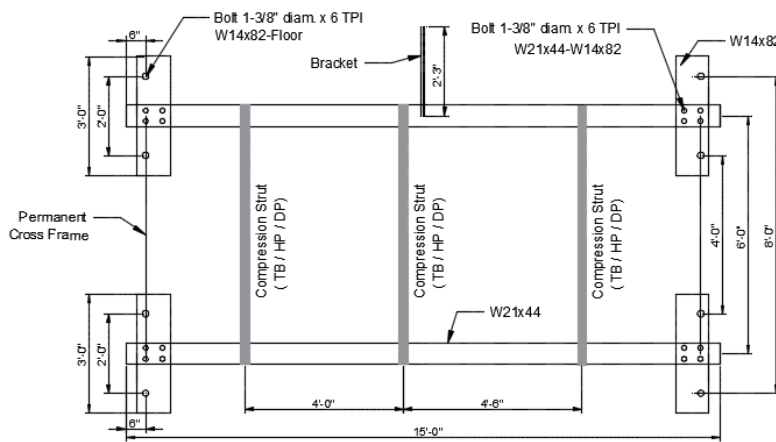


Figure D.24 Plan view for configurations with 3 compression struts (TB / HP / DP).

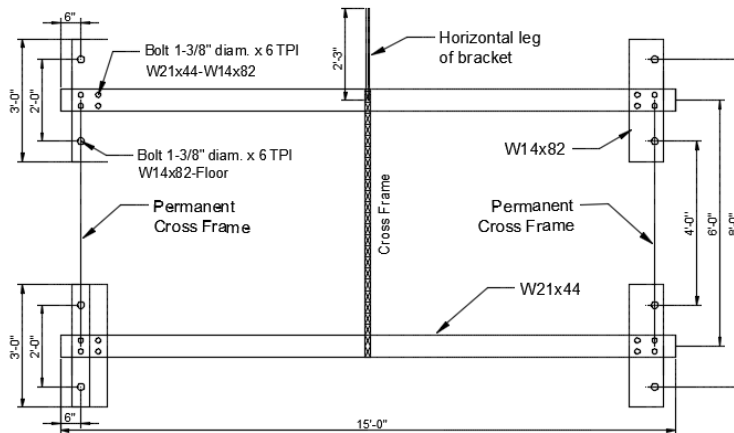


Figure D.25 Plan view for configurations with 1 intermediate cross frame at midspan.

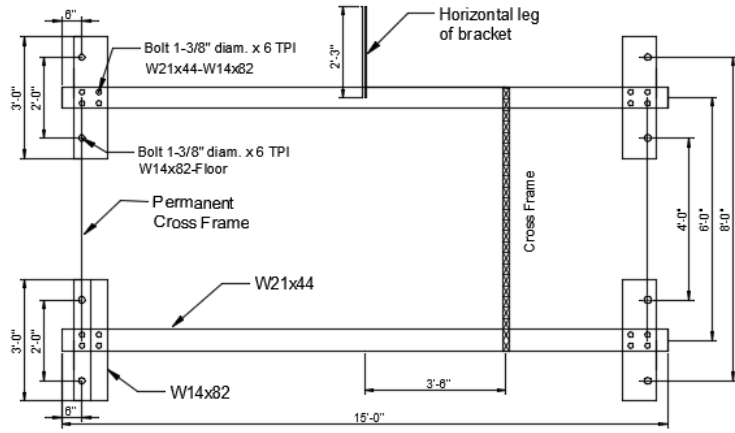


Figure D.26 Plan view for configurations with 1 intermediate cross frame not at midspan.

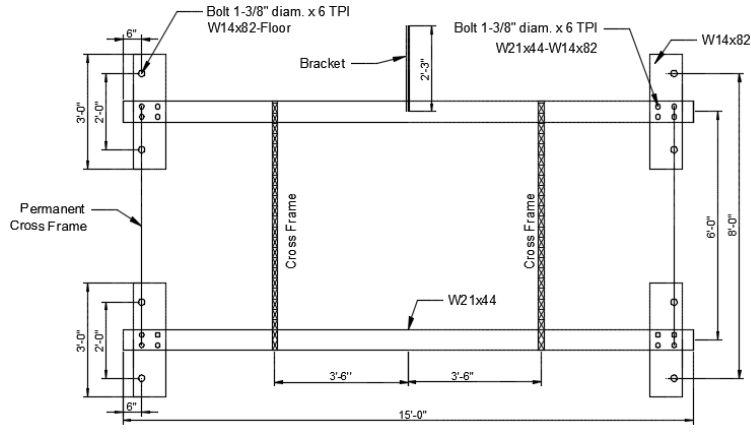


Figure D.27 Plan view for configurations with 2 intermediate cross frames.

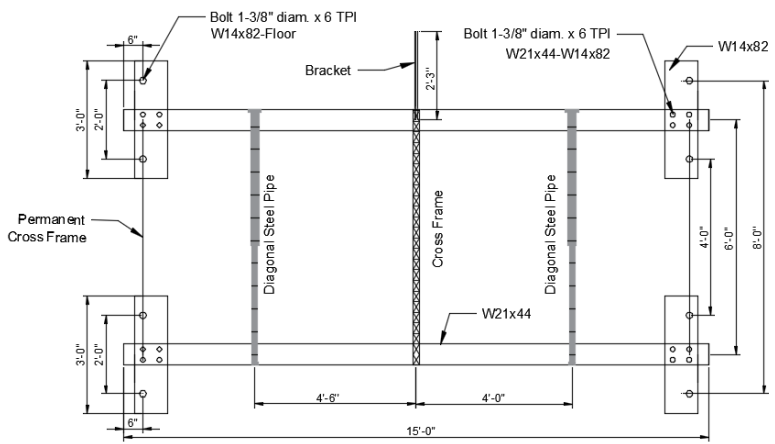
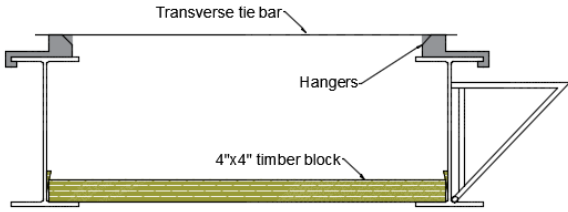
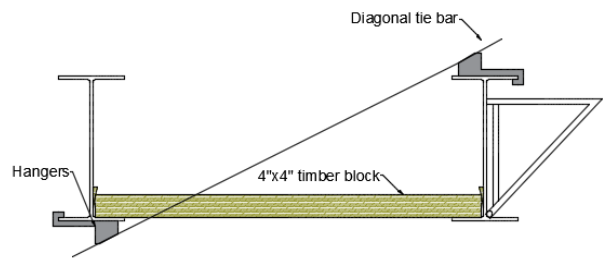


Figure D.28 Plan view for configurations with 1 intermediate cross frame at midspan and two diagonal pipes.



**Figure D.29 Cross section with transverse tie + timber block (TT + TB).**



**Figure D.30 Cross section with adjusted diagonal tie + timber block (ADT + TB).**

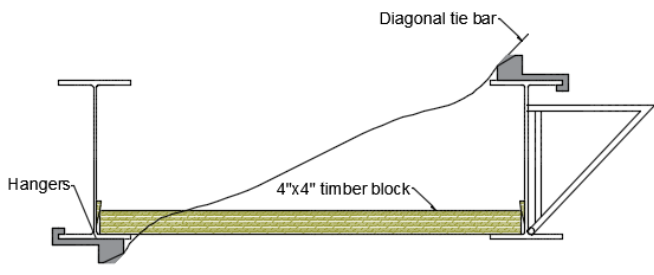


**Figure D.31 Cross section with transverse tie + unadjusted diagonal tie (UDT + TB).**

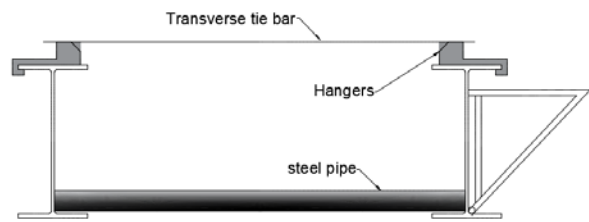


**Figure D.32 Cross section with transverse tie + horizontal pipe (TT + HP).**



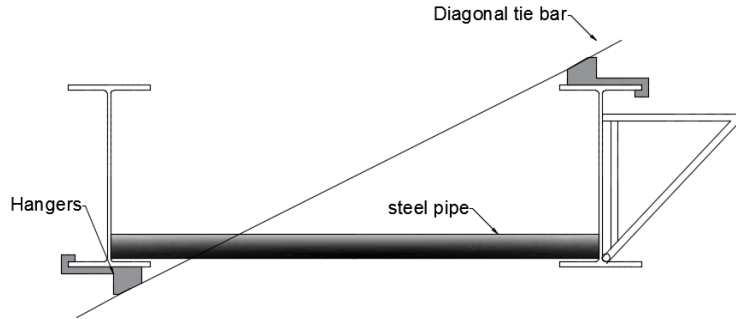


**Figure D.33. Cross section with adjusted diagonal tie + horizontal pipe (ADT + HP).**

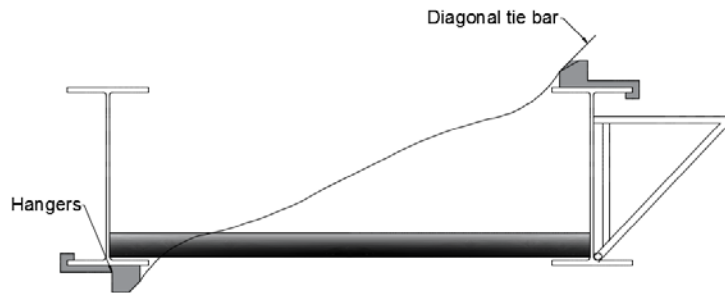


**Figure D.34 Cross section with transverse tie + horizontal pipe (UDT + HP).**

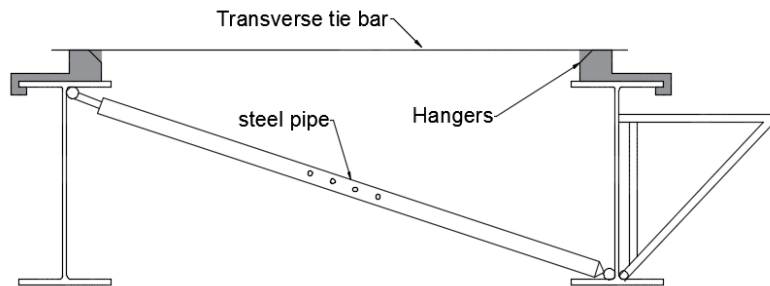


**Figure D.35 Cross section with transverse tie + horizontal pipe (TT + DP).**

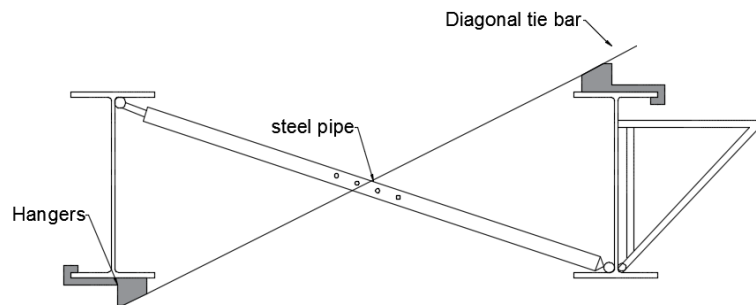


**Figure D.36 Cross section with adjusted diagonal tie + horizontal pipe (ADT + DP).**

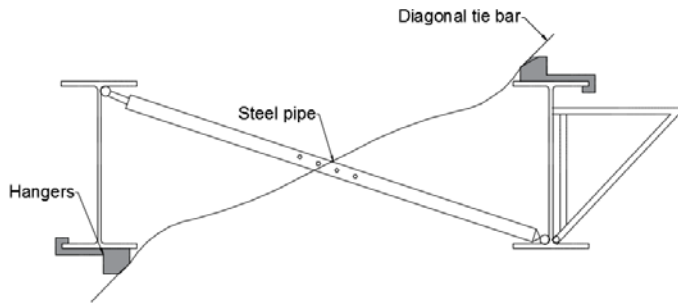


**Figure D.37 Cross section with transverse tie + horizontal pipe (UDT + DP).**

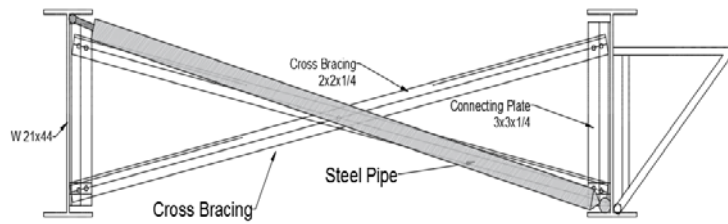


**Figure D.38 Cross section with cross frame + diagonal pipe (CF + DP).**

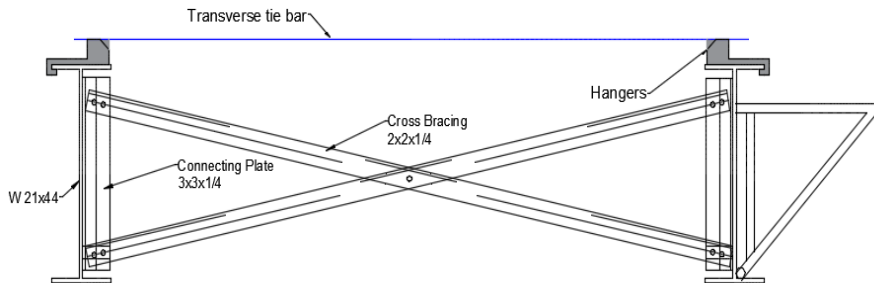


**Figure D.39 Cross section with transverse tie + cross frame (TT + CF).**

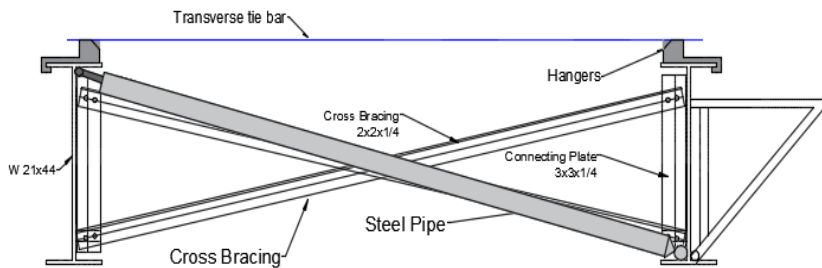


**Figure D.40 Cross section with cross frame + diagonal pipe + transverse tie (CF + DP + TT).**

**D.3 LABORATORY LAYOUTS AND MOST RELEVANT CROSS-SECTIONS FROM THE TESTED CASES IN THE EXPERIMENTAL PROGRAM**



**Figure D.41 3 transverse ties + 3 diagonal pipes (3-TT + 3-DP).**



**Figure D.42 1 cross frame at midspan + 3 transverse ties (1-CF@MS + 3-TT).**



**Figure D.43 1 Cross frame at midspan + 2 diagonal pipes+ 3 transverse ties (1-CF + 2-DP + 3-TT).**



**Figure D.44 4 transverse ties + 4 diagonal pipes (4-TT + 4-DP).**



**Figure D.45 3 adjusted diagonal ties + 3 horizontal pipes (3-ADT + 3-HP).**



**Figure D.46 3 unadjusted diagonal ties + 3 timber blocks (3-UDT + 3-TB).**



**Figure D.47 Cross frame not at midspan  
+ 2 diagonal pipes + 4 transverse ties  
(1-CF@ 3.5 ft. from midspan + 2-DP + 4-TT).**



**Figure D.48 4 transverse ties + 2 cross frames  
(4-TT + 2-CF @ 3.5 ft. from midspan).**



